Replication Fork Uncoupling Causes Nascent Strand Degradation and Fork Reversal

By

Tamar Kavlashvili

Dissertation

Submitted to the Faculty of the

Graduate School of Vanderbilt University

in partial fulfillment of the requirements

for the degree of

DOCTOR OF PHILOSOPHY

in

BIOCHEMISTRY

December 17, 2022

Nashville, Tennessee

Dr. James M Dewar, Ph.D.

Dr. David Cortez, Ph.D.

Dr. Brandt F. Eichman, Ph.D.

Dr. Houra Merrikh, Ph.D.

Dr. Emily Hodges, Ph.D.

To my grandmother Neli -

The most wonderful woman who valued my education above all else and was always there for me every step of the way

ACKNOWLEDGMENTS

It has been incredible 5 years at Vanderbilt and I am so grateful to have had such great support and excellent training environment in the department of Biochemistry. I would like to thank Dr. Beth Bowman for recruiting me to Vanderbilt and the IGP program for offering financial support for international trainees.

First and foremost, my gratitude goes to my mentor Dr. James Dewar who has been absolutely pivotal in my success in graduate school. I feel so lucky that I came across his poster during my first week at Vanderbilt and was lured in by the frog cartoons and candy. I was not planning on rotating in biochemistry or studying *in vitro* DNA replication but James's enthusiasm about science and the organization and support that his lab provided were unparalleled. James taught me how to critically think about science. He inspired me to trust the data and the process of science rather than making premature conclusions. I learned how to keep an open mind and go where the data led me. He ensured that I had all the tools to become successful. He encouraged collaborations, giving talks and networking at conferences, and always advocated for work-life balance. Every vacation I have gone on in the last 4 years, I have shared pictures and funny anecdotes with James and that shows that he cares about his trainees as people rather than just scientists. James has supported my every potential career choice and has ensured that I always had the resources to follow my passions – from time away from bench experiments to focus on learning data science and coding to networking with biotech companies in Boston, he never stood in the way of me expanding my professional toolkit. One of my favorite memories from grad school will always be how he called me on the lab landline phone to notify me that my paper was accepted by NSMB but first he pretended that one of the freezers were malfunctioning and of course I was

gloved up and doing a complicated immunodepletion experiment and freaked out. James believed from the first couple of preliminary experiments I did in 2018 that my discoveries would be big and impactful and he always kept the big picture in mind, reminding me to keep pushing even when I did not believe that I would publish a high impact story. I feel like I have grown immensely both as a scientist and as a person by being mentored by James. Reflecting on the last 4 years in the lab after publishing a high-impact paper and giving two high-profile talks at international conferences, I cannot help but feel immense gratitude for the mentorship and support I received. I will miss our daily interactions dearly knowing that he will be my mentor for life beyond graduate school.

I would like to thank the members of my committee for encouraging me and providing valuable insight over the years: Dr. Dave Cortez, Dr. Brandt Eichman, Dr. Emily Hodges and Dr. Houra Merrikh. Particularly, I'd like to thank Dr. Eichman for suggesting the RuvC experiment that definitively showed that remodeled forks were reversed forks. I would also like to thank the chair of my committee Dr. Dave Cortez for multitude of reasons. First, for having such a great discussion after my qualifying exam and making me feel extremely proud of my performance. That high has followed me throughout grad school and has gotten me through some of my lowest moments at the bench. Second, for cheering me on before and after my oral presentation in Trieste, Italy where I was very nervous. And finally for all the cellular data that our collaboration yielded that ensured success of my big grad school paper. I am very thankful that my committee is invested in my work and my success at Vanderbilt.

I would also like to thank past and present members of the Dewar Lab. I am proud to be one of the original members of the lab and James's first graduate trainee. And I am also proud of the culture of respect and camaraderie that we established in the lab. Kaylee, thank you for our

donut + dog adventures and being such a supportive lab mate and friend. Darren, I am so thankful for how deeply you always believed in my abilities and how excited you were about my project. You were the first one I told about passing my quals when I came back into the lab and I'll never forget how you said "well, of course you did!". I know you will be extremely successful in your life and career. Sabrina, thank you for all the little notes, countless loaves of sourdough and rolls, life chats and liters of borrowed TBE. I am so proud of how far you've come in graduate school. Emma, Sara and Steven, you have such bright futures ahead of you and I will miss our lab laughs. And if they install internet in Iowa we might even be able to keep in touch. Stedman, thank you for sharing my taste in music and being one of the funniest people. And last but not least, Lily! I am so grateful for our friendship. Our quarantine extract preps, frog accidents and labisms will go down in history.

I would also like to thank my undergraduate research mentor Dr. Shujie Yang for taking a chance on me, as well as Dr. Bob Kirby and Lindsey Marshall at Iowa Center for Research by Undergraduates (ICRU) for giving me funding for undergraduate research. Dr. Yang taught me so much about science and experimentation and I would not have chosen this path without her mentorship. In addition, huge thanks goes to the Ministry of Education and Science of Georgia for fully funding my undergraduate studies at the University of Iowa and my high school biology teacher Nona Solomonia for sparking my interest in the subject.

I would not have made it through grad school without all the friends I made here. My original IGP girl group: Sara Ramirez, Sarah Fong, Caye Arnaiz and Linh Trinh – I love you all dearly! You are all amazing scientists and brilliant women. Our friendship is my proudest accomplishment in grad school and our North Carolina trip will be the best grad school memory! Sam Lisy – you are

one of the most incredible people I have ever met. I am so grateful we became so close over my last year at Vanderbilt and I will miss our times in Nashville but know that we will be friends for life.

To my friends beyond graduate school – I feel so lucky to have kept in touch with you daily and so thankful how much you uplifted me and believed in my success. Elene, Maya, Likuna, and Kato. There aren't enough words to describe how grateful I am to have all of you in my life. You are all incredibly successful and marvelous women and I look up to you. Elene, thanks for flying to Nashville for my defense and surprising me in the best way possible. With you in the room, it felt like my Georgian family was here.

To my family who always believed in me even when they had no idea what I was doing in grad school, I am so grateful to have you. My cousin and best friend Mariam, I look forward to our lifelong adventures. My mom Natalia who is one of the most incredible human beings. I could not have done this without your love. My sister Nutsa who is always there to listen to my endless rants – I am grateful for you. My grandmother Tamri, who never hesitates to give honest advice and is one of the strongest women I know. My father Levan who encouraged me to keep learning and educating myself and quizzed me on novels I had read as a child – your dedication to my studies allowed me to come this far. And most importantly, my departed grandmother Neli who was so looking forward to seeing me defend my dissertation. I'm doing this in her honor. She was a marvelous self-made woman engineer who taught me math and science and did my homework with me as a child. I would not be earning this PhD without her sacrifice.

I recognize this PhD as an immense privilege and a collective effort of my scientific mentors, fellow lab members, friends and family. I am sharing this with all of you who have been by my side supporting me and motivating me for the last 26 years.

TABLE OF CONTENTS

Page

DEDICATION ii

ACKNOWLEDGEMENTS iii

LIST OF FIGURES xi

CHAPTER

I. INTRODUCTION 1

Overview of the mechanisms of vertebrate DNA replication 5
Causes and consequences of replication fork stalling 7
Replication fork reversal 8
Overview of fork reversal 8
Proteins that catalyze fork reversal 9
Molecular triggers of fork reversal 11
Replication fork protection 13
Overview of fork protection 13
Discovery of fork protection 15
Fork reversal in fork protection 19
Fork protection and chemosensitivity 21
Nascent strand degradation 23
Overview of NSD 23
NSD in the absence of fork protection 23
NSD in the presence of fork protection 24
NSD and fork reversal 25
Summary of the current model for fork reversal and NSD 25
Xenopus egg extracts to study DNA replication and repair 26
Thesis Project 88

II. MATERIALS AND METHODS 31

Xenopus egg extracts 31
Plasmid construction and preparation 31
DNA replication in Xenopus egg extracts 32
Protein purification 33
Nascent strand degradation assays 34
Antibodies and immunodepletions 35
2D gel electrophoresis 35
Nick translation of DNA 36
Plasmid pulldowns 36
siRNA knock downs 36
DNA fiber labeling analysis in human cells 37

III. DEVELOPING A BIOCHEMICAL SYSTEM TO STUDY NSD AND FORK REVERSAL IN XENOPUS EGG EXTRACTS 39

Introduction 39
Overview of the cell-free Xenopus egg extract system 39
Results 41
Triggering NSD in extracts 41
NSD is an initial response to fork stalling in human cells 45
A synchronous biochemical approach to study NSD 49

IV. NSD INVOLVES DNA2 EXONUCLEASE AND FORK REVERSAL 55

Introduction 55
Results 55
NSD involves DNA2 exonuclease in extracts 55
NSD involves DNA2 exonuclease in human cells 59
NSD involves fork remodeling 62
Remodeled forks are reversed forks 64
Requirements for fork remodelers in human cells 68

V. UNCOUPLING TRIGGERS NSD AND FORK REVERSAL 73

Introduction 73
Results 73
Both strands are degraded 73
Approach to inhibit uncoupling 77
Uncoupling elicits the onset of NSD 77
Uncoupling elicits NSD 79
Uncoupling elicits fork reversal 79

VI. CMG HELICASE IS RETAINED ON CHROMATIN DURING NSD 85

Introduction 85
Results 88
Approach to monitor binding of MCM6 and CDC45 during NSD 88
The CMG helicase is retained during NSD and fork reversal 88
NSD does not require replisome unloading 90

VII. NSD INVOLVES MULTIPLE SUBSTRATES 94

Introduction 94
Results 95
Approach to test whether multiple substrates for NSD exist 96
Y-shaped forks are substrates for NSD 96
NSD can occur in the absence of fork reversal in extracts 98

NSD can occur in the absence of fork reversal in human cells 100

VIII. DISCUSSION 103

Summary of dissertation work 103
Are all modes of NSD the same? 104
The role of the retention of CMG helicase during NSD and fork reversal 107
How does uncoupling elicit NSD? 108
Does ssDNA promote NSD? 109
Is uncoupling an absolute requirement for NSD? 110
Are post-replicative gaps uncoupled forks or degraded forks? 111
How does NSD lead to fork restart? 112
DNA2/WRN mediates fork processing and restart 113
Conversion of reversed forks to Y-shaped forks 115
What determines the choice between fork protection and NSD? 115

IX. APPENDIX A 118

SAMHD1 and FAN1 nucleases do not aid DNA2 in NSD 118
NSD involves WRN helicase/nuclease 120
NSD in extracts does not involve SMARCAL1 123
Proximity of the converging forks has no effect on NSD 123

X. REFERENCES 126

LIST OF FIGURES

Figure **Page**

1.1. Cartoon of fork reversal and NSD following genotoxic stress 16

1.2. Overview of vertebrate DNA replication 18

1.3. Cartoon of replication fork uncoupling 20

1.4. Cartoon of fork protection in vertebrates 26

1.5. Schematic of DNA fiber labeling assay 28

1.6. Models for NSD substrates 32

1.7. Overview of the Xenopus egg extract system 42

3.1. Analysis of DNA replication in *Xenopus* egg extracts 54

3.2. NSD is an initial response to fork stalling in extracts 57

3.3. Parental strands remain stable during NSD 58

3.4. NSD is an initial response to fork stalling in human cells 60

3.5. 2-D gel analysis of early replication structures 62

3.6. Schematic of triggering synchronous and localized uncoupling 64

3.7. Induction of synchronous and localized nascent strand degradation 66

3.8. Visualization of nascent strand degradation in extracts 68

4.1. Characterization of MRE11 and DNA2 activity during NSD 71

4.2. Nascent strand degradation involves DNA2 but not MRE11 in extracts 73

4.3. DNA2 and MRE11 inhibitors do not inhibit uncoupling 75

4.4. Nascent strand degradation involves DNA2 but not MRE11 in cells 78

4.5. Nascent strand degradation involves fork remodeling 80

4.6. Cartoon of how replication and repair intermediates migrate on 2-D gels 82

4.7. Remodeled forks are four-way junctions 84

4.8 Remodeled forks migrate as reversed forks 86

4.9. Requirement for fork remodeling enzymes in cells 87

5.1 Schematic for nascent strand degradation of both, leading or lagging strands 90

5.2 Both strands are degraded 92

5.3 An approach to inhibit uncoupling in extracts 94

5.4 Uncoupling promotes onset of nascent strand degradation 96

5.2 Uncoupling promotes extensive nascent strand degradation 98

5.3 Uncoupling promotes fork reversal 99

6.1 Two potential models for the fate of CMG helicase during NSD 100

6.2 Plasmid pulldown approach to measure protein binding 103

6.3 Replisome remains associated with DNA during NSD 104

6.4 Measuring replisome binding in the presence of p97-I 106

6.2 Impaired helicase unloading does not affect NSD 109

7.1 Schematic of different models for NSD substrates 110

7.2 DNA2 degrades replication forks and reversed forks 112

7.3 NSD can occur in the absence of fork reversal in extracts 114

7.4 NSD can occur in the absence of fork reversal in cells 116

8.1 Schematic of NSD contributing to fork restart 118

AA.1 SAMHD1 and Fan1 are not involves in NSD 136

AA.2 WRN and DNA2 function during NSD 138

AA.3 NSD in extracts does not involve SMARCAL1 139

AA.4 Proximity of converging forks has no effect on NSD 124

CHAPTER I

Introduction

DNA replication is a fundamental process that ensures faithful duplication of genomic material in every organism (Branzei & Foiani, 2010). Complete and accurate replication is essential to maintain genome stability. Although DNA replication has very high rate of fidelity, with less than 1 in a billion errors (Kunkel & Bebenek, 2000), several sources of endogenous and exogenous sources of stress can lead to DNA damage and subsequent accumulation of mutations. Exogenous sources of stress include environmental factors such as ultraviolet (UV) rays (Rastogi et al., 2010), ionizing radiation (IR) (Santivasi & Xia, 2014), as well as chemotherapeutic agents. While endogenous sources of damage arise from cellular metabolic processes and lead to oxidative damage, hydrolysis, alkylation etc. (Moretton & Loizou, 2020). Genome instability caused by a combination of these sources of damage is a hallmark of cancer and underlies almost all forms of neoplastic transformation (Negrini et al., 2010). Mechanisms have evolved to deal with genotoxic stress in order to minimize the mutations and maintain genome stability, but some of these mechanisms and how they are deployed are poorly understood.

DNA replication occurs at structures called replication forks, where parental DNA is unwound and daughter strands are synthesized. Various forms of genotoxic stress can lead to stalling of replication fork structures. Genotoxic stress and subsequent fork

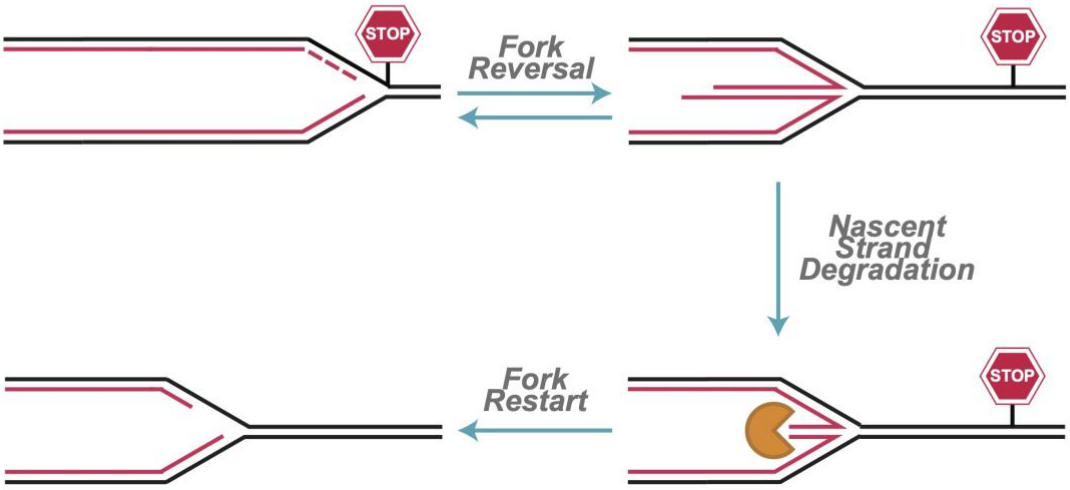

Figure 1.1. Cartoon of fork reversal and NSD following genotoxic stress

stalling is complex and involves a variety of pathways that become activated in order to stabilize forks and restart DNA synthesis. Reannealing and extrusion of nascent DNA strands to form a four-way junction termed a Reversed Fork (RF) is one of the primary responses to fork stalling (Zellweger et al., 2015) (Figure 1.1). Fork reversal is thought to be a mechanism to stabilize a fork before the damage is repaired and synthesis can be resumed (Berti, Cortez, et al., 2020). Additionally, fork reversal is important for replication restart following genotoxic stress (Thangavel et al., 2015). However, fork reversal also creates a substrate that resembles a double-stranded DNA end that can be subject to processing and degradation (Cortez, 2019). Cells possess mechanisms to reverse DNA synthesis by degrading the newly synthesized daughter strands (Figure 1.1). This is a highly conserved process across bacteria, viruses, yeast as well as metazoa. Degradation of newly synthesized DNA in response to genotoxic stress is termed Nascent Strand Degradation (NSD). Although NSD has been linked to fork restart (Thangavel et al., 2015), it has also been linked to generating aberrant chromosomes and promoting genome instability (Schlacher et al., 2011). Thus, it is unclear how cells elicit NSD and properly regulate the balance between degradation, reversal and restart. My thesis work has developed an *in vitro* system to study NSD and fork reversal in mechanistic detail and answer some of the key questions in the field.

In this chapter, I will overview vertebrate DNA replication in more detail, discuss how genotoxic agents induce fork stalling, and overview our current understanding of responses to fork stalling, mechanisms of fork protection and fork reversal.

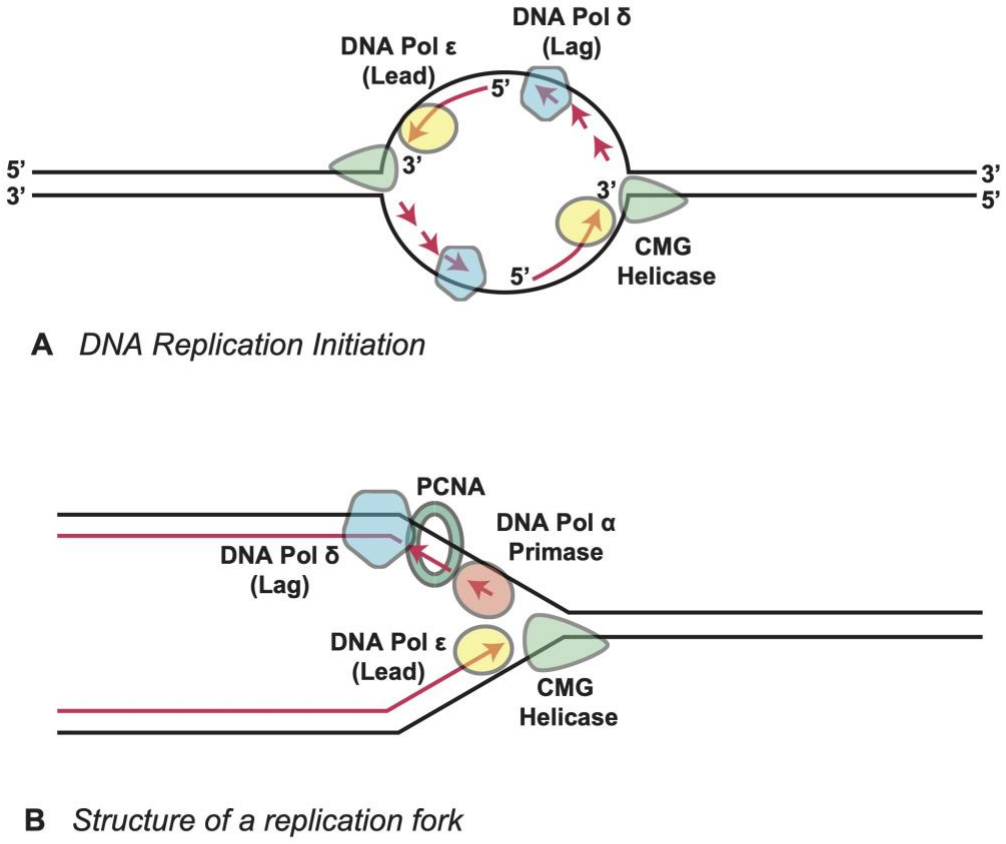

Figure 1.2. Overview of vertebrate DNA replication
(A) Schematic of DNA replication initiation. (B) Structure of a vertebrate replication fork.

Overview of the mechanism of vertebrate DNA replication

In vertebrates, DNA replication occurs in three distinct phases termed initiation, elongation, and termination (O'Donnell et al., 2013). During G1 phase of the cell cycle in vertebrates, pairs of MCM2-7 helicase complexes are loaded onto undefined origins of replication (Evrin et al., 2009). At the beginning of each S phase, inactive helicase complexes are converted to an active CMG complex by association of Cdc45 and GINS factors (Ilves et al., 2010). Active CMG complexes melt the DNA, generating single-stranded DNA (ssDNA) at origins and subsequently move away from one another bidirectionally to begin the elongation phase of DNA synthesis (Bochman & Schwacha, 2015; Li et al., 2015) (Figure 1.2 (A)). Each origin gives rise to two replication forks and each fork is replicated by a molecular machine termed the 'replisome' (Figure 1.2 (B)). The vertebrate replisome also includes DNA polymerases epsilon (Polε) (Waga et al., 2001) and delta (Polδ), synthesizing leading and lagging strands, respectively, and polymerase alpha primase (Polα), which generates a template to initiate replication of both leading and lagging strands during initiation, and continually primes the lagging strand template during elongation of DNA synthesis (Pellegrini, 2012). The replisome also includes the processivity and cell cycle signaling factor PCNA and many other accessory proteins that help coordinate DNA synthesis and coat ssDNA at forks (Sun et al., 2015). During termination, replisomes from adjacent origins converge and pass each other, nascent strands are ligated and replisomes are unloaded (Dewar et al., 2015; Dewar & Walter, 2017).

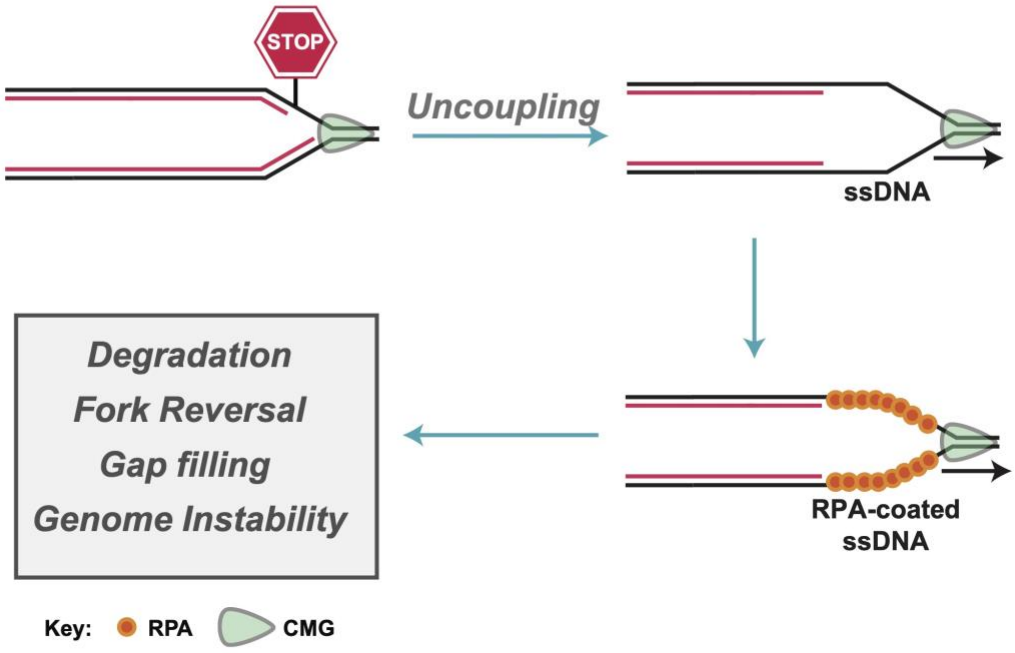

Figure 1.3. Cartoon of replication fork uncoupling

Causes and consequences of replication fork stalling

Introduction

Genome duplication is crucial for cellular division and thus, targeting DNA replication is a very common approach in cancer therapy. Several classes of genotoxic agents are utilized as chemotherapeutics that cause various types of DNA damage. All genotoxins broadly inhibit DNA replication. Most forms of genotoxic stress stall replication forks during DNA synthesis and pose a threat to genome integrity. Fork stalling can occur due to physical lesions in the DNA such as interstrand crosslinks (ICLs), DNA-protein crosslinks (DPCs), abasic sites, nicks in the DNA backbone etc. Additionally, stalling can occur at intact DNA templates due to decreasing pool of nucleotides (dNTPs) by hydroxyurea (HU) (Bianchi et al., 1986) or blocking of DNA polymerases by small molecule inhibitors such as aphidicolin (Ikegami et al., 1978) or CD437 (Han et al., 2016). When forks stall, DNA polymerases are unable to continue synthesis and this blocks the elongation of the nascent strands. CMG helicase continues unwinding parental DNA, which can generate excessive parental ssDNA (Byun et al., 2005; Michael et al., 2000; Zhou & Elledge, 2000). During normal DNA synthesis, activities of DNA polymerases and the CMG helicase are coupled. However, during polymerase stalling, CMG helicase continues its enzymatic activity while the polymerase is not synthesizing nascent DNA. This phenomenon is referred to as uncoupling and is thought to occur in response to various forms of genotoxins (Byun et al., 2005; Zellweger et al., 2015). Replication fork uncoupling leads to CMG helicase

slowing. The CMG helicase slows down ~8-10 fold following aphidicolin treatment (Graham et al., 2017; Sparks et al., 2019). Although helicase progression is slow, uncoupling still leads to generation of excessive ssDNA ahead of nascent strands (Byun et al., 2005) (Figure 1.3). Excessive ssDNA gaps can be mutagenic and thus, it is important that they are properly processed (Cong et al., 2021; Gambus et al., 2009; Nedelcheva et al., 2005). Uncoupled forks may undergo several types of processing in order to restart DNA synthesis such as repriming and subsequent post-replicative gap filling (Berti, Cortez, et al., 2020). They can also be targeted by structure-specific endonucleases that can cause fork breakage (Lemacon et al., 2017). Additionally, uncoupled forks may remodel into four-way junctions (Zellweger et al., 2015). This phenomenon is termed fork reversal and it is one of the most common responses to fork stalling. My dissertation work seeks to understand the molecular trigger for fork reversal and mechanisms that follow. I will explore fork reversal in more detail in the next section.

Replication fork reversal

Overview of fork reversal

One of the primary responses to fork stalling involves reannealing and extrusion of nascent DNA strands to generate a four-way junction sometimes termed as a ‘chicken-foot’ structure or an RF (Zellweger et al., 2015). This is a remarkably frequent mechanism that is observed in response to a wide variety of replication insults and

allows for replication fork stabilization and lesion bypass following genotoxic stress. Fork reversal was first observed in 1976 on an electron micrograph and was hypothesized as a potential model for using the sister nascent strand as a template for replication when parental template is damaged (Higgins et al., 1976). Back then, it was referred to as four-pronged replication fork and thought to be highly deleterious and mutagenic. More recently, fork reversal is seen as a way to stabilize stalled forks in order to avoid genome instability (Quinet et al., 2017). Fork reversal is a frequent and controlled process that occurs in response to a wide variety of genotoxins and other sources of replication stress.

Proteins that catalyze reversal

Fork reversal involves many proteins including a ssDNA binding protein RAD51, a Fox helicase 1 (FBH1), DNA translocase PICH and SNF family helicases SMARCAL1 (SWI/SNF-related, matrix associated, actin-dependent, regulator of chromatin, and subfamily A-like 1), ZRANB3 (zinc finger, RAN-binding domain containing 3), as well as HLTF (Helicase-Like Transcription Factor) (Hishiki et al., 2015). First, I will focus on SMARCAL1, ZRANB3 and HLTF roles in fork reversal. These enzymes all recognize different substrates *in vitro* (Poole & Cortez, 2017), however, their knockdown leads to some similar phenotypes *in vivo*, abrogation of fork reversal and excessive NSD following genotoxic treatment in fork protection deficient cells (Taglialatela et al., 2017). Mutations in SMARCAL1 cause Schmike immunoosseous dyplasia and it was first identified as an RPA binding genome maintenance protein overexpression or deficiency

of which led to activation of DNA damage response and hypersensitivity to genotoxins, respectively (Bansbach et al., 2009; Yuan et al., 2009). SMARCAL1 binds RPA and its RPA binding domain is essential in fork remodeling functions *in vivo* (Ciccia et al., 2009). This observation led to proposing the model that SMARCAL1 remodels forks with persistent ssDNA gaps at the fork junction (Taglialatela et al., 2017). dsDNA translocase activity of SMARCAL1 is also important for fork reversal, putting forth a model that reannealing of the parental strands drives reannealing of the nascent strands and fork reversal (Betous et al., 2012). ZRANB3 was first identified as a genome maintenance protein that localized to damaged forks via PCNA, K63-polyubiquitin chain interactions and also possesses a structure-specific endonuclease activity, generating an accessible 3' OH group of the leading strand template (Weston et al., 2012). ZRANB3 interacts with polyubiquitinated PCNA which promotes its fork remodeling activity (Ciccia et al., 2012; Vujanovic et al., 2017). HLTF is an ATP-dependent DNA translocase with a ubiquitin ligase activity (Unk et al., 2008). HLTF relies on its HIRAN domain that can interact with 3' OH and carry out fork reversal (Kile et al., 2015). In the absence of HLTF, DNA replication fails to slow down under genotoxic stress, which can lead to genomic instability (Achar et al., 2011; Bai et al., 2020).

FBH1 can catalyze fork regression both *in vitro* and *in vivo* (Fugger et al., 2015). FBH1 contains a helicase domain but also has ubiquitin ligase activity (Chiolo et al., 2007). FBH1 also controls RAD51 function (Chu et al., 2015), which could be how it indirectly affects fork regression. More recently, DNA translocase PICH emerged as a fork reversal factor. PICH together with SUMO E3 ligase ZATT and TOP2A is thought to drive extensive fork reversal downstream of SMARCAL1, ZRANB3 and HLTF mediated

initial reversal (Tian et al., 2021). Roles of RAD51 recombinase in fork reversal will be further expanded in the following section.

Overall, we know that all these proteins are capable of regressing replication forks. However, how they function together or how the pathway of choice is determined under different circumstances remain unclear.

Molecular triggers of fork reversal

Fork reversal allows for global slowing of replication fork elongation. This gives DNA repair machinery more time to repair or bypass certain lesions. However, reversed fork overhang also resembles a DNA double-strand break (DSB), which is highly mutagenic. Replication fork reversal can occur in response to a wide variety of genotoxic stress that can cause both replication fork stalling and uncoupling. Therefore, an exact molecular trigger for reversal is unclear. It has been hypothesized that ssDNA gaps in the wake of uncoupled forks an provide a platform for loading of fork reversal enzymes to promote remodeling, however, it has not been formally demonstrated. This evidence comes from the observation that upon wide sources of genotoxic stress, the median size of ssDNA stretches measured by EM correlate with the relative abundance of fork reversal (Zellweger et al., 2015). My thesis work in Chapter IV will identify one of the molecular triggers of fork reversal, which is replication fork uncoupling.

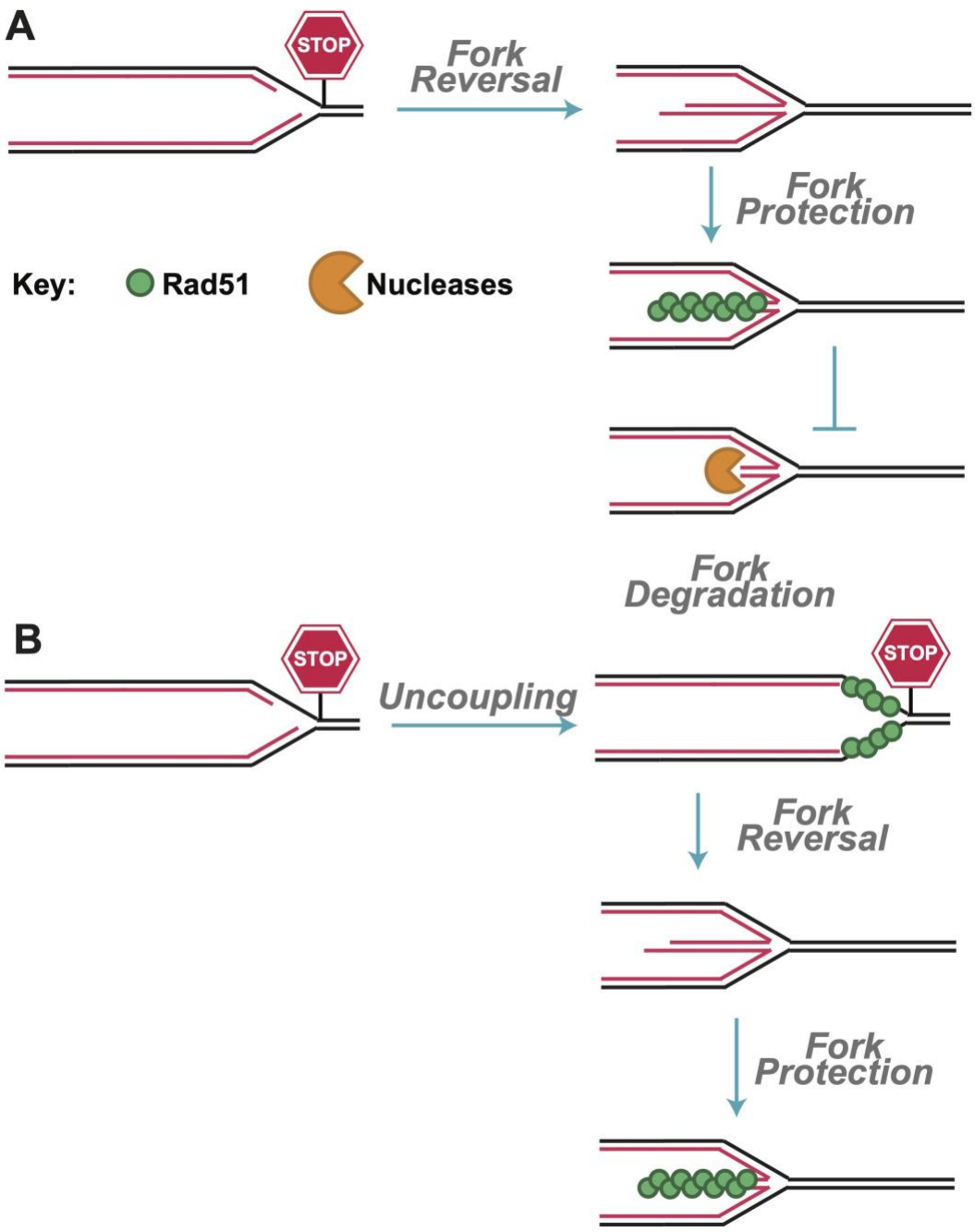

Figure 1.4. Cartoon of fork protection in vertebrates
(A) Schematic of fork reversal and RAD51 mediated protection of a reversed end. (B) Schematic of RAD51 function upstream of fork protection.

Replication fork protection

Overview of fork protection

Replication fork protection is a mechanism that protects reversed forks from aberrant processing (Berti, Cortez, et al., 2020; Hashimoto et al., 2010; He et al., 2018; Kolinjivadi et al., 2017; Lemacon et al., 2017; Liao et al., 2018; Przetocka et al., 2018a; Taglialatela et al., 2017) (Figure 1.4 (A)). Many different DNA repair proteins have been implicated in fork protection such as BRCA1/2, FANCD2, BOD1L and others (Higgs et al., 2015; Liu et al., 2020; Schlacher et al., 2012). Genotoxic stress in the absence of these factors causes NSD of unprotected reversed forks which leads to chromosomal aberrations and genomic instability. Excessive NSD can be rescued by depleting enzymes that catalyze fork reversal such as SMARCAL1, ZRANB3, HLTF, FBH1 or inhibiting nucleases that carry out NSD such as MRE11, EXO1 and CTIP (Cortez, 2019; Liu et al., 2020; Taglialatela et al., 2017). NSD can also be rescued by depleting RAD51, presumably by preventing fork reversal (Berti, Cortez, et al., 2020; Berti, Teloni, et al., 2020). However, the biochemical mechanisms underlying fork protection and degradation remain elusive. In this section, I will discuss the discovery and the evolving model for fork protection in vertebrates.

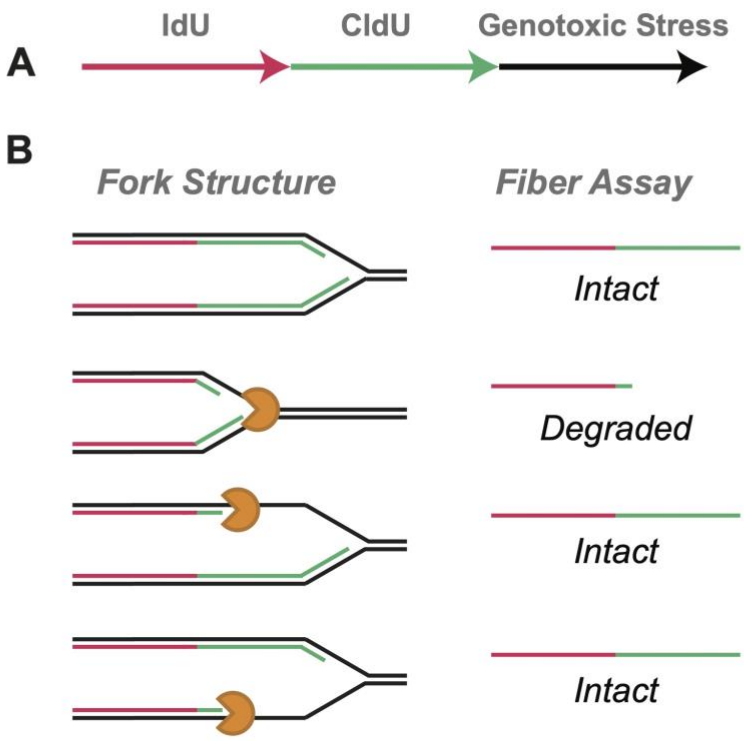

Figure 1.5. Schematic of DNA fiber labeling assay
(A) Schematic of sequential labeling with nucleotide analogs, followed by genotoxic stress to measure NSD. (B) Different fork structures corresponding to DNA fibers.

Discovery of fork protection

Fork protection was co-discovered in human cells and *Xenopus* egg extracts (Hashimoto et al., 2010; Schlacher et al., 2011). Both studies found unexpected roles for BRCA2/RAD51 and MRE11 nuclease independent of their canonical functions in double-strand break (DSB) repair (Holloman, 2011). The proposed mechanism included stabilization of RAD51 nucleofilaments on the ssDNA gaps behind the fork by BRCA2 in order to prevent nucleolytic processing of the overhang. This was supported by the evidence that stabilization, but not loading of RAD51 by BRCA2 was required to protect reversed forks from degradation by MRE11 (Schlacher et al., 2011). The cellular study hypothesized the role of fork reversal but did not formally test its involvement. In extracts, a study found that following MMS mediated DNA damage, ssDNA gaps accumulated on damaged templates in a RAD51-dependent manner(Hashimoto et al., 2010). When RAD51 binding to chromatin was inhibited using recombinant human BRC4 peptide, a motif of BRCA2 with a high affinity to RAD51, the number and the length of gaps increased significantly. Gaps were found to be suppressed by excess recombinant RAD51, showing the direct requirement for RAD51 recombinase in gap suppression (Figure 1.4 (B)). These gaps arose in MRE11 nuclease mediated manner. When MRE11 activity was inhibited by a small molecule inhibitor mirin, substantially lower amounts of gaps were detected by EM following MMS treatment. This study concluded that in the absence of RAD51 and the presence of genotoxic stress, MRE11 nuclease degrades nascent DNA behind forks leaving large ssDNA gaps.

A simultaneously published study in human, mouse embryonic and hamster cells reported similar findings (Schlacher et al., 2011). They utilized DNA fiber labeling analysis to monitor the stability of replication forks following hydroxyurea (HU) treatment, which is a genotoxic agent that inhibits ribonucleotide reductase and depletes deoxyribonucleoside triphosphate pools, thereby stalling replication forks. DNA fiber labeling sequentially pulses cells with two nucleotide analogs followed by genotoxic stress and provides a way to measure the length of replication forks following stress, as a proxy for degradation (Figure 1.5 (A)). Importantly, this assay cannot distinguish between leading versus lagging strand degradation because if either of the two strands are intact, signal appears unchanged (Figure 1.5 (B)). They found that in BRCA2-deficient cells, IdU tracts shortened over time following HU treatment, suggesting that nascent DNA was being degraded (Schlacher et al., 2011). This phenotype could be rescued by using BRCA2-proficient cells. Additionally, they did structure-function analysis on different domains of BRCA2 and found that a highly conserved C-terminus, which is dispensable for homologous recombination, is essential for maintaining replication fork stability. Thereby, providing evidence that stabilizing replication forks following genotoxic stress is done in an HDR independent manner. They further tested the direct involvement of RAD51 in maintaining nascent replication tracts following HU treatment. Similarly, to the study in *Xenopus* egg extracts, they expressed BRC4 peptide to perturb RAD51 nucleofilament formation, which led to substantially more degradation of nascent DNA. ATP hydrolysis by RAD51 is required

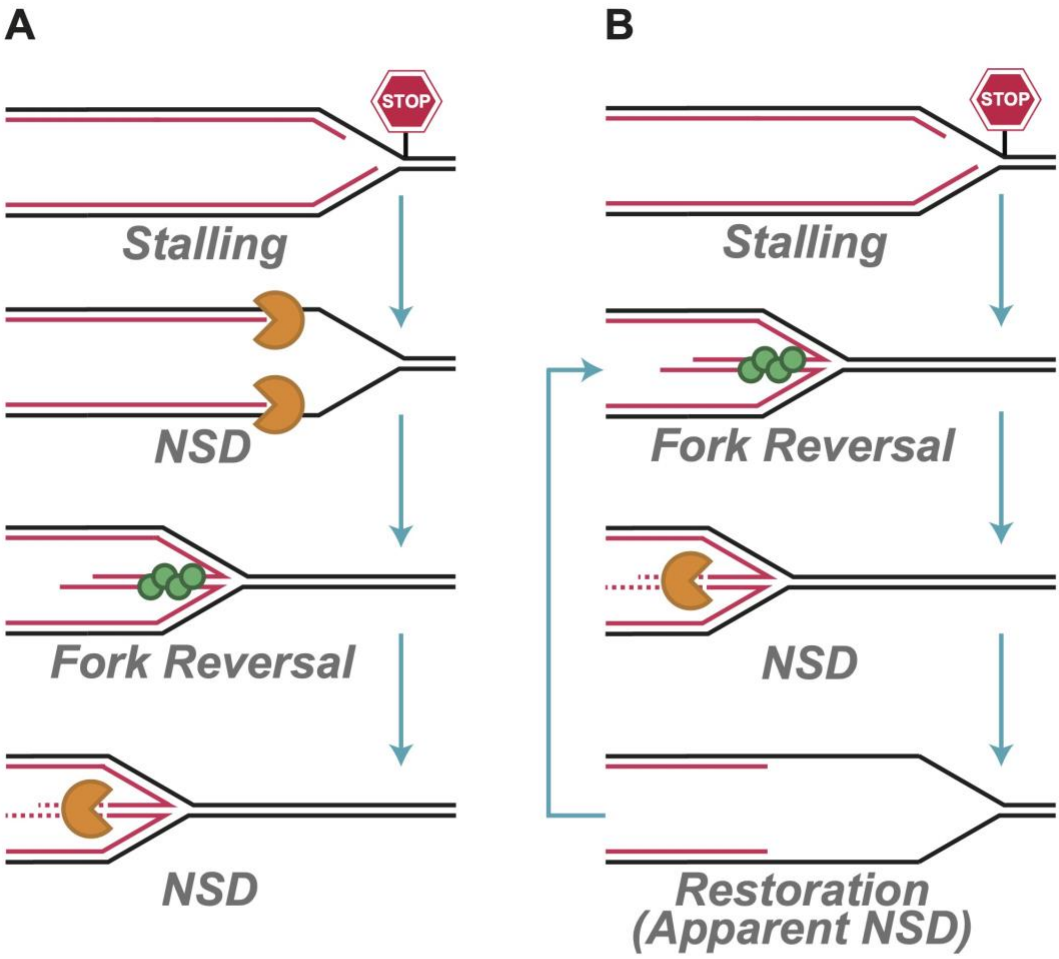

Figure 1.6. Models for NSD substrates
(A) A model for Double-Ys as substrates for NSD. (B) A model for reversed forks as substrates for NSD.

for RAD51 dissociation from DNA while allowing association and nucleofilament formation. Therefore, they expressed the K133R form of RAD51 which is devoid of the ATPase activity and forms very stable filaments. Expression of this mutant stabilized replication forks and rescued the protection phenotype, thereby providing evidence that stabilization of RAD51 filaments by BRCA2 is important for fork stability following genotoxic stress. This study also showed the involvement of MRE11 nuclease in nascent strand degradation. They also hypothesized that fork reversal might play a role in this process but did not formally test it. Most recently, new evidence came to light showing that the protective function of RAD51 during fork protection largely involves its capacity to bind dsDNA (Halder et al., 2022), in stark contrast to previous models which put forth a model that RAD51 coats ssDNA overhang of a reversed fork to protect it against nucleolytic degradation. The evidence that supported their findings is as follows. First, they showed that inhibiting dsDNA binding of RAD51 by BRC4 abrogates end protection. They additionally tested a RAD51 bacterial homolog RecA, which binds dsDNA poorly, and found that it does not confer protection to DNA ends. Finally, they show that ssDNA overhangs are dispensable for RAD51 protecting reversed forks against nucleolytic degradation. However, this study was done *in vitro* on synthetic DNA templates using recombinant proteins, which might not accurately represent cellular circumstances.

These studies laid a foundation for numerous others that explored fork protection in more detail and found that many more replication and repair factors are involved. Most of those mechanisms we still do not fully understand. Particularly, how all the

different fork reversal and fork protection factors function to maintain genome stability and which contexts are these different pathways deployed in are unclear.

Role of fork reversal in fork protection

Following these initial discoveries, a trio of papers were published reporting similar findings in both *Xenopus* egg extracts and human cells and discovering the involvement of fork reversal in fork protection and nascent strand degradation. The Xenopus study found that SMARCAL1 mediated fork reversal triggers MRE11 nuclease mediated nascent strand degradation in the absence of BRCA2 and RAD51 mediated fork protection (Kolinjivadi et al., 2017). First, they found that BRCA2 promotes binding of RAD51 to DNA during unperturbed DNA replication. Then they recapitulated earlier findings, showing that under MMS mediated replication stress, BRCA2 depleted extracts show ssDNA gaps that are subject to S1 nuclease mediated cleavage. Importantly, they showed that treatment with aphidicolin, also led to a similar gap formation phenotype, suppressed by both mirin treatment and rescuing extracts with recombinant BRCA2 domains. Their novel finding was that following aphidicolin treatment, they observed reversed fork structures by EM (Kolinjivadi et al., 2017). Reversed fork frequency was decreased by depleting both SMARCAl1 translocase and RAD51, and further decreased by co-depleting both factors. Thus, the study concluded that ssDNA gaps behind the replication fork following genotoxic stress are remodeled into reversed forks in RAD51 and SMARCAL1 mediated fashion and this reversal prevents degradation of reversed forks by MRE11 and other nucleases. A study

published simultaneously found that in addition to SMARCAL1, other 2 members of the SNF2 family fork remodelers, ZRANB3 and HLTF are also important for fork reversal following genotoxic stress in human cells (Taglialatela et al., 2017). They utilized DNA fiber labeling analysis to measure the length of nascent DNA tracts following HU treatment. As expected, they found that in cells devoid of fork protection, nascent strand degradation occurs following genotoxic stress. Importantly, they could rescue degradation and restore tract length by knocking down ZRANB3, HLTF and SMARCAL1. Another study in the same issue, showed that replication fork slowing and reversal upon genotoxic stress requires PCNA polyubiquitination and ZRANB3 translocase activity (Vujanovic et al., 2017). Another study also showed that BRCA2 defective cells undergo fork reversal and MRE11 mediated nascent strand degradation in response to HU treatment. In addition to MRE11, they defined a role for PTIP and RAD52 proteins in degradation of stalled forks (Mijic et al., 2017).

In addition to fork protection, RAD51 is also important for fork reversal (Zellweger et al., 2015). A study showed that siRNA-mediated knockdown of RAD51 inhibited fork reversal upon CPT, MMC and HU induced genotoxic stress (Zellweger et al., 2015). Several others reported that RAD51 cooperates with SNF2 family translocases to carry out fork reversal (Betous et al., 2012; Ciccia et al., 2012; Kile et al., 2015; Vujanovic et al., 2017; Zellweger et al., 2015). Importantly, RAD51 has been reported to be necessary for fork reversal in all genetic backgrounds of fork protection loss (Liu et al., 2020). Although the mechanistic role of RAD51 in protection of reversed forks is more well understood, how it catalyzes fork reversal remains elusive. One important finding is

that amount of RAD51 protein determines fate of stalled forks (Bhat & Cortez, 2018). Higher cellular levels of RAD51 are required for fork protection than fork reversal, so when RAD51 is partially knocked down, stalled fork reversal and degradation can still take place, but reversed forks are deprotected (Bhat et al., 2018). Additionally, RAD51 small molecule inhibitor B02 which inhibits RAD51 nucleofilament assembly and foci formation, blocks fork protection (Taglialatela et al., 2017) but does not inhibit fork reversal, providing further mechanistic insight on how roles of RAD51 during these two processes are distinct.

Fork protection in chemosensitivity

In addition to fork protection, BRCA1/BRCA2 and RAD51 proteins play a key role during error-free DSB repair by homologous recombination. Patients with mutations in these proteins are predisposed to breast, ovarian and pancreatic cancers. Cells devoid of these proteins, as well as patients with mutations are very sensitive to DNA damaging agents such as cisplatin and poly(ADP-ribose) polymerase (PARP) inhibitors. Since the discovery of the roles of BRCA1/2 and RAD51 in fork protection and fork reversal beyond their canonical functions in HR, scientists have been curious to know how defective fork stability affects chemotherapy sensitivity and whether restoration of fork stability can confer chemoresistance. Mouse and cellular studies showed that restoring fork protection correlates with chemotherapy resistance in HR deficient settings (Ding et al., 2016; Dungrawala et al., 2017; Ray Chaudhuri et al., 2016; Yazinski et al., 2017). One particular study, found a causal relationship between

restoring fork protection and gaining chemoresistance (Ray Chaudhuri et al., 2016). However, some studies have shown that restoration of fork protection has no effect on modulating chemosensitivity (Feng & Jasin, 2017). Overall, the majority of the chemoresistance can be attributed to restoration of homologous recombination, but fork protection also serves a role (Dias et al., 2021).

Nascent Strand Degradation

Overview of NSD

Nascent strand degradation is a complex mechanism that occurs downstream of genotoxic stress. Small amounts of degradation could be beneficial to promote fork restart however, excessive degradation leads to genome instability and chromosomal aberrations. NSD can be carried out by many different nucleases in different genetic backgrounds. Below I will discuss our current understanding of NSD in the presence or absence of fork protection.

NSD in the absence of fork protection

In the absence of fork protection factors, genotoxic stress causes excessive NSD. One of the initial studies that discovered fork protection, also found that excessive NSD leads to aberrant chromosomal structures during metaphase such as radial and broken chromosomes (Schlacher et al., 2011). Importantly, they were able to rescue the chromosomal abnormalities by inhibiting NSD by inactivating MRE11 nuclease. Interestingly, accumulation of these aberrant chromosomal structures, did not lead to increased cell death, suggesting that BRCA2 deficient cells upon genotoxic stress will be able to undergo increased mutagenesis without compromising survival. Subsequent studies showed that loss of many other proteins such as FANCD2, ABRO1, BOD1L,

VHL, FANCA, EXD2, and 53BP1 also leads to aberrant degradation by MRE11, CTIP and DNA2 nucleases (Espana-Agusti et al., 2017; Higgs et al., 2015; Higgs & Stewart, 2016; Liu et al., 2020; Nieminuszczy et al., 2019; Xu et al., 2017). How these different fork protection factors function together and whether there are multiple fork protection pathways that function in response to different insults are unclear.

NSD in the presence of fork protection and fork restart

In addition to NSD that occurs in the absence of fork protection, degradation of nascent DNA strands has also been observed in wild-type (WT) cells under the conditions of prolonged HU stalling (Thangavel et al., 2015). This form NSD is driven by DNA2 nuclease (Zheng et al., 2020) and WRN helicase, is antagonized by RAD51 and does not involve MRE11, EXO1, EXD2 or CTIP nucleases. This mode of degradation is thought to be important for fork restart after genotoxic stress. However, it is unclear whether this controlled NSD occurs in the presence of fork protection or whether they are two separate pathways deployed under different conditions. It is also unclear whether NSD under fork protection proficient conditions can only occur after 8+ hours of stalling or whether it is a primary response to stalling and leads to fork recovery. My thesis work will explore this further.

NSD and fork reversal

Replication fork reversal and NSD are tightly linked. All known modes of NSD can be fully inactivated by knockdown of fork reversal factors, which serves as an indirect readout for fork reversal being required for NSD. However, a question still remains of whether NSD can occur in the absence of fork reversal and whether fork reversal is a necessary entry point for nucleolytic degradation of newly synthesized DNA (Berti, Cortez, et al., 2020) (Figure 1.6) My thesis work in Chapter VII will address is unanswered question.

Summary of the current model for fork reversal and NSD

Below is the current model of stalled fork processing in vertebrates. Stalled forks are remodeled into reversed forks, which are subject to fork protection to guard them against aberrant nucleolytic processing. Nascent strand degradation can also occur in fork protection proficient cells after prolonged fork stalling, and this is thought to be important for fork restart. Reversed forks are thought to be necessary entry points for nascent strand degradation. However, key mechanistic questions about fork reversal and nascent strand degradation remain. For instance, what is a molecular trigger for fork reversal? Is NSD ever deployed as a first response to genotoxic stress? Are these other substrates for NSD? What is the fate of the replicative helicase during fork reversal and NSD? My thesis work aimed to address these questions by developing an *in-vitro* system using cell-free *Xenopus* egg extracts.

Xenopus egg extracts to study DNA replication and repair

Xenopus egg extracts provide an excellent system to study DNA replication and repair in mechanistic detail. These cell-free extracts contain all necessary components to carry out in vitro DNA replication (Lebofsky et al., 2009) and have been used to discover many fundamental processes, including fork protection(Hashimoto et al., 2010). Broadly, oocytes are isolated from female frogs and processed into cytosolic and nuclear extracts which provide means for DNA licensing, and DNA replication, respectively (Figure 1.7). Custom plasmid DNA templates, as well as chromosomal DNA can be efficiently replicated in extracts. I will explore the utility of the *Xenopus* egg extract system in more detail in Chapter III.

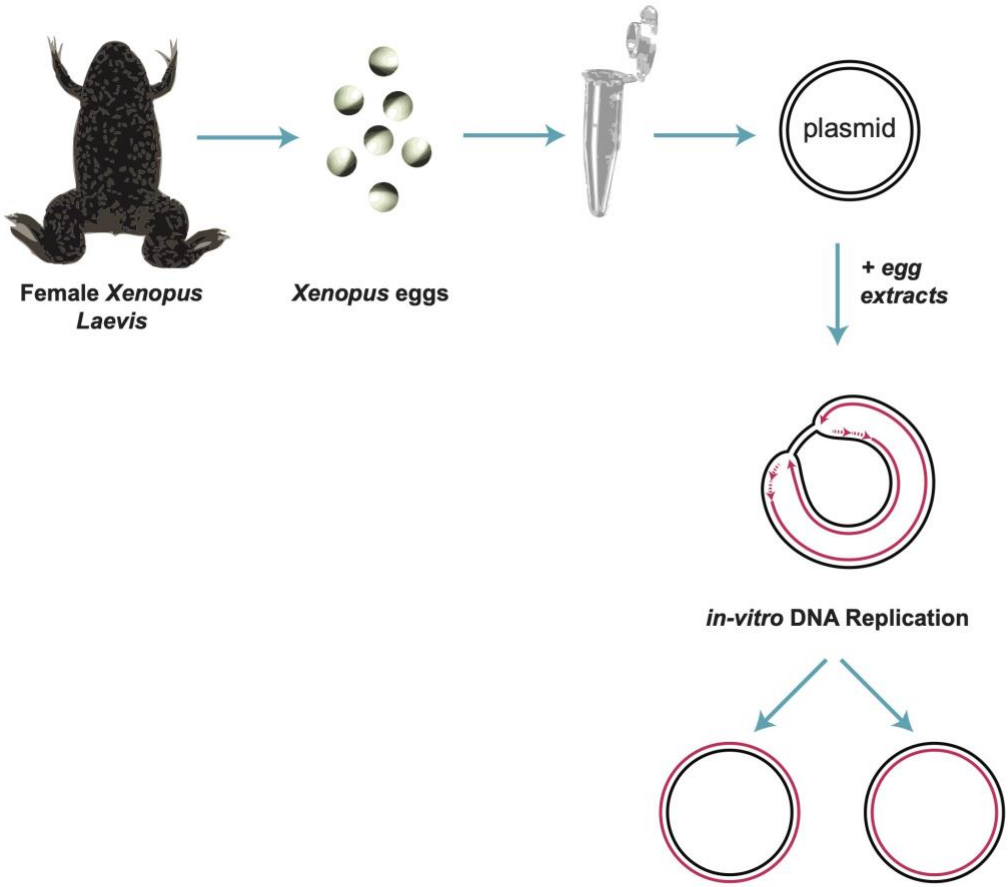

Figure 1.7. Overview of the *Xenopus* egg extract system

Thesis Project

Genotoxic stress stalls replication forks during DNA replication and causes fork reversal and NSD. Over the last decade, numerous studies have identified and characterized fork protection, NSD and fork reversal and they have identified many tumor suppressor proteins that function in these pathways. These processes are crucial to maintain genome stability in response to genotoxic stress, however our mechanistic understanding on how they are triggered or carried out is limited. One big question in the field is precisely which aspect of fork stalling triggers NSD? Uncoupling has been correlated with fork reversal and NSD, but it has not been formally demonstrated that uncoupling can trigger NSD. In addition, it is unclear what DNA structures are targeted for degradation and whether fork reversal is a necessary entry point for resection. It is possible that different substrates can be degraded, and degradation of Y-shaped forks might precede or even promote fork reversal. Another gap in our knowledge of these mechanisms is what is the fate of the replicative helicase during NSD and fork reversal? CMG helicase translocates on ssDNA of the leading strand template and fork reversal creates a four-way double stranded junction which is theoretically incompatible with CMG binding. Does CMG unload from the fork prior to fork reversal? If so, what are the mechanisms that promote unloading and how can efficient restart be ensured to safeguard genome integrity? Conversely, does CMG stay bound to the fork structure during fork reversal and if so, does it get trapped in a ssDNA bubble or translocates on dsDNA somehow avoiding triggering ubiquitination and unloading? Most importantly, is NSD a primary response to fork stalling or does it only occur following impaired fork

protection and a very prolonged stalling? How physiological is this process? These are all important questions that conventional approaches lack the temporal and spatial resolution, as well as sensitivity to answer. My thesis project has focused on initially developing an approach to study fork reversal and NSD, and subsequently answering key mechanistic questions about these fundamental biochemical processes which are outlined above. I sought to develop a system that synchronized replication forks in order to study the dynamics of NSD and fork reversal in mechanistic detail. In Chapter II, I provide the methods that we used to develop the assays in order to study NSD and fork reversal. In Chapter III, I describe the development of the biochemical system to study NSD and fork reversal in *Xenopus* egg extracts. In Chapter IV, I describe the results validating that our approach can trigger and monitor NSD that is in line with what has been described in the literature. In Chapter V, I describe our novel findings that fill some of the crucial gaps in the literature. In Chapter VI, I overview my thesis findings and discuss the implications and future directions of my work. First, I observed that NSD is an initial response to replication fork stalling. Then, I showed that replication fork uncoupling, but not stalling, is a trigger for both NSD and fork reversal. Additionally, I discovered that Y-shaped forks, in addition to reversed forks, can be substrates for NSD and that degradation of canonical Y-shaped forks precedes degradation of reversed forks. Finally, my work has showed that replicative helicase CMG remains bound to DNA throughout NSD and fork reversal and that impaired helicase unloading does not impair NSD. Overall, my thesis has made significant contributions to understanding the molecular triggers and mechanisms of fork reversal and NSD and has provided a new

method for further elucidating how various genotoxic agents affect replication fork stability.

CHAPTER II

MATERIALS AND METHODS

Xenopus egg extracts

Xenopus egg extracts were prepared from *Xenopus laevis* wild-type males and females (Nasco) as previously described (Lebofsky et al., 2009) and approved by Vanderbilt Division of Animal Care (DAC) and Institutional Animal Care and Use committee (IACUC).

Plasmid Construction and Preparation

pJD145, pJD156, and pJD90 were described previously(Dewar et al., 2015). To create pJD161 (p[*lacO*x25]-XhoI-[*lacO*x25]) DNA oligonucleotides JDO120 (GTACAAGTAAATCAGAGCCAGATTTTTCCTCCTCTCGGAATTGTGAGCGGATAACA ATTCCCTCGAGCCAATTGTGAGCGGATAACAATTGGAAGTGCAGAACCAATGCATG CAGGAGATTTGAC) and JDO121 (GT ACGTCAAATCTCCTGCATGCATTGGTTCTGCACTTCCAATTGTTATCCGCTCACAAT TGGCTCGAGGGAATTGTTATCCGCTCACAATTCCGAGAGGAGGAAAAATCTGGCT CTGATTTACTT) were annealed to create a DNA fragment that contained a XhoI site flanked by a lacO sequence on each side. The JDO120/JDO121 duplex was then cloned into the BsrGI site of pJD90 (p[*lacO*x24]). This cloning procedure regenerated the BsrGI

site, which was then used as the target for insertion of a BsrGI-BsiWI fragment from pJD90 that contained 24 tandem *lacO* repeats. The resulting plasmid was then digested with BsrGI and BsiWI to create a fragment containing 50 tandem *lacO* repeats with a XhoI site in the middle. This fragment was inserted into the BsiWI site of pJD145 to yield pJD161.

DNA replication in Xenopus egg extracts

High Speed Supernatant (HSS) was supplemented with nocodazole (3 ng/µl) and ATP regenerating system (ARS; 20mM phosphocreatine, 2 mM ATP and 5 ng/µl creatine phosphokinase) then incubated at room temperature for 5 minutes. To license plasmid DNA, 1 volume of 'licensing mix' was prepared by adding plasmid DNA to HSS at a final concentration of 15 ng/µl, followed by incubation at room temperature for 30 minutes. NucleoPlasmid Extract (NPE), extract was supplemented with ARS, DTT (final concentration: 2 mM), [α-^{32}P]dATP (final concentration: 350 nM) and diluted to 45% in 1X Egg Lysis Buffer (ELB, 250 mM Sucrose, 2.5 mM MgCl2, 50 mM KCl, 10 mM HEPES, pH 7.7). To form a replication barrier, LacR was bound to *lacO* repeats as previously described. To initiate replication, 2 volumes of NPE mix were added to 1 volume of Licensing mix. Replication forks were stalled at the LacR-bound *lacO* array and then released by IPTG addition as described previously(Dewar et al., 2015). Reactions were stopped by addition of 10 volumes Extraction Stop Solution (0.5% SDS, 25 mM EDTA, 50 mM Tris-HCl, pH 7.5). Samples were subsequently treated with RNase A (final concentration: 190 ng/µl) and then Proteinase K (909 ng/µl) before either

direct analysis by gel electrophoresis or purification of DNA as described previously (Dewar et al., 2015).

For most experiments pJD156 (p[*lacO*x32]) was used as the template for replication. For the experiments in Fig. 3F-H and Supplemental Fig. S4J-K pJD161 (p[*lacO*x25]-XhoI-[*lacO*x25]) was used. pJD145 (p[CTRL]) did not contain a *lacO* array, which allowed it to fully replicate in the presence of LacR, and was used as a loading control because its small size allowed it to be readily distinguished from pJD156 and pJD161. In most experiments, pJD145 was added to the licensing mix at a final concentration of 1 ng/µl and the plasmid replicated prior to induction of NSD due to the absence of any LacR array. Radiolabeled pJD145 was added to NPE at a concentration of 1 ng/µl prior to initiation of DNA replication and the plasmid did not replicate because it had not undergone prior licensing of the DNA.

Aphidicolin from *Nigrospora sphaerica* (Sigma-Aldrich) was dissolved in DMSO and added to reactions at a final concentration of 330 µM. Mirin (Selleckchem) was dissolved in DMSO and added to reactions at a final concentration of 500 µM. C5 (AOBIOUS) (Liu et al., 2016) was dissolved in DMSO and added to reactions at a final concentration of 3.5 mM. NMS-873 (Selleckchem) was dissolved in DMSO and added to reactions at a final concentration of 200 µM. For drugs dissolved in DMSO the final reaction concentration of DMSO was 4% (V/V).

Protein Purification

Biotinylated LacR was expressed in *Escherichia coli* and purified as described previously (Dewar et al., 2015).

Nascent Strand Degradation assays

To monitor DNA synthesis, samples were separated on a 1% agarose gel at 5 V/cm. Radiolabeled DNA was visualized by phosphorimaging to measure incorporation of radiolabeled nucleotides. Signal was quantified using ImageQuant (GE Healthcare) and ImageJ and normalized to the loading control in each lane.

To monitor NSD, samples were purified and then digested with 0.4 U/µl XmnI in CutSmart Buffer (NEB) for 30 minutes at 37°C and then separated on a 1% agarose gel at 5 V/cm. Radiolabeled DNA was detected by phosphorimaging and Double-Y signal was quantified and normalized to pJD145 signal, which served as a loading control.

To monitor disappearance of intact nascent strands, purified NSD intermediates were digested with 0.4 U/µl AlwnI (NEB) in CutSmart Buffer (NEB) for 1 hour at 37°C. Digest was stopped by adding EDTA to a final concentration of 30 mM. Reaction was then prepared for electrophoresis by adding Alkaline Loading Buffer 6X (EDTA, Ficoll, Bromocresol green, Xylene Cyanol and NaOH (10N)) to a final concentration of 1X. Nascent strands were then separated on a 1.5% denaturing alkaline gel at 1.5 V/cm.

Denaturing gel was then neutralized by gentle agitation in 7% TCA solution and radiolabeled DNA was detected by phosphorimaging as described above.

Antibodies & Immunodepletions

Antibodies targeting Xenopus CDC45, MCM6 and RPA were previously described (Dewar et al., 2017), as were antibodies targeting Xenopus SAMHD1(Coquel et al., 2018) and FAN1(Klein Douwel et al., 2014). Antibody (i) targeting Xenopus SMARCAL1 was raised against a peptide of CKRRKIDDYFAL (New England Peptide 3850) while antibody (ii) was previously described (Kolinjivadi et al., 2017). Immunodepletions were performed as described (Heintzman et al., 2019), but with three rounds of depletion instead of two. Antibodies targeting human RAD51 (AB63801) were obtained from Abcam.

2D gel electrophoresis

2D gels were performed as described with slight modifications (Heintzman et al., 2019). Briefly, purified DNA was digested with XhoI and DraIII (Fig. 4H) or XmnI (all other gels) and digested DNA was separated on a 0.4% agarose gel at 1 V/cm for 22 hours. A second dimension gel containing 1.2% agarose and 0.3 µg/ml ethidium bromide was cast over the first dimension gel slice and separated at 5 V/cm for 12 hours at 4°C. Radiolabeled DNA was then detected by phosphorimaging as described above.

Nick translation of DNA

To radiolabel parental DNA strands, 60 ng/µl plasmid DNA was resuspended in 1X NEB Buffer 2.1 and treated with 0.5 U/µl Nt.BbvCI at 37°C for 1 hour, followed by heat inactivation at 80°C for 20 minutes. To perform nick translation the reaction was supplement with 0.5 volumes of dNTPs (12.5 mM each of dCTP, dGTP, dTTP), 3 U/µl *E. coli* DNA Polymerase 1, and 0.33 mM [α^{32}P]-dATP in 1X NEB Buffer 2.1 and incubated at 16°C for 10 minutes then on ice for 5 minutes. Nick-translated DNA was purified into 10 mM Tris-HCL, pH 8.0 using micro Bio-Spin columns (Bio-Rad) and used for replication and NSD assays.

Plasmid pull downs

Plasmid pull downs were performed as previously described (Dewar et al., 2017).

siRNA knock downs

siRNAs targeting MRE11, DNA2, and RAD51 were previously described (Liu et al., 2020). siRNAs targeting PICH (L-031581-01), HLTF (L-006448-00), FBH1 (L-017404-00), FAN1 (L-020327-00), and SAMHD1 (L-013950-01) were ON-TARGETplus siRNA from Horizon. siRNA targeting ZRANB3 was s38488 from ThermoFisher. SMARCAL1 was targeted using siRNA GCUUUGACCUUCUUAGCAA. All siRNA

transfections were performed using DharmaFECT reagents according to the manufacturer's instructions. Experiments were performed 3 days after transfection.

DNA fiber analysis in human cells

DNA fiber spreading experiments were performed as described previously(Liu et al., 2020). Cells were labeled with 20 μM CldU followed by 100 μM IdU for 20 min each, then treated as indicated with the following concentrations of drugs: aphidicolin (10 μM, unless otherwise indicated), RAD51 inhibitor B02 (25 μM), DNA2 inhibitor C5 (20 μM), MRE11 inhibitor Mirin (20 μM), HU (4 mM). Following stretching and fixation on glass slides, DNA was denatured in 2.5 M HCl for 80 min, washed three times with phosphate-buffered saline (PBS), and blocked in 10% goat serum/PBS with 0.1% Triton X-100 for 1 hour. Slides were immunoblotted with 1% (v/v) rat anti-CldU antibody (Abcam ab6326) and 1% (v/v) mouse anti-IdU antibody (BD B44) for 2 hours, then washed 3 times with PBS followed by 0.4% (v/v) secondary antibody incubation for 1 hour. Slides were then washed with PBS 3 times, then mounted with prolong gold without DAPI 508 (Invitrogen P36930). Fibers were imaged using a Nikon Ti-DH immunofluorescence microscope. At least 100 fibers were counted for each sample. Statistical analyses were performed using Prism. For experiments with more than two samples, a Kruskal-Wallis test was used and corrected for multiple comparisons. A two-tailed t test was used to compare two samples with normally distributed data. P-values are reported in the figures. Non-significant comparisons are indicated as 'ns'. No statistical methods or criteria were used to estimate sample size or to include/exclude

samples. All experiments were performed at least twice and a representative experiment is shown.

CHAPTER IIII

Developing a biochemical system to study NSD and fork reversal in *Xenopus* egg extracts

Overview of the cell-free *Xenopus* egg extract system

The cell-free *Xenopus* egg extracts have been used to study a variety of cellular processes that led to many discoveries. More specifically, the egg extract system described in this chapter (Walter et al., 1998) supports *in vitro* DNA replication using the full set of vertebrate cellular proteins. Using this approach, all stages of replication can be monitored in detail using custom DNA templates. First, plasmids are incubated in high-speed supernatant (HSS), which contains soluble interphase proteins and supports 'licensing' of DNA or loading of the inactive Mcm2-7 complexes onto replication origins by ORC, CDC6 and CDT1 (Figure 3.1 (A, i)). HSS contains very low concentrations of CDK and DDK kinases, which are essential to 'fire' origins or initiate DNA replication. In order words, incubating plasmid DNA in HSS resembles the G1 phase of the cell cycle. To trigger replication initiation, reactions are supplemented with Nucleoplasmic Extract (NPE), which contains a high concentration of nuclear factors and CDK and DDK kinases. This results in the activation of Mcm2-7 complexes by association of Cdc45 and GINS forming the CMG helicase (CDC45-MCM2-7-GINS) and replication forks are established (Figure 3.1 (A, ii)). Subsequent incubations of plasmid DNA in HSS and NPE results in a single round of DNA replication, strictly enforced by destruction of Cdt1

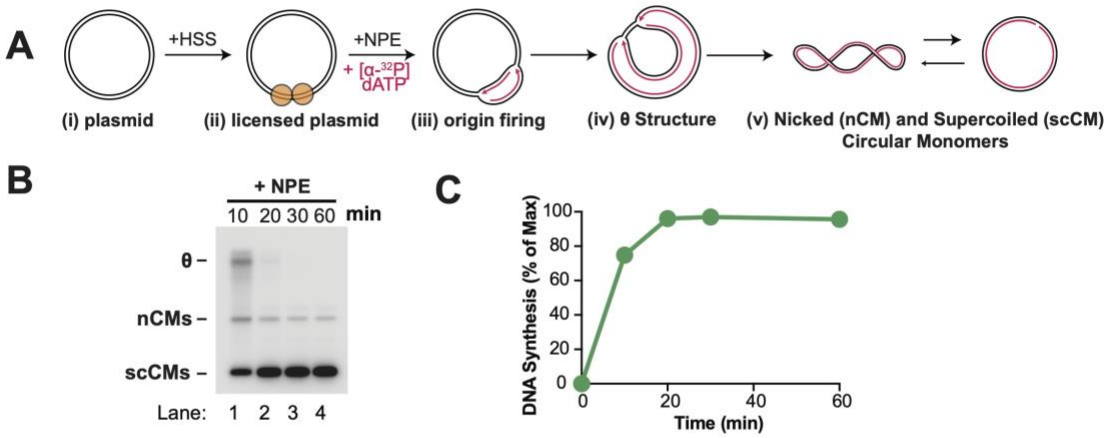

Figure 3.1. Analysis of DNA replication in *Xenopus* egg extracts
(A) Overview of plasmid DNA replication in extracts. (B) Samples from (A) were separated on an agarose gel and visualized by autoradiography. (C) Quantification of total signal from (B).

at the onset of DNA synthesis (Arias & Walter, 2005) (Figure 3.1 (A, i-v)). Replication is visualized by separating radiolabeled plasmids on a native agarose gel (Figure 3.1 (B)) (Kavlashvili & Dewar, 2022). At early timepoints, most of the signal is present as a smear corresponding to different sizes of theta structures (Figure 3.1 (B, lane 1)), an intermediate formed during replication of circular DNA templates. Later, all the signal is present as nicked circular monomers (nCM) and supercoiled circular monomers (scCM), suggesting that every plasmid got fully replicated (Figure 3.1 (B, lanes 2-4)). Overall, the *Xenopus* egg extract system allows for mechanistic analysis of different stages of DNA replication and multiple DNA repair processes.

Triggering NSD in extracts

To determine whether NSD can be triggered in Xenopus egg extracts, we examined the stability of nascent DNA strands after stalling forks. To this end, we replicated plasmid DNA and labeled nascent DNA strands by inclusion of radiolabeled nucleotides (Figure 3.2 (A (i))). We simultaneously pre-radiolabeled a smaller control plasmid and supplemented NPE with it, thereby inhibiting the licensing and replication of the control (Figure 3.2 (A (ii))). Shortly after initiation, we supplemented the reactions with aphidicolin, a small molecule inhibitor of DNA polymerases which induces fork stalling by inhibiting DNA polymerases (Couch et al., 2013; Toledo et al., 2013) and has previously been shown to induce fork reversal and NSD in Xenopus egg extracts (Figure 3.2 (A) (Kolinjivadi et al., 2017). Aphidicolin also mimics the effects of HU, which is the most commonly used reagent to trigger NSD in cells (Higgs et al., 2015; Liu et al.,

2020; Schlacher et al., 2011; Thangavel et al., 2015). In contrast with HU, however, aphidicolin does not induce reactive oxygen species (ROS) accumulation in the nucleus (Somyajit et al., 2021). I will discuss the implications of ROS in NSD in Chapter VIII. In addition, *Xenopus* egg extracts contain high pre-existing pools of nucleotides and thus are insensitive to HU treatment. Samples were withdrawn at different timepoints, purified and digested to remove all topological effects and quantify the total radioactive signal relative to a loading control (Figure 3.2 (B)). In vehicle treated extracts, radioactive signal increased and then plateaued, as expected for completion of single round of replication (Figure 3.2 (C lanes 1-5, D-E). In contrast, signal in aphidicolin treated extracts was reduced by 60 minutes and almost completely absent at 120 minutes, indicating that nascent strands got degraded (Figure 3.2 C lanes 6-10, D-E). This was an interesting observation. In contrast to published studies, we observed that NSD is an immediate response to fork stalling in *Xenopus* egg extracts. We therefore wanted to formally demonstrate that only nascent strands were being degraded and the parental template remained intact to formally demonstrate that NSD is an immediate response to stalling.

To test whether this degradation corresponded to both strands or only nascent strands, and ensure that we were observing true NSD, we radiolabeled the parental strands instead of nascent strands. We again replicated radiolabeled plasmid DNA, without inclusion of free radiolabel in the reaction, and supplemented them with aphidicolin shortly after initiation to stall the forks. We then purified and digested DNA and quantified total radioactive signal against the loading control (Figure 3.3 (A)).

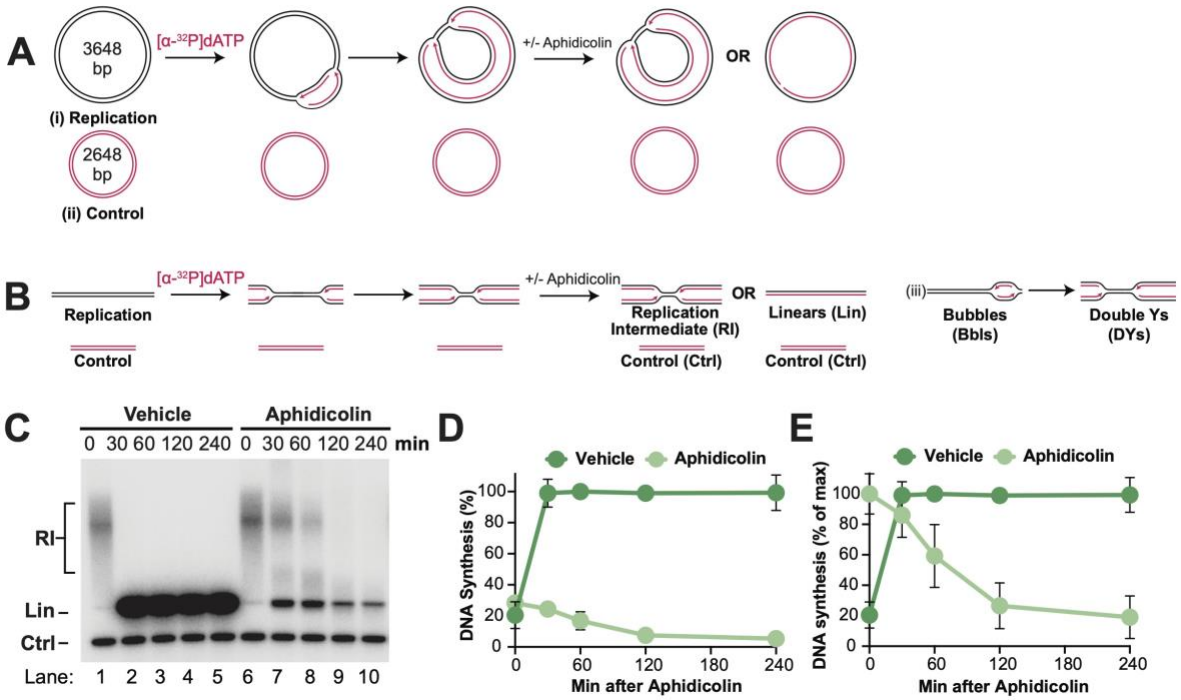

Figure 3.2. Nascent strand degradation is an initial response to fork stalling in extracts

(A) To stall replication forks in vitro, plasmid DNA was replicated using Xenopus egg extracts and newly-synthesized nascent strands were radiolabeled by inclusion of [α-32P]dATP. In this system, plasmid templates replicate semi-synchronously from a single origin per plasmid. 6 minutes after initiation, reactions were treated with aphidicolin, to stall DNA synthesis, or vehicle control. As a loading control (Ctrl) the reactions include a smaller plasmid that was radiolabeled prior to the experiment and did not undergo replication. (B) DNA structures from (d) were purified and digested with XmnI, which cuts the plasmid once. (C) Samples from (e) were separated on an agarose gel and visualized by autoradiography. Time after aphidicolin addition is indicated. (D) Quantification of DNA synthesis from (g) normalized to the maximum signal across all time points and conditions. Mean ± S.D., n=3 independent experiments. (E) Quantification of DNA synthesis in (g) normalized to the maximum signal for each condition across all time points. Mean ± S.D., n=3 independent experiments.

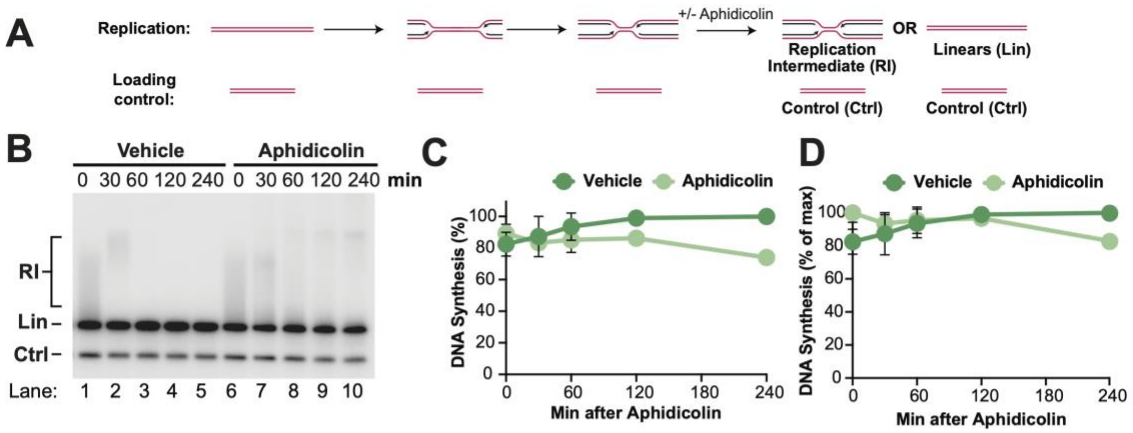

Figure 3.3. Parental strands remain stable during nascent strand degradation
(A) To test whether degradation in Figure 3.2 corresponded to both strands or nascent strands only, pre-radiolabeled plasmid DNA was replicated using Xenopus egg extracts. 6 minutes after initiation, DNA synthesis was inhibited by the addition of Aphidicolin, similarly to Figure 3.2. (B) XmnI digested molecules were separated on an agarose gel and visualized by autoradiography. As a loading control (Ctrl) the reactions include a smaller radiolabeled plasmid that did not undergo replication. (C) Quantification of (B) as in Figure 3.2 (D). Mean ± S.D., n=3 independent experiments. (D) Quantification of (B) as in Figure 3.2 (E). Mean ± S.D., n=3 independent experiments.

Parental strand signal was relatively stable with only a small difference between aphidicolin and vehicle treatment, suggesting that degradation we observed corresponded to NSD (Figure 3.3 (B-D). Our data show that NSD occurs rapidly after fork stalling and thus is an initial response to fork stalling in vertebrates.

NSD is an initial response to fork stalling in human cells

We were surprised by our observation that NSD occurs so rapidly after aphidicolin addition (Figures 3.2 & 3.3). Our data suggests that in extracts, NSD is an immediate and first response to fork stalling. In cells, however, NSD occurs in either fork protection deficient cells (Cortez, 2019; Costanzo, 2011; Liu et al., 2020; Przetocka et al., 2018b; Rickman et al., 2020; Schlacher et al., 2011) or after prolonged high dose HU treatment (Thangavel et al., 2015). In fact, HU is the most commonly used genotoxin to stimulate NSD in cells. HU induced NSD is thought to be a consequence of fork stalling. However, recent literature has shown that HU also induces formation of ROS (Somyajit et al., 2017). ROS were reported to be required for NSD(Somyajit et al., 2021). Therefore, we wanted to test whether NSD took place in human cells following the treatment with aphidicolin, which induces fork stalling by inhibiting DNA polymerases, but does not induce oxidative stress (Somyajit et al., 2021). In order to measure NSD in human cells, we used the DNA fiber labeling approach. This approach includes pulsing cells with two halogenated nucleotide analogs which are incorporated into DNA during elongation and subsequently fluorescently labeled to measure tract lengths as a proxy for length of nascent strands. Importantly, fiber labeling assay does

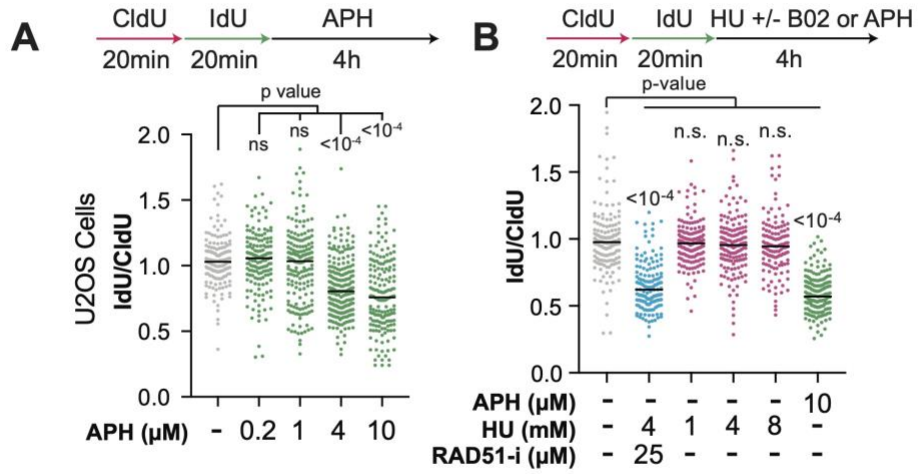

Figure 3.4. NSD is an initial response to fork stalling in human cells (A) U2OS cells were pulse-labeled with CldU then IdU followed by treatment with the indicated concentrations of aphidicolin so that loss of the IdU labeled tracks could be monitored as a measurement of NSD. DNA fiber analysis was performed to determine the lengths of CldU and IdU labeled DNA tracks in each condition. (B) U2OS cells were pulse labeled with CldU and IdU, then treated with the indicated concentrations of aphidicolin, hydroxyurea (HU) and B02. DNA fiber analysis was performed to determine the lengths of CldU and IdU labeled DNA tracks in each condition. Experiments in Figure 3.4 were performed by Wenpeng Liu.

not offer the resolution to distinguish between leading versus lagging strand degradation and rather shows when both or neither of the strands are degraded (Figure 1.5 (B)). U2OS cells were pulse-labeled with CldU then IdU followed by treatment with the indicated concentrations of aphidicolin so that loss of the IdU labeled tracks could be monitored as a measurement of NSD. We found that increasing doses of aphidicolin, induced NSD in human cells (Figure 3.4 (A)). This data suggests that fork stalling by aphidicolin is sufficient to trigger NSD in U2OS cells without inactivation of any fork protection proteins or induction of oxidative stress. Interestingly, aphidicolin induced NSD in a dose-response manner with 4 μM and above concentrations being sufficient to trigger NSD. We then measured NSD side by side using HU alone, HU in conjunction with RAD51-I B02 as a positive control and aphidicolin. Co-addition of the RAD51-I B02 with HU has previously shown to trigger NSD, as the B02 treatment inactivates fork protection. As expected, HU+B02 treatment led to extensive NSD, as previously shown (Taglialatela et al., 2017). In contrast, increasing concentrations of HU did not result in any detectable NSD, which is consistent with previous literature showing that HU alone in fork protection proficient settings leads to limited degradation (Thangavel et al., 2015). 10 μM Aphidicolin treatment however led to the same level of NSD as HU treatment and the RAD51-I addition (Figure 3.4 (B)). These data show that fork stalling by aphidicolin alone, without imposing any metabolic stress on cells, leads to extensive NSD as is observed in fork protection deficient cells under genotoxic stress.

This exciting finding that NSD is an immediate response to fork stalling in *Xenopus* egg extracts, that we recapitulated in human cells prompted us to develop an

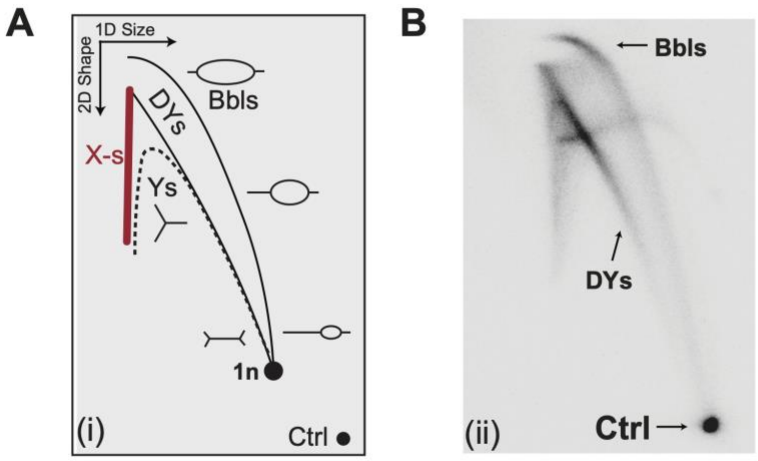

Figure 3.5. 2-D Gel analysis of early replication structures
(A) 2-D gel schematic of replication structures. (B) DNA structures from Figure 3.2 (B, lane 1) were purified and digested with XmnI, which cuts the plasmid once, separated by 2-D gel electrophoresis and visualized by autoradiography.

in vitro system in extracts to mechanistically dissect NSD. As I previously mentioned, cellular approaches of measuring NSD such as fiber labeling assays do not offer the high temporal and spatial resolution that is necessary to understand key mechanistic details about this process. We sought to develop a system that would allow us to study NSD by monitoring the entire population of forks over time and measuring both signal intensity and the shape of DNA molecules undergoing resection and remodeling. To this end we designed a synchronous, biochemical approach to study NSD in *Xenopus* egg extracts, which I describe in more detail below.

A synchronous biochemical approach to study NSD

Our approach to stall forks shortly after initiation resulted in a heterogenous population of replication forks that were replicated to different extents and stalled at different locations as demonstrated by a smear of thetas throughout the lane (Figure 3.2 (C, lane 1)). To formally demonstrate that the population of forks at early timepoints was extremely heterogenous, we purified and digested replication intermediates and analyzed them by 2-D gel electrophoresis. This method allowed us to monitor the size and shape of replication intermediates and distinguish between Double-Ys, Bubbles that arise from origin firing events, as well as control linear plasmid. When we analyzed the 2-D gel, we found that the signal was distributed throughout the Double-Y and Bubble arcs, corresponding to some forks just initiating replication and others being farther along, demonstrating heterogeneity (Figure 3.5 A-B).

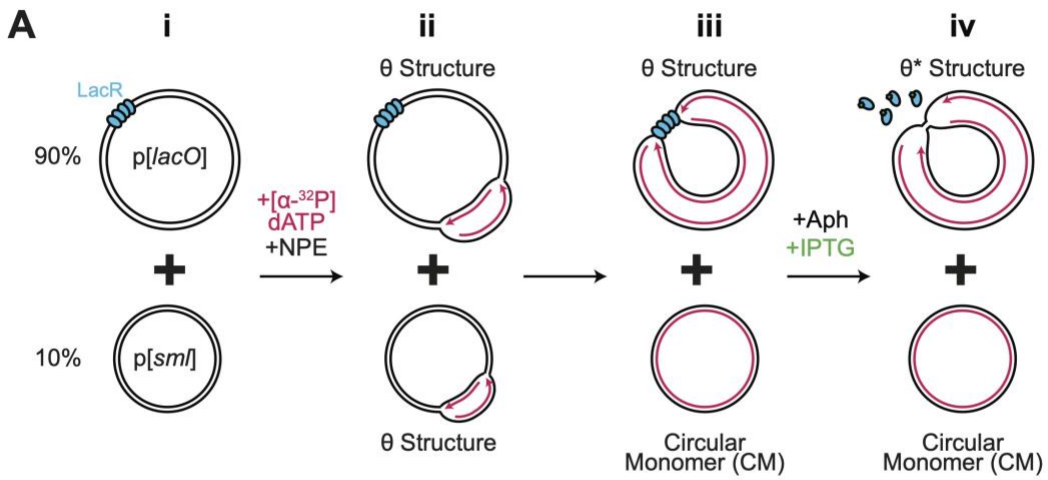

Figure 3.6. Schematic of triggering synchronous and localized uncoupling

(A) A schematic of plasmid DNA harboring a LacR array and a control plasmid without a LacR array being replicated using Xenopus egg extracts and subsequent induction of uncoupling by aphidicolin and IPTG treatment.

In order to carefully monitor NSD with high temporal and spatial resolution, we needed to come up with a way to synchronize replication forks. To this end, we utilized a site-specific reversible replication barrier (Dewar et al., 2015). We pre-incubated a plasmid containing Lac operator sequences (*lacO)* with Lac Repressor (LacR) and then replicated it in *Xenopus* egg extracts (Figure 3.6 (A, i-ii)). This approach allows replication forks to arrest at both sides of the LacR barrier, thereby synchronizing them. When forks arrive at the LacR array, this gives rise to a θ structure, as expected(Figure 3.6 (A, iii)). To induce uncoupling – forks arrested at the LacR array were treated with aphidicolin and reactions were simultaneously supplemented with IPTG to disrupt the LacR array and allow uncoupling of the replicative helicase, as it occurs when HU is used in cells (Figure 3.6 (A, iv)). Upon aphidicolin and IPTG treatment, θs were converted to θ* structures (Figure 3.7 (B, lanes 1-2)). These structures arose from reannealing of unwound parental DNA strands in detergent treated samples and the mobility shift of θs to θ*s shows that uncoupling occurred (Figure 3.7 (A,iii-iv)). We confirmed that the mobility shift corresponds to uncoupling by digesting θs and θ*s with Topoisomerase II alpha (Top2) which removes catenanes (Figure 3.7 (D)). While θs were unaffected by Top2 treatment, θ*s shifted back up to the original mobility, suggesting that mobility shift occurred due to compensatory catenane formation after uncoupling (Figure 3.7 (D, lanes 1-3, 2-4)). These data demonstrate that we have developed a system to trigger site specific uncoupling.

To remove any topological effects and definitively identify replication fork structures, we purified the DNA and performed restriction digest to visualize replication

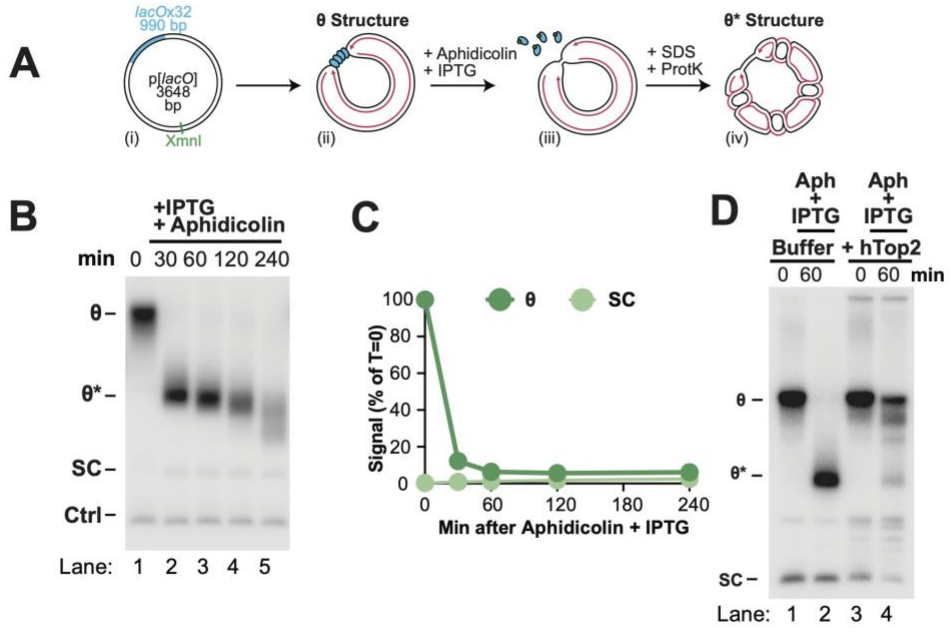

Figure 3.7. Induction of synchronous and localized nascent strand degradation

(A) Plasmid DNA harboring a LacR array was replicated using Xenopus egg extracts and dATP[α-32P] was added to label newly-synthesized DNA strands. Once forks were localized at the LacR barrier, replication was restarted by addition of IPTG, which removed the LacR barrier, and replication forks were stalled by addition of aphidicolin. (B) Samples from (A) were separated on an agarose gel and visualized by autoradiography. As a loading control (Ctrl) the reactions include a fully-replicated plasmid. (C) Quantification of θ structures and supercoiled monomers (SC) from (b). Mean ± S.D., n=3 independent experiments. (D) DNA structures from (A) were treated with human topoisomerase II (hTop2) or buffer control, then separated on an agarose gel and visualized by autoradiography.

fork structures (Figure 3.8 (A)). This method allowed us to visualize Double-Ys and linear replication products over time and measure their abundance to the levels of the loading control. Double-Ys disappeared over time without any appreciable increase in linear products of replication, suggesting that nascent DNA strands got degraded (Figure 3.8 (B)). Accordingly, the majority of the nascent DNA signal was lost (Figure 3.8 (C)). Collectively, these results show that we have developed a synchronous biochemical approach to induce NSD. In the next chapter, I will validate that the NSD we observed in extracts involves the same nuclease and fork remodeling events as previously described in the literature.

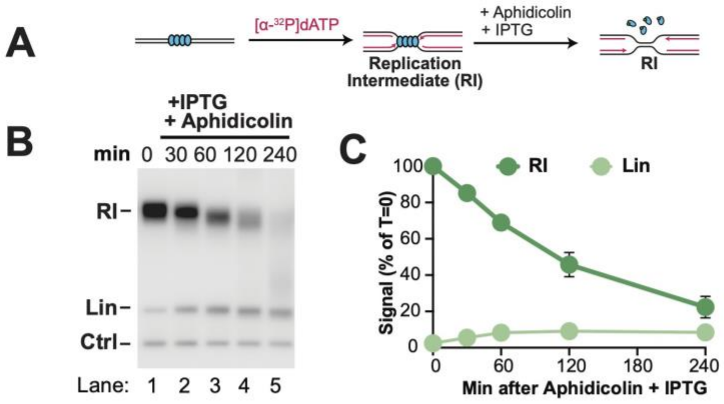

Figure 3.8. Visualization of nascent strand degradation in extracts

(A) Samples from Figure 3.9 (A) were digested with XmnI to allow unambiguous identification of replication intermediates (RIs) and linear products of replication (Lin). (B) Samples from (A) were separated on an agarose gel and visualized by autoradiography. (C) Quantification of RI and Lin structures in (B). Mean ± S.D., n=5 independent experiments.

CHAPTER IV

NSD INVOLVES DNA2 EXONUCLEASE AND FORK REVERSAL

Introduction

In a previous chapter, I describe how I have developed an *in vitro* system to study NSD in *Xenopus* egg extracts. All previous modes of NSD that have been described in the literature involve either DNA2 or MRE11 nucleases, as well as replication fork remodeling into reversed forks. These enzymes canonically function during DSB repair where MRE11 initiates resection and DNA2 carries out long-range resection (Paudyal et al., 2017). In this chapter, I will describe how we validated that the NSD we are observing corresponds to the NSD that has been previously described in the literature and involves the same factors and molecular events.

NSD involves the DNA2 exonuclease in extracts

NSD that has been described in the literature typically involves DNA2 or MRE11 exonucleases (Figure 4.1 (A)). To determine which exonuclease was involved in the NSD we observed, we used small molecule inhibitors C5 (DNA2-i) and Mirin (MRE11-i)

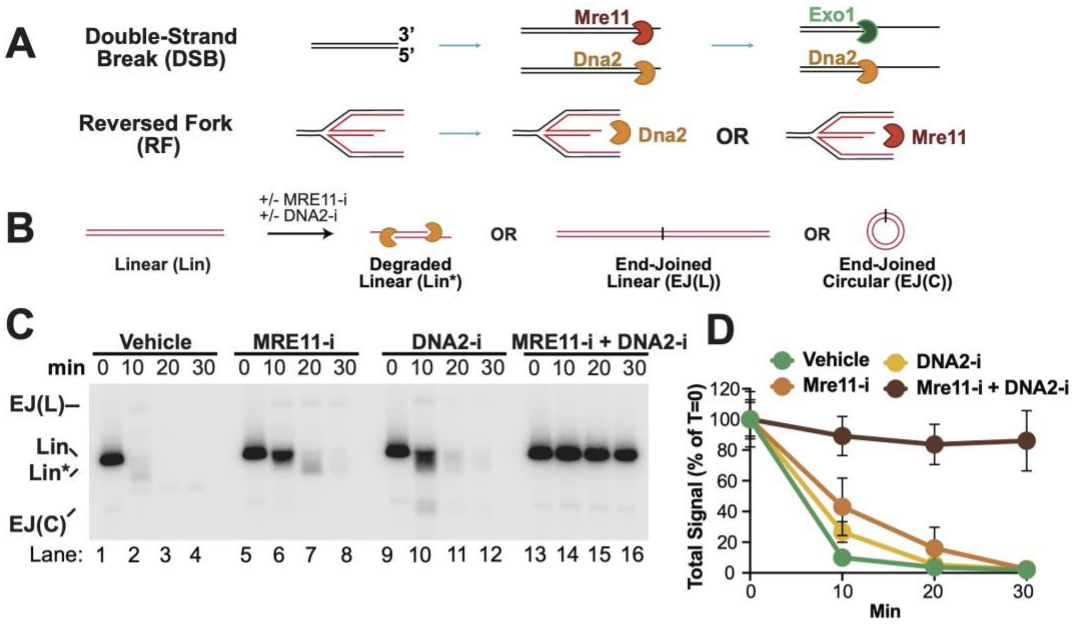

Figure 4.1. Characterization of MRE11 and DNA2 activities during NSD

(A) Cartoon depicting the roles of MRE11 and DNA2 in resection at double-strand breaks and reversed forks. (B) Cartoon of linear radiolabeled DNA incubated in Xenopus egg extracts in the presence of MRE11 inhibitor (MRE11-i) or DNA2 inhibitor (DNA2-i) or both. (C) Samples from (B) were separated on an agarose gel and visualized by autoradiography. (D) Quantification of total signal from (C). Mean ± S.D., n=3 independent experiments.

inactivating their targets, we first targeted DNA2 and MRE11 during DSB resection,

which involves both of these enzymes in egg extracts and is blocked by simultaneously inactivating both nucleases (Figure 4.1 (A)). We first radiolabeled and subsequently linearized plasmid DNA to generate a linear substrate for resection (Figure 4.1 (B)). Then we incubated linear radiolabeled DNA in *Xenopus* egg extracts and monitored their degradation, as a read-out for the extent of resection (Figure 4.1 (C)). In vehicle treated extracts, the control linear substrate was rapidly degraded, as expected. We also observed several additional products that arose from end-joining of resected molecules. The combined treatment with DNA2-I and MRE1-I almost completely blocked resection, while individual addition of these inhibitors partially inhibited resection, as expected (Figure 4.1 (D)). This assay demonstrated that both DNA2-I and MRE1-I were able to efficiently block their targets in *Xenopus* egg extracts.

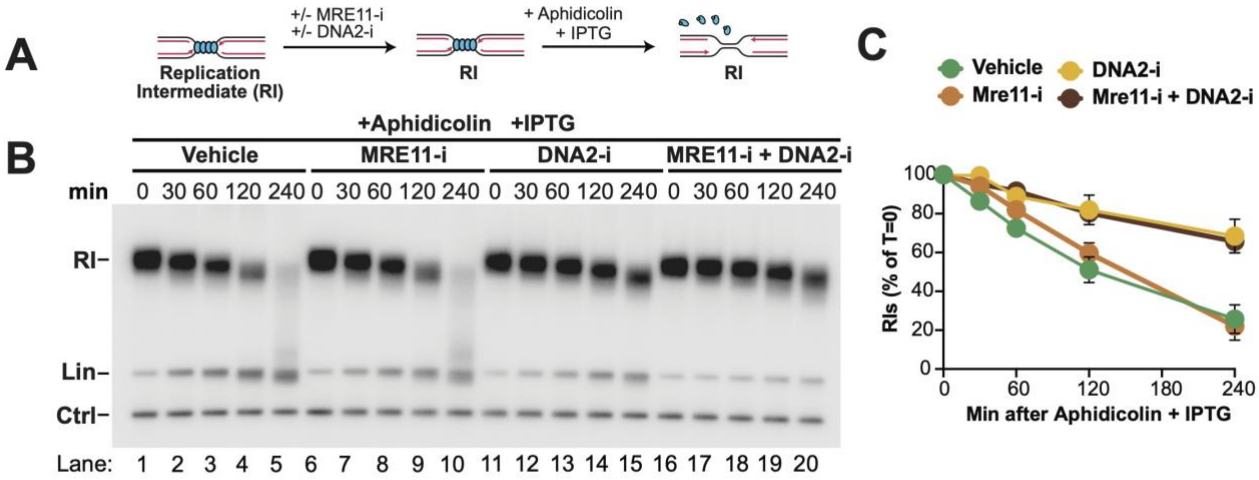

Figure 4.2. Nascent strand degradation involves DNA2 but not MRE11 in extracts

(A) Forks were localized to a LacR barrier and NSD was induced by addition of IPTG and aphidicolin in the absence or presence of MRE11-i and DNA2-i. Purified DNA was subjected to restriction digest so that replication fork structures could be visualized as RIs. (B) Samples from (A) were separated on an agarose gel and visualized by autoradiography. (C) Quantification of RI signal from (b). Mean ± S.D., n=3 independent experiments.

presence of either MRE11-I, DNA2-I or both. We replicated plasmid DNA containing LacR Array in the presence of radionucleotides to label the daughter strands and then induced uncoupling by addition of IPTG and aphidicolin. Simultaneously we either included Vehicle, MRE11-I, DNA2-I or both. We then purified and digested the DNA to identify Double-Ys (Figure 4.2 (A)). In Vehicle treated extracts, we observed efficient NSD. DNA2-I treatment blocked the majority of NSD while MRE11-I treatment has little to no effect either alone, or in combination with DNA2-I (Figure 4.2 (B-C)). These data suggest that NSD involves DNA2 exonuclease in *Xenopus* egg extracts.

Next we wanted to ensure that neither inhibitor inhibited uncoupling. To this end, we performed the same experiment but we did not digest NSD intermediates and separated them on the agarose gel (Figure 4.3 (A)). We observed that neither inhibitor prevented uncoupling (Figure 4.3 (B)). Collectively, these data show that NSD we observe involved DNA2 but not MRE11, consistent with previously published literature.

NSD involves the DNA2 exonuclease in human cells

Since aphidicolin alone has never been reported to induce NSD in cells, we decided to also investigate whether DNA2 had a role in aphidicolin induced NSD in cells. To this end, we treated U2OS cells with siRNAs against MRE11 and DNA2 and both. Subsequently, we treated cells with aphidicolin and monitored NSD by DNA fiber

labeling analysis. We observed that siRNA knockdown of DNA2, but not MRE11 rescued NSD, as expected based on our data in *Xenopus* (Figure 4.4 (A)). We then validated our siRNA knockdown results with the same small molecule inhibitors we used in extracts. Aphidicolin treated U2OS cells experienced rampant NSD as expected, which was rescued by DNA2-I but not MRE11-I, as expected based on our previous results (Figure 4.4 (B)). Importantly, as a control we treated cells with HU + B02 to trigger NSD in the absence of fork protection which is mediated by MRE11 nuclease. As expected, MRE11-I blocked NSD in this setting (Figure 4.4 (B)). Collectively, our data show that in both *Xenopus* egg extracts and human cells, NSD that is triggered by aphidicolin involves DNA2 exonuclease.

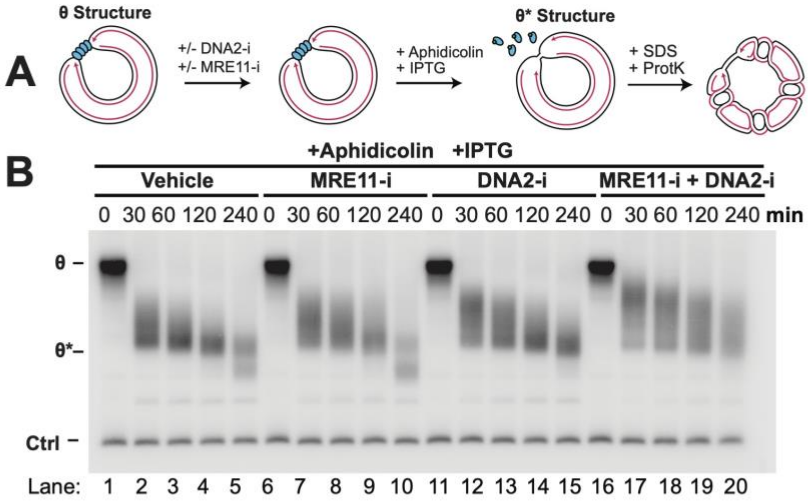

4.3. DNA2 and MRE11 inhibitors do not inhibit uncoupling
(A) Forks were localized to a LacR barrier and NSD was induced by addition of IPTG and aphidicolin in the absence or presence of MRE11-i and DNA2-i. (B) Samples from (A) were separated on an agarose gel and visualized by autoradiography.

NSD involves fork remodeling

We next wanted to examine other aspects of NSD. NSD typically involves replication fork reversal (Bhat & Cortez, 2018; Kolinjivadi et al., 2017; Schlacher et al., 2011; Thangavel et al., 2015; Zellweger et al., 2015). To test whether this was also the case in our experiments, we triggered uncoupling as previously described, purified and digested the DNA and performed 2-D gel electrophoresis in order to monitor different DNA structures formed during NSD (Figure 4.5 (A)). 2D gel electrophoresis separates DNA structures based on their relative size and shape, allowing to distinguish various replication intermediates such as bubbles that arise from origin firing, double-ys which represent canonical replication forks, linear replication products as well as repair intermediates such as holliday junctions, hemicatenanes, reversed forks etc (Figure 4.5 (B)). At early timepoints, radiolabeled DNA signal was broadly distributed throughout the bubble and double-y arcs, due to initiation of replication throughout the plasmid (Figure 4.5 (B(i))). When replication forks arrested at the LacR barrier and before induction of NSD, majority of the signal was present as a discrete spot on the double-Y arc, corresponding to forks localized to the barrier (Figure 4.5 (B(ii))). Interestingly, we also observed a small population of forks that did not represent canonical fork structures and corresponded to remodeled forks. After NSD was induced, abundance of Double-Ys rapidly declined while remodeled forks increased ~3 fold, indicating that Double-ys were being converted to remodeled forks (Figure 4.5 (B(iii))). Importantly, the frequency of

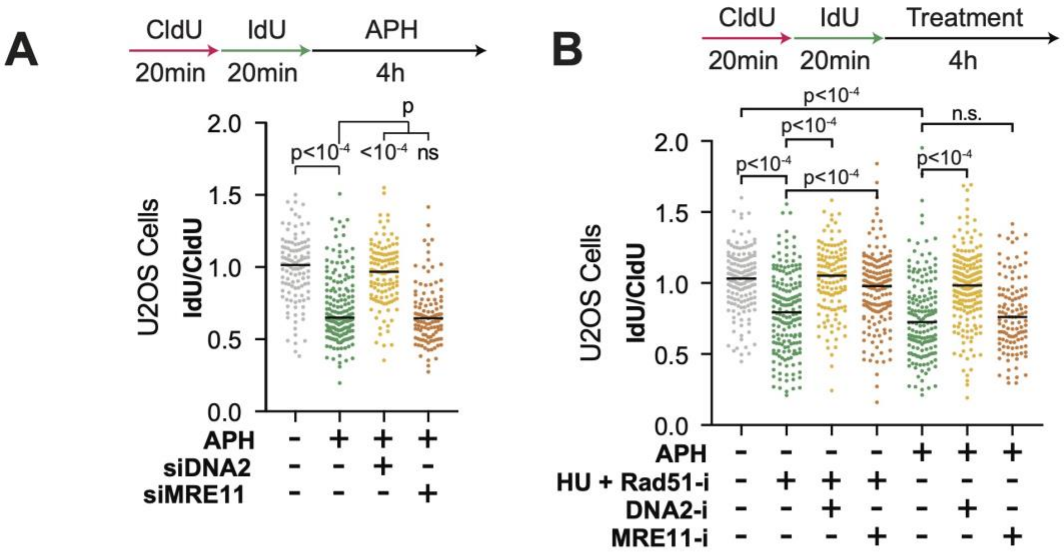

Figure 4.4. Nascent strand degradation involves DNA2 but not MRE11 in cells

(A) U2OS cells were transfected with the indicated siRNA, pulse labeled with CldU and IdU, then treated with aphidicolin. DNA fiber analysis was performed to determine the lengths of IdU and CldU labeled DNA tracks in each condition. (B) U2OS cells were pulse labeled with CldU and IdU, then treated with either aphidicolin, or hydroxyurea combined with RAD51-i. MRE11-i, DNA2-i, or vehicle control were also added, as indicated. DNA fiber analysis was performed to determine the lengths of IdU and CldU labeled DNA tracks in each condition. Experiments in Figure 4.4 were performed by Wenpeng Liu.

to remodeled forks. Additionally, the mobility of both structures decreased over time,

indicating that both structures included partially degraded molecules (Figure 4.5 (B(iv))). Thus, we observed that NSD causes progressive remodeling of replication forks (Figure 4.5 (C)). These data show that canonical replication forks undergo some form of remodeling throughout NSD, but it does not definitively show that fork reversal is taking place.

Migration of remodeled forks did not correspond to canonical Holliday junctions or hemicatenanes and is potentially consistent with fork reversal (Figure 4.6 (A, i-ii)). However, here we are observing two forks simultaneously. Migration patterns of two forks where one or both of the forks are reversed are not well documented in the literature. In addition, one of the forks could represent a D-loop or a hemicatenane and migrate as a remodeled fork. From this data it is unclear whether remodeled forks correspond to reversed forks. In order to formally identify the identity of the remodeled forks, we used two independent approaches outlined below.

Remodeled forks correspond to reversed forks

Previous approach of monitoring remodeling fork structures on 2D gels included Double-Y structures where each molecule contains 2 forks. DNA structures resulting from reversal of one or both of the forks of a Double-Y molecule are currently undefined so a clear assignment could not be made. Furthermore, remodeled forks could in

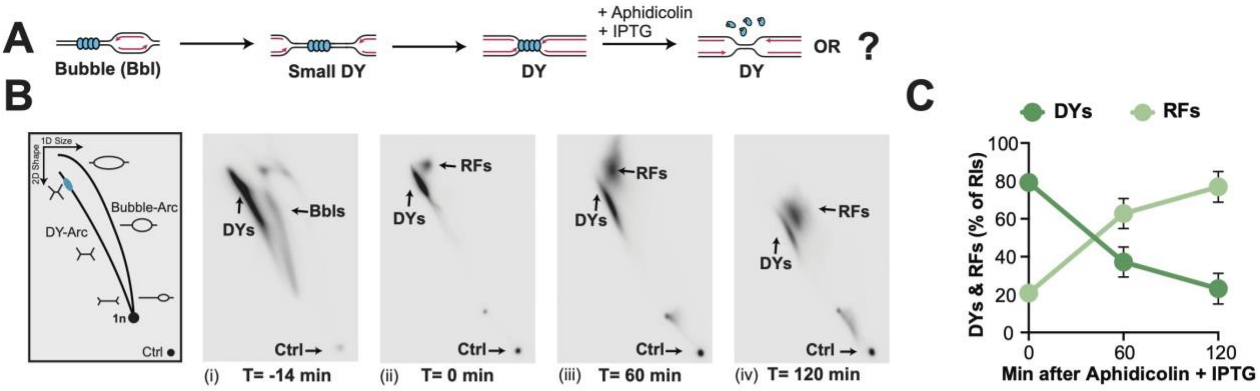

Figure 4.5. Nascent strand degradation involves fork remodeling
(A) Cartoon depicting the different DNA structures formed during replication of plasmid DNA harboring a LacR array and induction of NSD. The structures depicted arise from restriction digest using an enzyme that cuts the plasmid template once. (B) 2-D gel migration pattern of the DNA structures depicted in (A). The blue spot on the Double Y-arc (DY-arc) indicates the expected migration of DY structures localized to the LacR array. DNA structures from (A) were analyzed by 2-D gel electrophoresis and visualized by autoradiography. T=0 is the point at which IPTG and aphidicolin were added. DY, bubble (Bbl), and remodeled fork (RF) structures are indicated. (C) Quantification of DY and RF structures from (B) as a percentage of replication intermediates (RIs) at each time point. Mean ± S.D., n=3 independent experiments.

both forks. In order to definitively identify the identity of remodeled forks, first we tested whether they corresponded to four-way junctions, consistent with fork reversal. To examine this, we treated the Double-Y and remodeled fork species with RuvC enzyme, which cleaves reversed forks and Holliday junctions, but not hemicatenanes or other replication fork structures. RuvC treatment has essentially no effect on Double-Y structures, as expected, but reduced the abundance of remodeled forks by ~5-fold (Figure 4.7 A-B). This data shows that remodeled forks contain four-way junctions and thus either correspond to reversed forks or replication forks followed by a Holliday junction i.e. D-loops.

To further distinguish between these possibilities, we took advantage of the fact that migration pattern of reversed forks and D-loops during 2-D gel electrophoresis is well defined for molecules that contain only a single fork structure. We therefore utilized a different plasmid with a second restriction digest site in the middle of the LacR array. We treated NSD intermediates with a pair or restriction enzymes to yield two replication forks of differing sizes that could be separated by gel electrophoresis (Figure 4.8 (A)). This approach allowed us to detect the large fork only and thus determine whether remodeled forks correspond to reversed forks. We induced NSD as previously described, purified and digested DNA to yield two forks and separated them on 2-D gels (Figure 4.8 (B)). Shortly after initiation, signal was distributed between bubble and Y-arcs, due to initiation of replication throughout the plasmid (Figure 4.8 (C(i))). Immediately prior to NSD, most signal was present as a discrete spot on the Y arc,

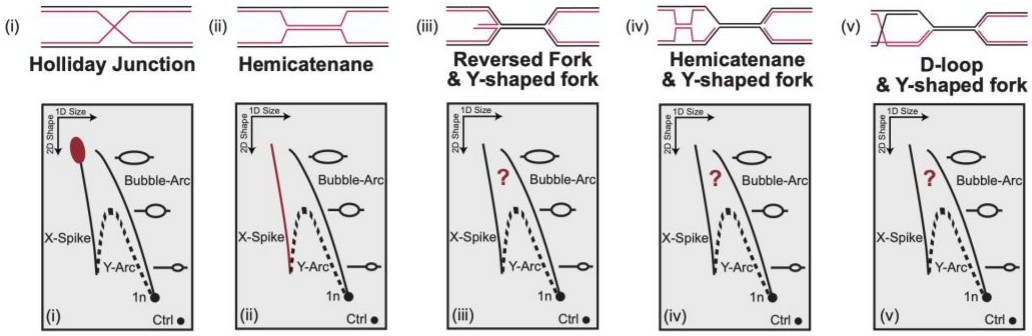

Figure 4.6. Schematic of how different DNA replication and repair intermediates migrate on 2-D gels

forks was observed immediately prior to NSD. Importantly, this species migrated mid-way down the X spike in the expected position for a reversed fork and not along the Y-arc, as would be expected for a D-loop. Surprisingly, this species did not increase in abundance during NSD in contrast to the remodeled forks observed previously. Instead, we observed two additional species during NSD that also migrated along the X-spike with a similar mobility to reversed forks (Figure 4.8 (C(iii))). These species almost completely disappeared following DNA2-i treatment, which also led to a corresponding increase in RF signal (Figure 4.8 (C(iv))). Thus, during NSD reversed forks are generated that are normally degraded by DNA2. Overall, these data show that NSD induced by our approach involves progressive conversion of replication forks to reversed forks, which are then degraded by DNA2. Collectively, these data validate that NSD we are observing corresponds to NSD that is physiologically relevant and occurs in cells. Furthermore, the new approaches of monitoring NSD gives us more mechanistic insight into this process and allows us to answer questions posed by the current models.

Requirements for fork remodeling enzymes

We next wanted to test whether fork reversal is involved in aphidicolin induced NSD we had observed in cells. We therefore tested the role of canonical fork reversal enzymes. To this end, U2OS cells were treated with siRNA targeting SMARCAL1, ZRANB3, HLTF, FBH1, and PICH and then DNA fiber analysis was performed to monitor and measure NSD. siRNA knockdown of SMARCAL1, FBH1 and PICH reduced

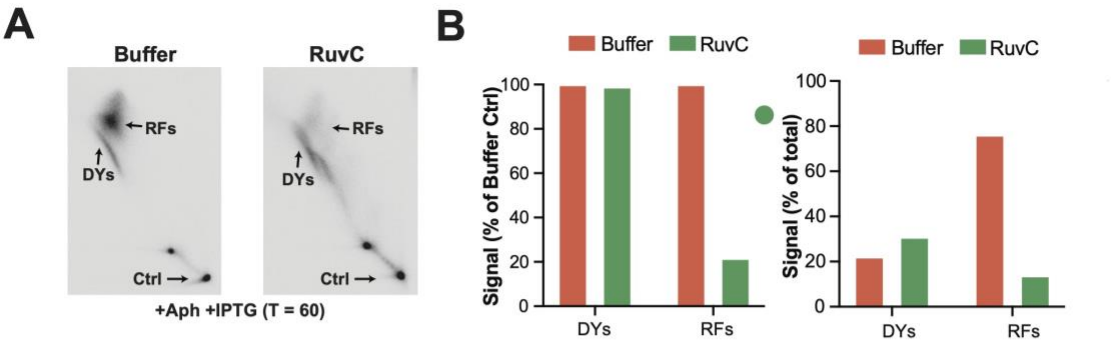

Figure 4.7. Remodeled forks are four-way junctions
(A) Samples from Figure 4.5 were treated with buffer or RuvC and analyzed by 2-D gel electrophoresis. (B) Quantification of DYs and RFs following RuvC treatment in (A) expressed relative to the abundance of each structure in the buffer treated condition and as relative to total signal on each gel.

human cells (Figure 4.9 (A)). Interestingly, knockdown of ZRANB3 and HLTF did not affect NSD. This is surprising because these enzymes have always been reported to cooperate with SMARCAL1 to carry out fork reversal in other NSD contexts.

To test this observation in extracts, we immunodepleted SMARCAL1 and cross validated the depletion with a published antibody that has previously shown to interfere with fork reversal (Figure 4.10 (A)). Then we triggered NSD in mock versus SMARCAL1 depleted extracts (Figure 4.10 (B)). To our surprise, NSD in *Xenopus* egg extracts did not involve SMARCAL1, suggesting that other fork reversal enzymes might operate (Figure 4.10 (C-D)). We therefore conclude that aphidicolin induces NSD and fork reversal in human cells and *Xenopus* egg extracts but not that in extracts only a subset of cellular pathways might operate. Further studies are needed to identify which of the cellular pathways operate in extracts during NSD. I will expand upon this topic in the discussion in Chapter VIII.

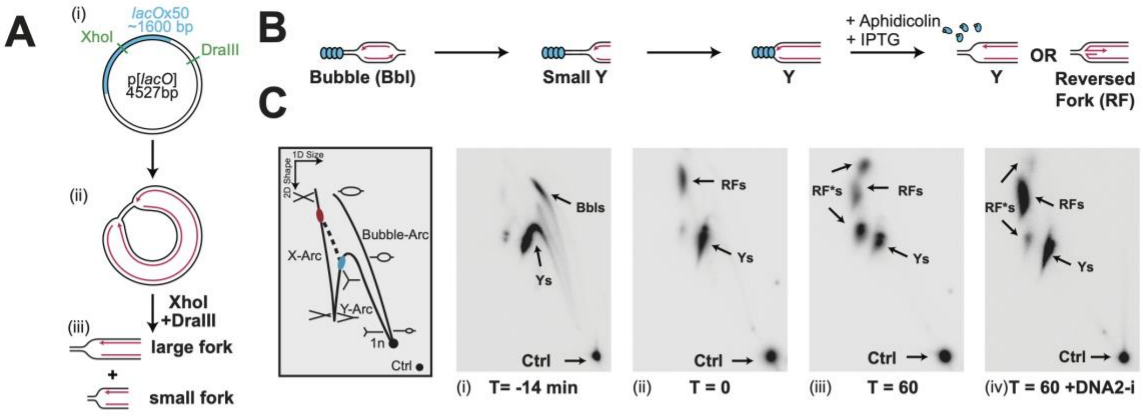

Figure 4.8. Remodeled forks migrate as reversed forks
(A) An approach to analyze a single fork by 2-D gel electrophoresis. (B) Cartoon depicting the same structures in Figure 4.5 after restriction digest using two different enzymes to release a single large fragment. (C) 2-D gel migration pattern of the DNA structures depicted in (B).The blue spot on the Y-arc indicates the expected migration of Y structures localized to the LacR array. The red spot indicates the expected migration of reversed fork structures arising from the Y structures within the black spot. DNA structures from (B) were analyzed by 2-D gel electrophoresis and visualized by autoradiography.

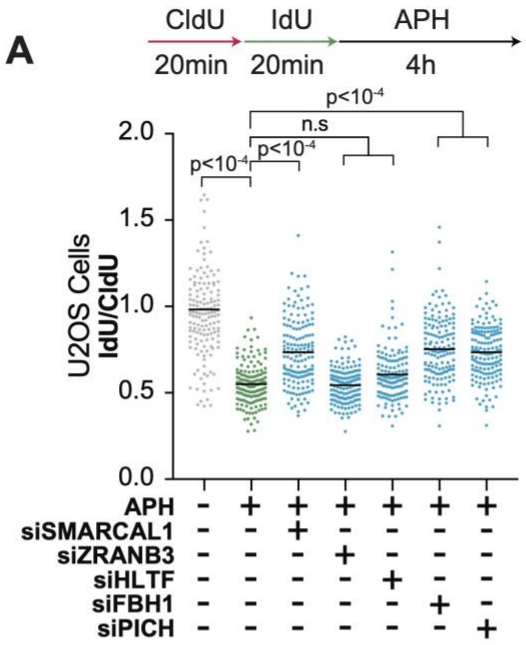

Figure 4.9. Requirement for fork remodeling enzymes in cells
(A) U2OS cells were transfected with the indicated siRNA. 72 hours later cells were pulse labeled with CldU and IdU, then treated with aphidicolin. DNA fiber analysis was performed to determine the lengths of CldU and IdU labeled DNA tracks in each condition. Experiment in Figure 4.9 was performed by Taha Mohamed.

CHAPTER V

UNCOUPLING TRIGGERS NSD AND FORK REVERSAL

Introduction

In previous chapters, I described the development and validation of the *in vitro* synchronous system to study NSD in *Xenopus* egg extracts. In chapter V, I will use the previously defined and validated approach to answer some key mechanistic questions that current models pose about NSD and fork reversal and uncover novel findings. First, we sought to identify the molecular trigger for NSD. Although it has been hypothesized that uncoupling leads to NSD, uncoupling also rapidly leads to helicase slowing (Graham et al., 2017; Sparks et al., 2019) and stalling. Therefore, stalling of the replicative helicase rather than uncoupling *per se* could be a trigger for NSD. In this chapter I describe an approach to distinguish between stalled and uncoupled forks and identification of the trigger for NSD and fork reversal in *Xenopus* egg extracts.

Both Strands are degraded

NSD in cells involves degradation of both nascent leading and lagging strands. This is evident from the complete disappearance of the nascent DNA tract in response

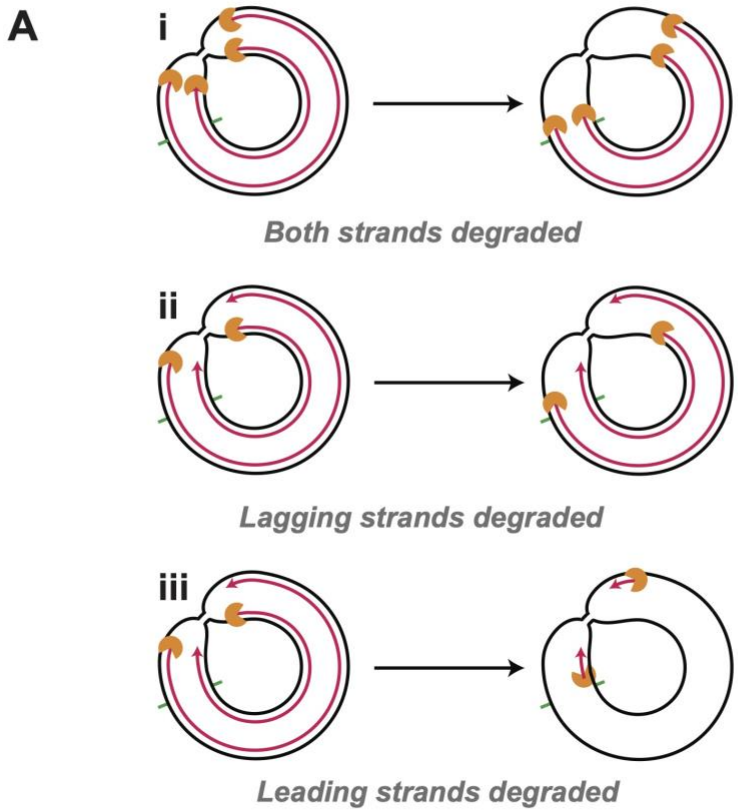

Figure 5.1. Schematic of nascent strand degradation of both, leading or lagging strands only.
(A) Depiction of different models for degradation of leading and lagging strands during NSD.

appear intact. We wanted to test whether this was the case in our in vitro *Xenopus* egg extract system as well. To this end, we used an approach outlined below. We digested and subsequently separated NSD intermediates on a denaturing gel, separately monitoring the nascent strands from the large fork and the small fork. This model outlines different possible outcomes from this experiment (Figure 5.1). In (i) both leading and lagging strand are degraded simultaneously and synchronously, which should result in disappearance of RWS before LWS. In (ii) lagging strands only are degraded synchronously, which should result in persistence of ~50% of RWS and LWS until the leading strand are degraded by nuclease activity that initiated at lagging strands of the opposite fork. This would result in biphasic kinetics of degradation. In (iii) lagging strands only are degraded asynchronously, which should result in loss of RWS and LWS at the same rate.

To test which one of these outcomes was the case in our in vitro *Xenopus* egg extract system, NSD DNA intermediates were purified, restriction digested and then separated on an agarose gel under denaturing conditions (Figure 5.2 (A)). This approach allowed us to get a very high sensitivity read out and monitoring of intact nascent strands (Kavlashvili & Dewar, 2022). This served as a more direct read out for the onset of NSD rather than measurement of the total Double-Y signal. Upon addition of IPTG and aphidicolin, intact nascent strands were readily lost and degraded strands could be visualized (Figure 5.2 (B)). The disappearance of essentially all intact strands

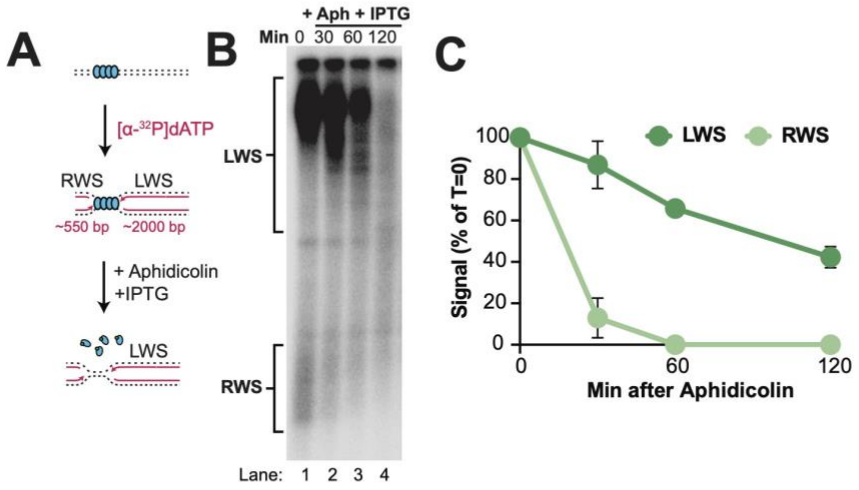

Figure 5.2. Both strand are degraded
(A) Forks were localized to a LacR barrier and aphidicolin was added in the absence or presence of IPTG. Purified DNA was restriction digested to yield leftward strands (LWS) and rightward strands (RWS) of different sizes. (B) Samples from (A) were purified and separated on an alkaline denaturing agarose gel and visualized by autoradiography. (C) Quantification of LWS and RWS as a % of signal at T=0. Mean ± S.D., n=3 independent experiments.

indicated that both leading and lagging strands were being degraded. Further analysis of both nascent strands confirmed that both strands were degraded (Figure 5.2 (C)).

Thus NSD we observe involves degradation of both nascent strands, as previously reported in the literature.

Approach to inhibit uncoupling

Next we wanted to identify the precise molecular trigger for NSD. Fork stalling by aphidicolin results in both uncoupling of the replication fork and helicase stalling. Therefore, it's unclear whether it's the stalling of the replicative helicase or physical uncoupling of the polymerase and helicase activities that is a molecular trigger for NSD and fork reversal. To directly test this, we took advantage of the LacR barrier. While aphidicolin stalls the polymerases, helicase uncoupling is facilitated by IPTG. Therefore, we decided to withhold IPTG from one of the reactions, thereby inhibiting helicase uncoupling (Figure 5.3). This approach allows us to separately monitor stalled versus uncoupled replication forks.

Uncoupling elicits the onset of NSD

To formally demonstrate whether stalling or uncoupling causes NSD, we used the approach outlined above. We localized forks to the LacR barrier, added aphidicolin and either added or omitted IPTG to facilitate or inhibit uncoupling, respectively (Figure

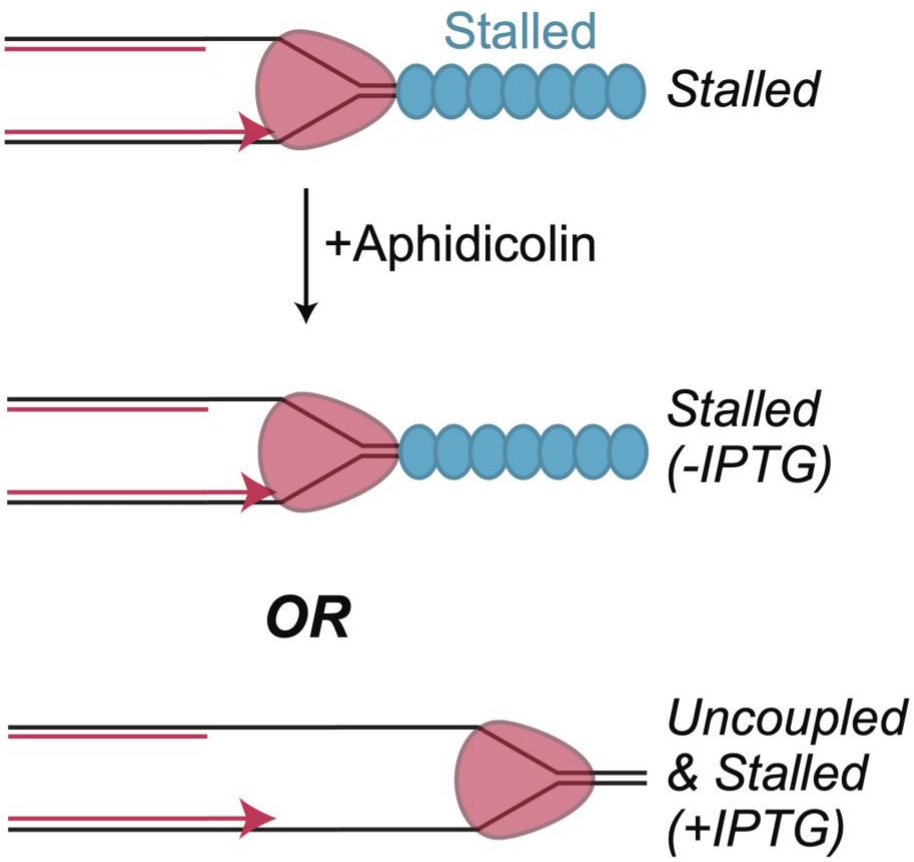

Figure 5.3. An approach to inhibit uncoupling in extracts
(A) Cartoon depicting a strategy to distinguish between helicase stalling and uncoupling in extracts.

to uncoupled fork, as expected (Figure 5.4 (B, lanes 5-6)). When IPTG was omitted however, uncoupling was strongly inhibited, but not fully blocked, as expected based on prior observations that LacR barrier allows for slow helicase movement (Figure 5.4 (B, lanes 1-2). Subsequently, we separated stalled or uncoupled nascent strands on a denaturing gel (Figure 5.4 (C-D). Omission of IPTG, or inhibition of uncoupling, caused nascent strands to persistent, suggesting that inhibiting uncoupling inhibits the initiation of resection (Figure 5.4 (E)). We were surprised by this observation and next wanted to test whether uncoupling leads to more extensive NSD and fork reversal.

Uncoupling elicits NSD

To test whether uncoupling leads to more extensive degradation, we localized forks to the LacR barrier, added aphidicolin and either added or omitted IPTG to facilitate or inhibit uncoupling, as previously described (Figure 5.5 (A)). We then monitored the abundance of Double-Ys in the presence or absence of DNA2-I. Following IPTG treatment, Double-Ys readily got degraded, corresponding to NSD which was inhibited with DNA2-I (Figure 5.5 (B, lanes 11-15). When IPTG was withheld, overall degradation was dramatically reduced (Figure 5.5 (B, lanes 1-5)) and when combined with DNA2-I treatment, almost fully blocked (Figure 5.5 (B, lanes 6-10)) (Figure 5.5 (C)). These data show that uncoupling promotes extensive NSD.

Uncoupling elicits fork reversal

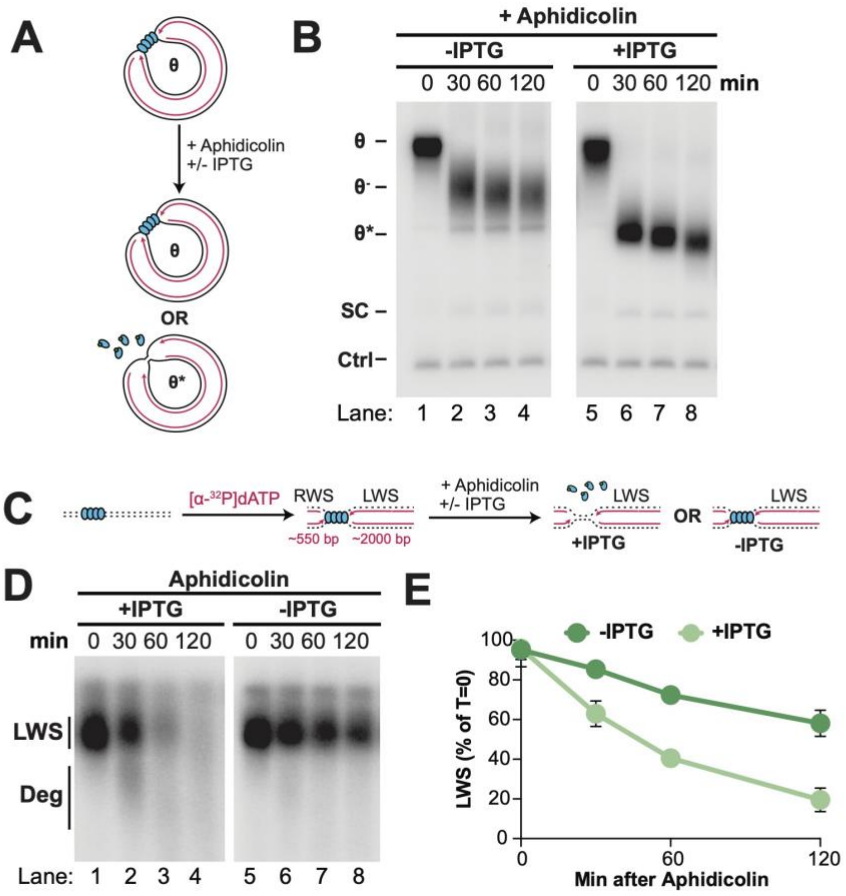

Figure 5.4. Uncoupling promotes onset of nascent strand degradation

(A) Forks were localized to a LacR barrier and aphidicolin was added in the absence or presence of IPTG. (B) Samples from (A) were separated on an agarose gel and visualized by autoradiography. (C) Forks were localized to a LacR barrier and aphidicolin was added in the absence or presence of IPTG. Purified DNA was restriction digested to yield leftward strands (LWS) and rightward strands of different sizes. (D) DNA structures from (C) were separated on an alkaline denaturing agarose gel and visualized by autoradiography. (E) Quantification of intact LWS strands from (D). Mean ± S.D., n=3 independent experiments.

Next we wanted to test whether fork reversal is also stimulated by replication fork uncoupling, since we found that NSD we observe involves fork reversal. To this end, we localized forks to the LacR barrier, added aphidicolin and either added or omitted IPTG to facilitate or inhibit uncoupling, similarly to previous experiments (Figure 5.6 (A)). We then extracted DNA, digested NSD intermediates and performed 2-D gel analysis to monitor the abundance of reversed forks during NSD. After 60 minutes of aphidicolin and IPTG treatment, we observed that Double-Ys had reduced in abundance and increased in mobility, as expected (Figure 5.6 (B(ii))). In stark contrast, omission of IPTG essential blocked the accumulation of reversed forks (Figure 5.6 (B(iii))). When we quantified the percent of reversed forks as a measure of total replication intermediates, we found that while uncoupling promoted ~3 fold increase in reversed forks, inhibiting uncoupling fully blocked this accumulation (Figure 5.6 (C)). These data suggests that replication fork uncoupling promotes fork reversal. Overall, our data show that replication fork uncoupling can stimulate both NSD and fork reversal. These are novel insights into NSD and fork reversal.

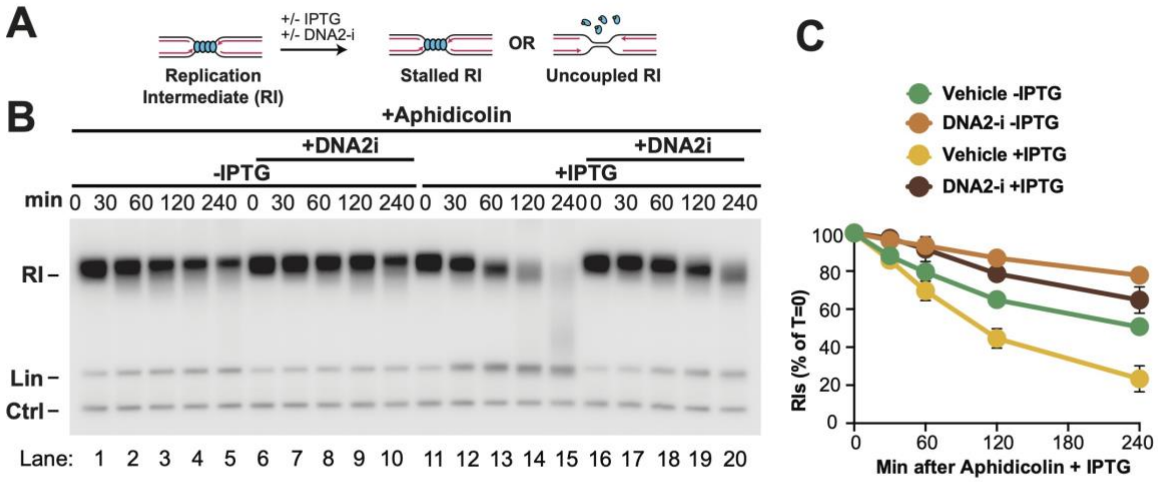

Figure 5.5. Uncoupling promotes extensive nascent strand degradation
(A) Forks were localized to a LacR barrier and aphidicolin was added in the absence or presence of IPTG and DNA2-i. (B) Samples from (A) were digested with XmnI, separated on a native agarose gel and visualized by autoradiography. (C) Quantification of RI signal from (B). Mean ± S.D., n=3 independent experiments.

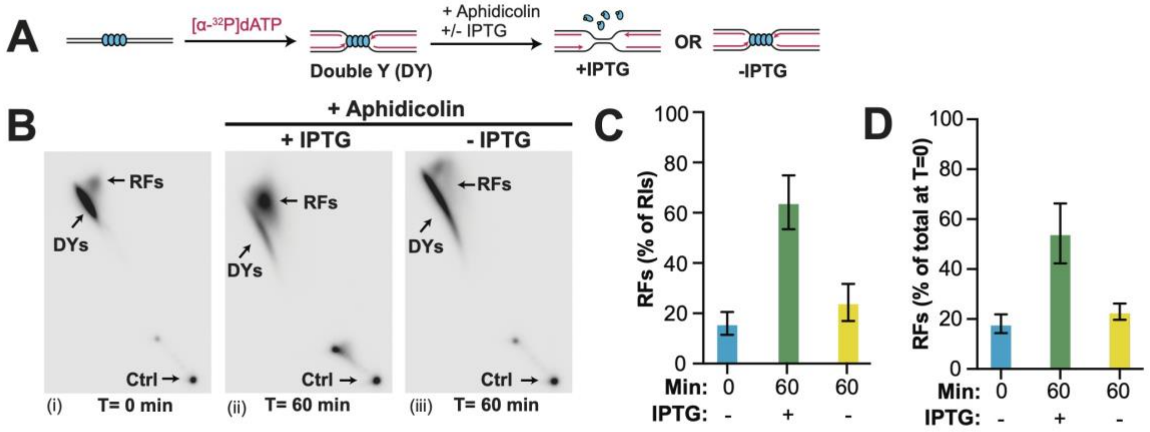

Figure 5.6. Uncoupling promotes fork reversal
(A) Forks were localized to a LacR barrier and aphidicolin was added in the absence or presence of IPTG. (B) DNA structures from (A) were analyzed by 2-D gel electrophoresis and visualized by autoradiography. (C) Quantification of RFs from (B) as a percentage of replication intermediates (RIs) at each time point. Mean ± S.D., n=3 independent experiments. (D) Quantification of RFs from (B) as a percentage of total signal at T=0.

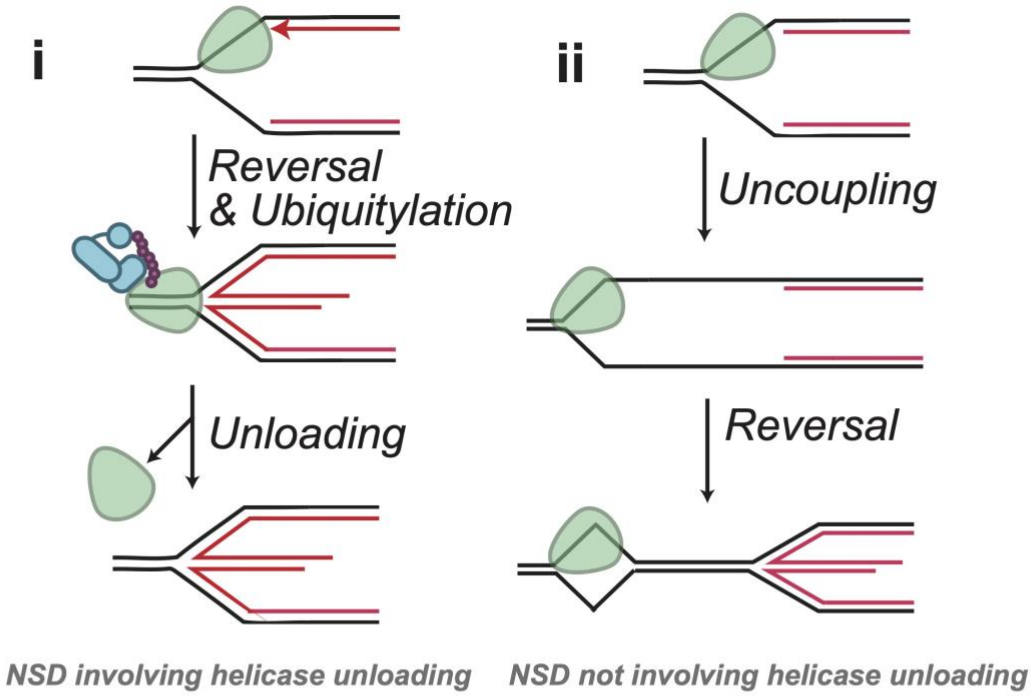

Figure 6.1. Two potential models for the fate of the CMG helicase during NSD
(A) Model for CMG unloading during NSD. (B) Model for CMG entrapped in a ssDNA bubble during NSD.

CHAPTER VI

THE CMG HELICASE IS RETAINED ON CHROMATIN DURING NSD AND FORK REVERSAL

Introduction

The fate of the CMG replicative helicase during NSD and fork reversal has been a long-standing question and remains largely elusive. CMG consists of six MCM subunits (MCM2-7) and forms an active helicase ring together with CDC45 and GINS hetero-tetramer (Georgescu et al., 2017). CMG translocates on a ssDNA template for leading strand synthesis (Langston & O'Donnell, 2017). However, fork reversal creates a four-way dsDNA junction which is in principle incompatible with CMG binding. These are several models hypothesizing what happens to the helicase during these processes. One model stipulates that CMG translocates onto double-stranded DNA during fork reversal (Figure 5.7 (i)). If CMG was to translocate onto dsDNA, this would trigger its rapid ubiquitylation and proteolysis, which would pose threat to genome stability since CMG cannot be re-loaded during S-phase. Therefore, there must be a way to retain CMG onto chromatin. However, unloading of the CMG helicase has also been reported to be required for fork reversal during ICL repair (Amunugama et al., 2018), and in principle a second converging fork could rescue the absence of CMG from one fork. Another model that we considered involves replisome remaining associated with the

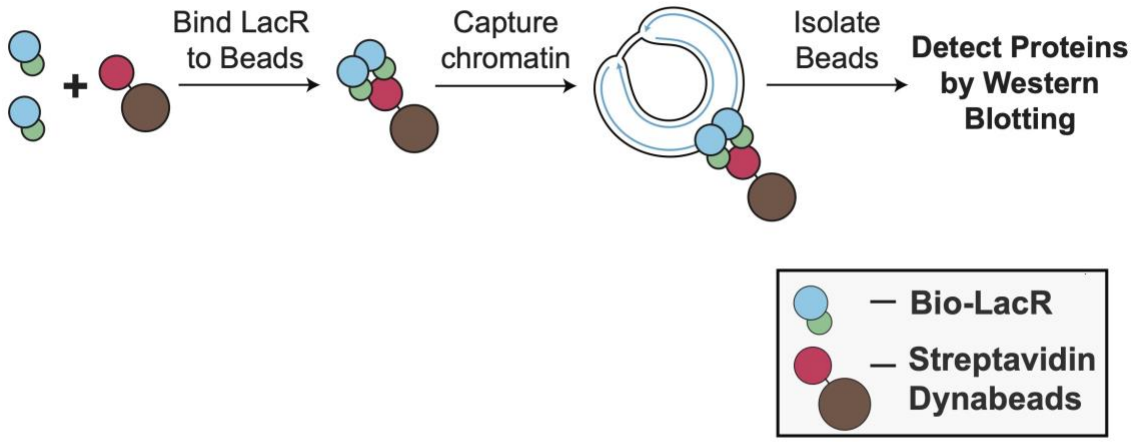

Figure 6.2. Plasmid pulldown approach to measure protein binding
(A) Schematic for measuring protein binding to chromatin using Bio-LacR and Streptavidin dynabeads.

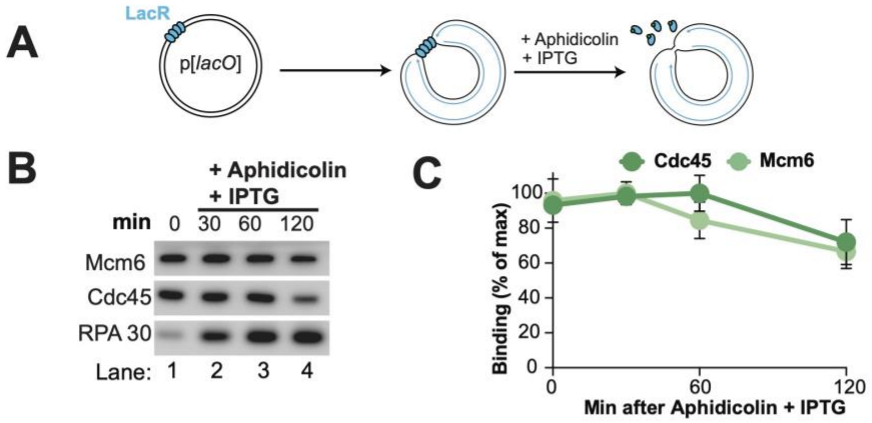

Figure 6.3. The replisome remains associated with DNA during NSD
(A) Forks were localized to a LacR barrier and NSD was induced by addition of IPTG and aphidicolin. At different time points chromatin-bound proteins were recovered. (B) Proteins from (A) were detected by Western Blotting. (C) Quantification of CDC45 and MCM6 from (B). Mean ± S.D., n=3 independent experiments.

nascent DNA, consistent with the published literature showing the long-term retention of the replisome under genotoxic stress that can cause fork reversal (Figure 5.7 (ii)) (Dungrawala et al., 2015). In this Chapter, I will describe an assay to monitor the abundance of replisome components on DNA during NSD and fork reversal and uncover that CMG remains bound to DNA during these processes, and impaired CMG unloading does not affect NSD.

The CMG helicase is retained during NSD and fork reversal

Binding of MCM6 and CDC45 during NSD and Fork Reversal

To determine the fate of the replisome during NSD and fork reversal, we utilized the plasmid pulldown approach. This approach allows for efficient recovery of chromatin bound proteins during different timepoints of replication (Figure 5.9). To this end, we induced NSD as previously described and recovered chromatin at different timepoints and subsequently performed Western blotting to monitor the abundance of replisome components Cdc45 and Mcm6 (Figure 5.10 (A)). We also measured the relatively levels of ssDNA binding protein RPA as a measure of uncoupling and NSD. As expected, RPA levels accumulated and then plateaued, consistent with the presence of high levels of ssDNA during both uncoupling and NSD. Importantly, levels of the CMG helicase components MCM6 and CDC45 were essentially unaltered for the first 60 minutes, which is when the majority of fork reversal takes place and NSD onset occurs at essentially all forks (Figure 5.9 (B-C)). This data shows that the CMG helicase remains

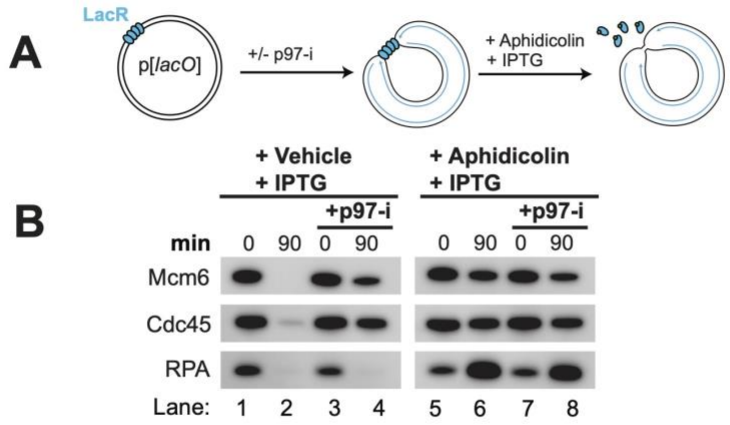

Figure 6.4. Measuring replisome component binding in the presence of p97-I
(A) NSD was monitored as in Figure 6.3 in the absence or presence of p97-i alongside normal replication. (B) Proteins from (A) were detected by western blotting.

bound to DNA during NSD and fork reversal, in contrast with some of the previous models but in line with other observations.

NSD does not require replisome unloading

Although replisome component association to chromatin was relatively stable at earlier timepoints of our NSD assays, we noticed an ~25% decrease in MCM6 and CDC45 signal by 120 minutes (Figure 5.10 (C)). This could be due to full degradation of subset of plasmids. Alternatively, it could be that subset of NSD events might require replisome unloading. Although the levels of unloading couldn't account for all NSD events, we decided to formally test whether replisome unloading has any role in NSD that we are observing. To this end, we monitored the onset of NSD by denaturing gel analysis in the presence of a small molecule inhibitor of p97 (p97-i), which inhibits all known replisome unloading pathways (Figure 5.10 (A))(Deng et al., 2019; Dewar et al., 2015). When replication forks were allowed to complete DNA synthesis in the absence of aphidicolin, p97-I led to retention of MCM6 and CDC45, but not RPA, consistent with a specific role for p97 in unloading of the replicative helicase but not other replication fork components (Figure 5.10 (B-C)). When aphidicolin was added and NSD was induced however, p97-I had little effect on levels of MCM6 or CDC45 (Figure 5.10 (B-C)). This data is consistent with replisome being largely stable.

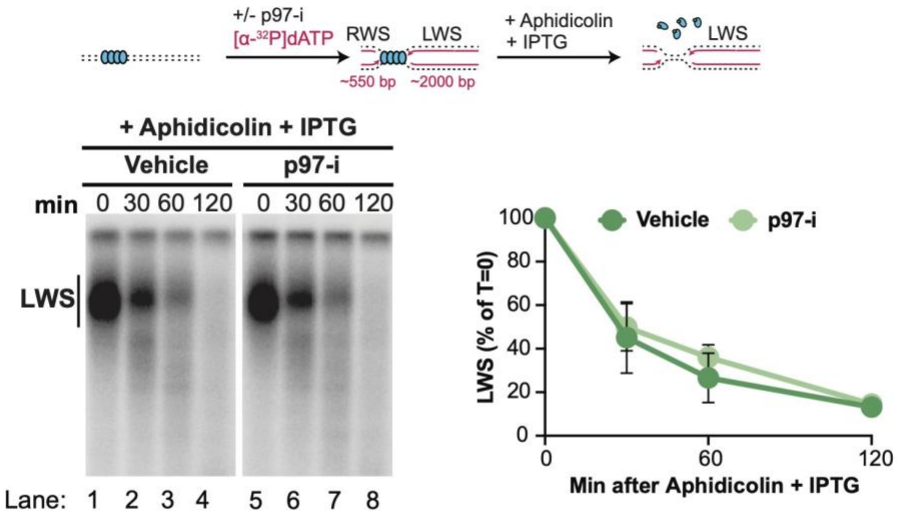

Figure 6.5. Impaired helicase unloading does not affect NSD
(A) NSD was monitored as in Figure 5.4 in the absence or presence of p97-i. (B) Samples from (A) were separated on an alkaline denaturing agarose gel and visualized by autoradiography. (C) Quantification of intact LWS strands from (B). Mean ± S.D., n=3 independent experiments.

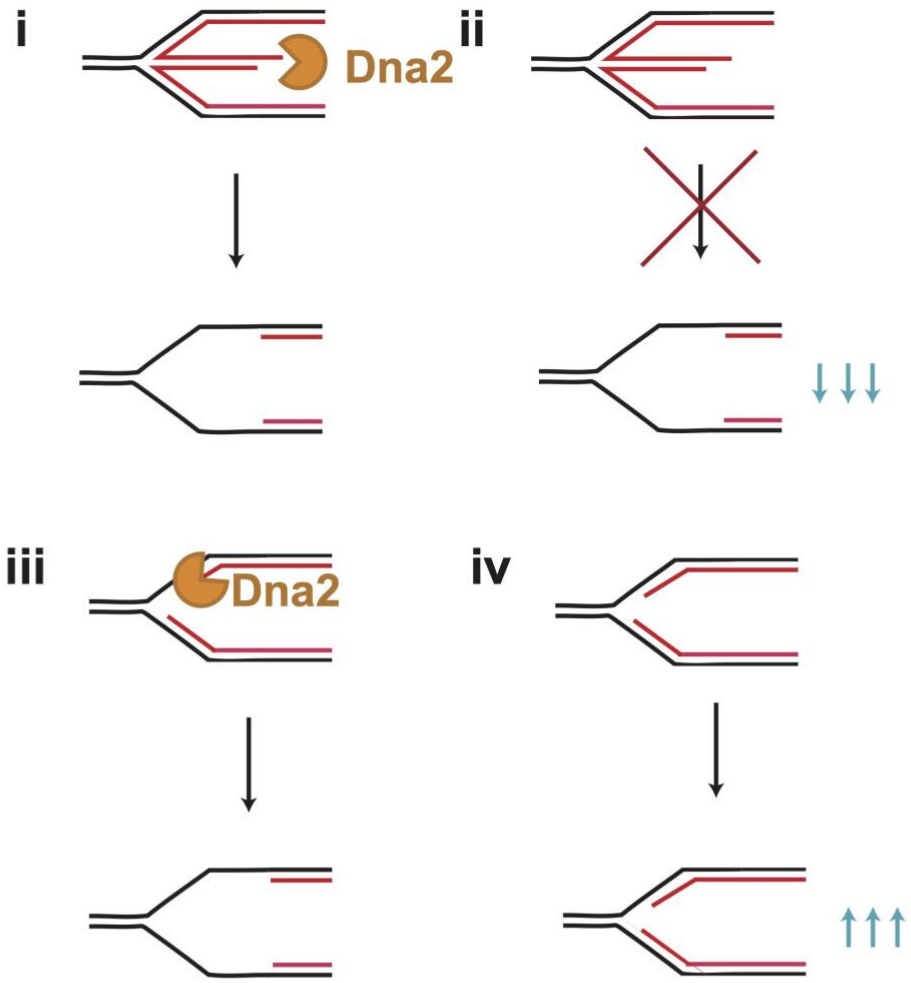

Figure 7.1. Schematic of different models for NSD substrates
(A) Cartoon of different models to explain a role for DNA2 in degrading Y-shaped forks during NSD and the expected impact of loss of DNA2 activity on Y-shaped forks in each case. (i) depicts a model where DNA2 degrades reversed forks to generate Y-shaped forks. In this model the Y-shaped forks are degraded as consequence of prior DNA2 activity at reversed forks. (ii) depicts the impact of impaired DNA2 activity on (i). Y-shaped forks should decrease in abundance as less degradation of reversed forks should reduce the formation of Y-shaped forks. (iii) depicts a model where DNA2 degrades forks prior to fork reversal. (iv) depicts the impact of impaired DNA2 activity on (iii). Y-shaped forks should increase in abundance due to less degradation of nascent strands, which is the source of the radioactive signal that is measured.

degradation compared to the control (Figure 5.11 (A-C)). Overall, our data rule out any requirement for replisome unloading in the vast majority of the NSD events that we observe.

CHAPTER VII

NSD INVOLVES MULTIPLE SUBSTRATES

Introduction

All current models of NSD suggest that fork reversal precedes NSD. However, whether fork reversal is a necessary entry point for nucleases remains elusive. Our data include two very interesting observations that might suggest that reversed forks are not the only substrates for NSD. Firstly, our 2-D gel analysis showed that the mobility of canonical Double-Y shaped molecules decreased over time (Figure 5.6 (B(ii))). This indicates that these over time, Double-Ys are getting smaller, thereby being degraded. However, this observation could be explained by the fact that degradation of reversed forks and subsequent attempts of fork restart could convert degraded reversed forks back to Y-shaped forks, as has been proposed by current models. Second observation provided more firm evidence that NSD might occur independently of fork reversal. When we inhibited uncoupling by omitting IPTG from our standard NSD assays, we fully blocked fork reversal, however small amounts of degradation by DNA2 still occurred (Figure 5.6 (B, iii) and Figure 7.3 (B, ii-iii)). These data suggests that forks can be degraded prior to fork reversal. In this Chapter, I will describe an approach to test whether multiple substrates for NSD exist and subsequently show that both Y-shaped forks and reversed forks can be substrates for NSD and that degradation of Y-shaped forks precedes fork reversal.

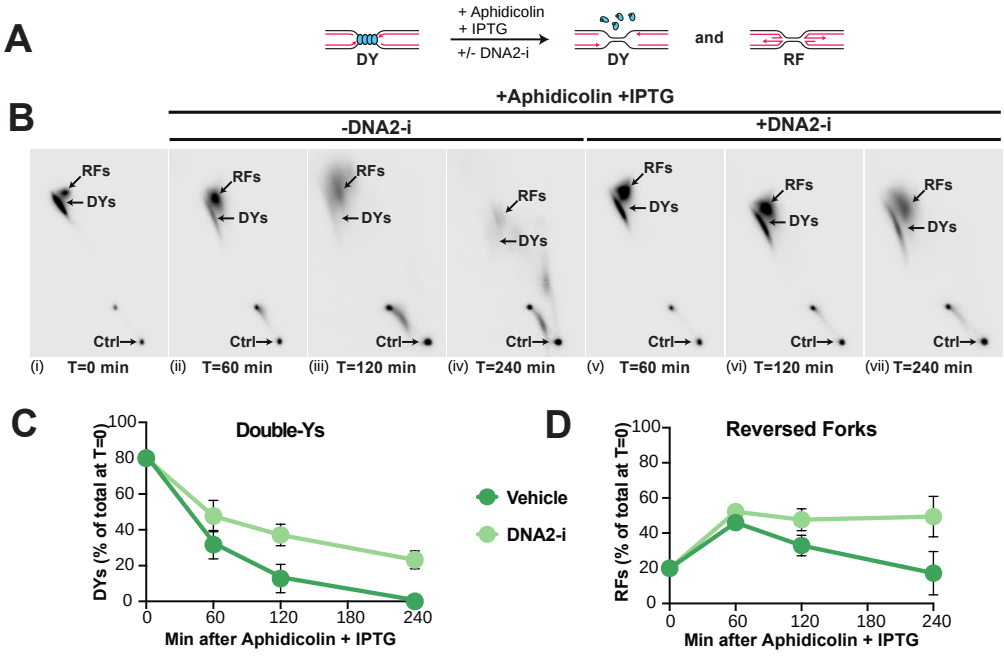

Figure 7.2. DNA2 degrades replication forks and reversed forks
(A) Forks were localized to a LacR barrier and NSD was induced by addition of IPTG and aphidicolin in the absence or presence of DNA2-i. Purified DNA was subjected to restriction digest so that replication fork structures could be visualized. (B) Double-Y (DY) and reversed fork (RF) structures from (a) were separated by 2-D gel electrophoresis. (C) Quantification of DY structures from (b) as a percentage of total signal at T=0. Mean ± S.D., n=3 independent experiments. (D) Quantification of RF structures from (d) as a percentage of total signal at T=0.

Our approach to test whether multiple substrates for NSD exist

To test whether Y-shaped forks can substrates for NSD, in addition to reversed forks, we used the approach outline below. We envisaged two possible sources of degraded Double-Y molecules. First, they could arise from degradation of reversed forks and their subsequent conversion to smaller Y-shaped forks (Figure 5.13 (i-ii)). Alternatively, they could arise from degradation of Y-shaped forks, without first converting them to four-way junctions (Figure 5.13 (iii-iv)). To test which of these scenarios held true in our system, we took advantage of the fact that DNA2 nuclease carries out degradation. We inhibited degradation by treating extracts with DNA2-I and monitored the abundance of Double-Ys and Reversed Forks by 2-D gel electrophoresis (Figure 5.14 (A)). If reversed forks are the only substrates for degradation, we expected DNA2-I treatment to over time increase abundance of reversed forks and decrease the abundance of Y-shaped molecules, as over time they would become converted to reversed forks but not degraded. Alternatively, if Y-shaped forks can also undergo resection, DNA2-I treatment should increase the abundance of Y-shaped forks.

Y-shaped forks are substrates for NSD

We performed an experiment outlined above and monitored the abundance of Double-Ys and Reversed Forks over 60 minutes, 120 minutes and 240 minutes throughout NSD (Figure 5.14 (A)). When we did this, we observed that abundance of Double-Ys was increased by DNA2-I at every timepoint, suggesting that Double-Ys are

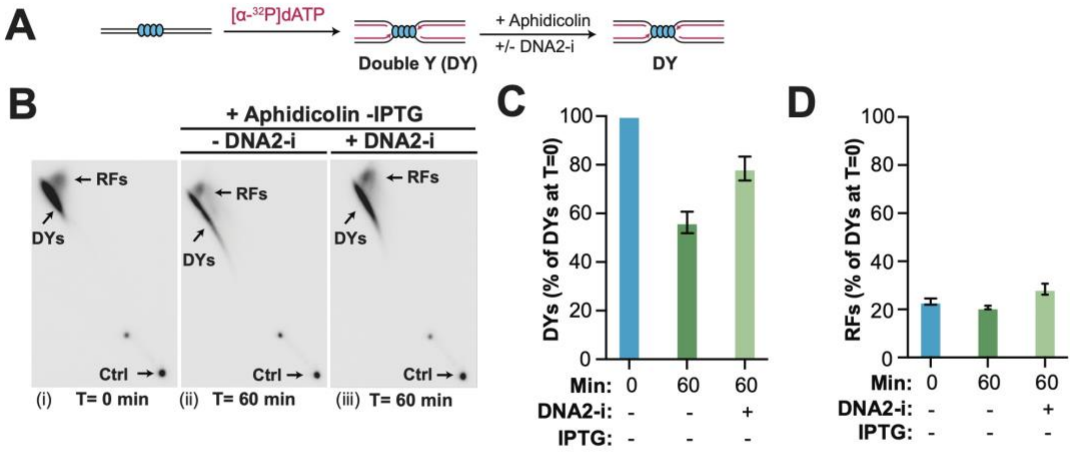

Figure 7.3. NSD can occur in the absence of fork reversal in extracts
(A) Forks were localized to a LacR barrier and aphidicolin was added in the absence or presence of DNA2-i. IPTG was omitted to retain the intact LacR barrier. (B) Samples from (A) were separated by 2-D gel electrophoresis. (C) Quantification of DY structures from (B) as a percentage of total signal at T=0. Mean ± S.D., n=3 independent experiments. (D) Quantification of RF structures from (B) as a percentage of total signal at T=0. Mean ± S.D., n=3 independent experiments.

normally degraded by DNA2 during NSD (Figure 5.14 (B(ii-iv)). We also observed that the abundance of Reversed Forks were increased at all timepoints (Figure 5.14 (D)). These data show that both Double-Ys and Reversed Forks are substrates for NSD. These observations provide novel insight into the mechanism of NSD, showing that fork reversal is not a necessary entry point for degradation and multiple substrates for degradation exist.

NSD can occur in the absence of fork reversal in extracts

We previously had observed that Double-Ys can undergo DNA2 mediated nucleolytic degradation, however, we did those experiments on uncoupled forks which also undergo reversal. We wanted to formally show that degradation of Double-Ys can occur even in the absence of fork reversal in extracts. To this end, we took advantage of the fact that inhibition of uncoupling inhibits fork reversal. We replicated plasmid DNA, stalled forks at the LacR array, treated extracts with Aphidicolin but omitted IPTG in order to induce helicase stalling (Figure 5.15 (A)). Then we either added or omitted DNA2-i. We purified DNA and analyzed the NSD intermediates by 2-D gel electrophoresis (Figure 5.15 (B)). At T=0, majority of the signal was present as a discrete spot on the double-Y arc, corresponding to forks localized to the barrier, with small amount of forks present when reversed forks migrate (Figure 5.15 (B(i))). 60 minutes following fork stalling, reversed forks did not accumulate, however Double-Ys decreased in abundance and increased in mobility, signifying that they were being degraded (Figure 5.15 (B(ii))). Importantly, DNA2-I treatment did not affect the

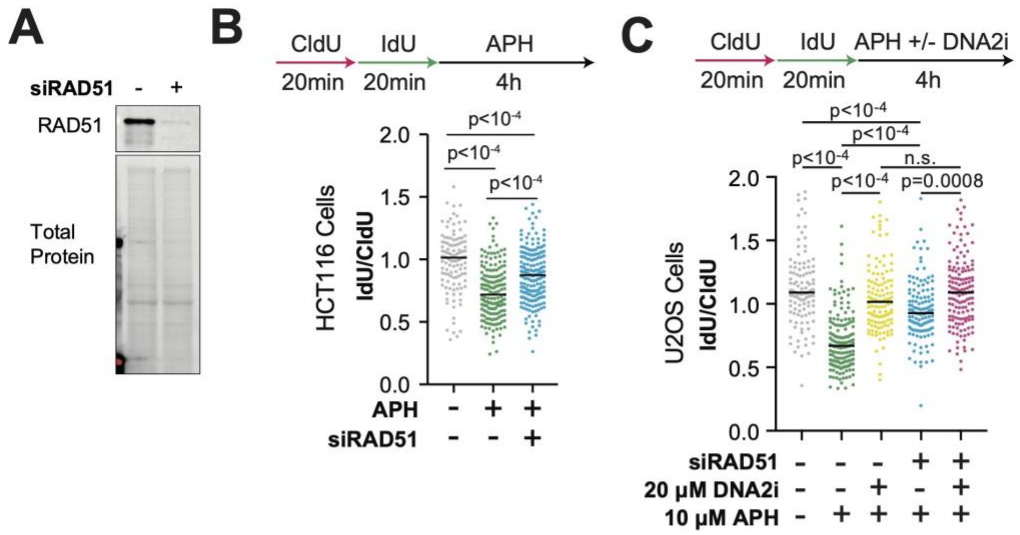

Figure 7.4. NSD can occur in the absence of fork reversal in cells
(A) Western blot confirmation for Rad51 knockdown. (B) HCT116 cells were transfected with control or RAD51 siRNA, pulse labeled with CldU and IdU, and then treated with vehicle or aphidicolin. DNA fiber analysis was performed to determine the lengths of the CldU and IdU labeled DNA tracks in each condition. (C) U2OS cells were transfected with control or RAD51 siRNA, pulse labeled with CldU and IdU, then treated with aphidicolin and/or DNA2-i. DNA fiber analysis was performed to determine the lengths of the CldU and IdU labeled DNA tracks in each condition. Experiments in Figure 7.4 were performed by Wenpeng Liu.

abundance of reversed forks but it increased the abundance and decreased the mobility of Double-Ys, suggesting that DNA2-I treatment reduced the degradation of Double-Y molecules (Figure 5.15 (B(iii))). Quantification of these results confirmed that while abundance of reversed forks were unchanged, DNA2-I treatment increased the abundance of Double-Ys (Figure 5.15 (C-D)). These data show that Y-shaped forks can be degraded in conditions where reversed forks do not form in *Xenopus* egg extracts.

NSD can occur in the absence of fork reversal in human cells

Next we wanted to test whether same holds true in human cells. In order to do this, we decided to inactive RAD51 recombinase which is involved in all reported NSD pathways and is thought to be an absolute requirement for fork reversal (Berti, Cortez, et al., 2020; Bhat & Cortez, 2018; Zellweger et al., 2015). Our previous observations that NSD can occur prior to fork reversal and in the absence of fork reversal suggested to us that we might be able to observe RAD51-independent NSD in human cells. To this end, U2OS cells were treated with siRNA targeting RAD51 and NSD was measured by DNA fiber labeling analysis. We verified that siRNA knockdown depleted cellular levels of RAD51 by Western Blotting (Figure 5.16 (A)). siRNA knockdown of RAD51 reduced, but did not block NSD (Figure 5.16 (B)). This is consistent with RAD51 and fork reversal independent NSD. We also repeated this experiment in HCT116 cells and the same observation held true. Furthermore, addition of DNA2-I reduced the amount of NSD following RAD51 knockdown (Figure 5.16 (C)). These data suggest that fork reversal

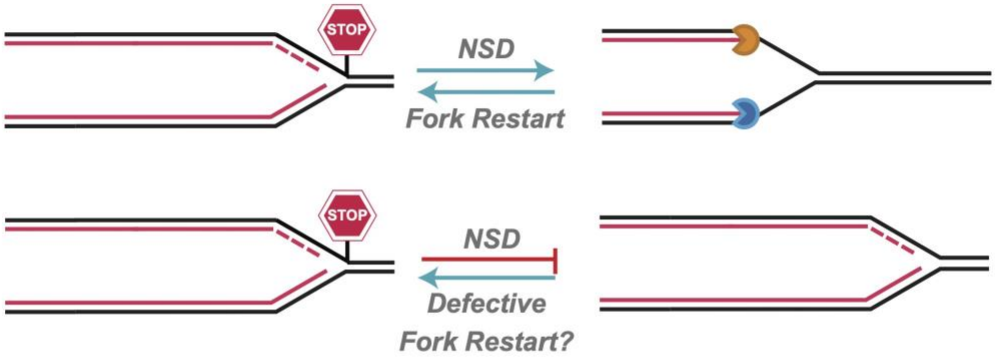

Figure 8.1. Schematic of NSD contributing to fork restart

independent NSD occurs in cells treated with aphidicolin, similarly to our prior findings in *Xenopus* egg extracts.

Chapter VIII

DISCUSSION AND FUTURE DIRECTIONS

Summary of Dissertation Work

DNA replication is a fundamental biochemical process that occurs before every single cell division. Various forms of endogenous and exogenous genotoxic stress challenge replication forks and pose a threat to the fidelity of this process. These stresses can arise from endogenous cellular processes such as aldehydes derived from lipid oxidation and ROS derived from mitochondrial metabolism. These molecules can cause direct DNA damage that can stall replication forks. In addition, cells are constantly subject to exogenous sources of stress such as UV light, ionizing radiation as well as chemotherapeutic drugs that can cause replication fork stalling. In response to these forms of genotoxic stress, replication forks stall. Properly processing stalled forks is crucial for resuming DNA synthesis and maintaining genome stability. My thesis work focuses on understanding the mechanistic underpinnings of two of the most common responses to fork stalling – fork reversal and nascent strand degradation.

My dissertation work has focused on developing a biochemical system in *Xenopus* egg extracts to answer these mechanistic questions. Our work demonstrated that NSD can be an initial response to fork stalling, which has implications in the importance of NSD in fork restart. Additionally, we found that NSD and fork reversal are

stimulated by helicase uncoupling, rather than stalling. Additionally, we showed that NSD can occur at canonical replication fork structures prior to fork reversal, indicating that there is an extra degradation step that the current models do not include. Furthermore, we show that the replicative helicase (CMG) remains bound to DNA throughout NSD and fork reversal. This observation suggests that CMG continues to reside on ssDNA during reversal and degradation. This is in support with the model that the CMG becomes trapped in the ssDNA bubble ahead of the replication fork. Collectively, the observations of my thesis work inform a new model for NSD and fork reversal in vertebrates. Many other questions remain that can be addressed by utilizing the system that I have developed. I will explore them in more detail in the discussion below.

Are all modes of NSD the same?

NSD can occur in response to many genotoxic agents such as MMC, HU, aphidicolin, cisplatin etc. NSD can also occur in wild type cells after prolonged genotoxic stress or cells devoid of one of the many fork protection factors after shorter periods of genotoxic stress. It can be mediated by many nucleases such as MRE11, DNA2, WRN, EXO1, CTIP and others. The question arises of how these different modes of NSD are deployed under different cellular circumstances. In the paragraph below, I will overview what we currently know about HU versus aphidicolin mediated NSD and how my thesis findings challenge the recent evidence showing that the oxidative stress rather than replication fork stalling alone is a trigger for NSD.

HU is the most common genotoxic agent used to induce NSD in human cells. HU inhibits ribonucleotide reductase (RNR) thereby reducing the pool of available dNTPs, which stalls DNA polymerases (Bianchi et al., 1986). In addition to depleting dNTP pools, inhibition of RNR causes cellular metabolic stress by elevating the levels of reactive oxygen species (ROS) (Somyajit et al., 2017). A study found that a short pulse of low concentrations of HU, while having no effect on dNTP pools, caused marked fork slowdown and rapid accumulation of superoxide and hydroxyl radicals, which could be rescued by treatment with ROS quencher NAC. The same study also found that Peroxiredoxin 2 (PRDX2), a ROS sensor protein, was enriched at forks and interacted with a replisome accelerator protein TIMELESS. Elevated ROS levels caused dissociation of both PRDX2 and TIMELESS from chromatin, mitigating the pathological consequences of DNA replication stress. A subsequent study from the same group showed that nascent strand degradation triggered by HU in fork protection deficient cells can be recapitulated by other genotoxic agents that causes ROS accumulation in the nucleus, such as GluOx, Rotenone and H2O2 (Somyajit et al., 2021). This study found that aphidicolin, which stalls forks by inhibiting DNA polymerases, does not induce accumulation of ROS. They, however, did not find that aphidicolin causes NSD at the same level of fork stalling as HU. These observations collectively led to them concluding that metabolic stress, as opposed to fork stalling alone, leads to NSD. In contrast, my work has shown that aphidicolin alone can lead to rampant NSD response in both cells and *Xenopus* egg extracts. Interestingly, work from our collaborators in Cortez lab has showed that aphidicolin induces NSD in a dose-response manner in

human cells. It is likely that the dose used in this study was not high enough to induce NSD. It is evident however that oxidative stress can cause NSD. However, oxidative stress also rapidly leads to replication fork stalling, which can rapidly lead to uncoupling. Therefore, future studies are needed to understand exactly what aspect of metabolic stress leads to NSD and whether it is replication fork uncoupling that follows ROS accumulation that is an actual molecular trigger for NSD or some other aspect of metabolic stress. For instance, metabolic stress could trigger a level of fork stalling that is only seen at higher aphidicolin concentrations. I believe this hypothesis is very likely to hold true because Timeless/Tipin complex has been hypothesized to be important for coupling helicase and polymerase activities in cells (Cho et al., 2013) and resist genotoxic stress (Chou & Elledge, 2006) and their dissociation from replisome could be a trigger for uncoupling, which could subsequently lead to NSD. Additionally, Timeless/Tipin in extracts have been shown to be crucial for fork restart following aphidicolin mediated genotoxic stress (Errico et al., 2007). Additionally, Tipin deficiency in Xenopus egg extracts leads to accumulation of reversed forks, suggesting that Tipin coupling activities could normally be restraining uncoupling and inhibiting fork reversal (Errico et al., 2014). Impaired fork restart has been previously shown to induce excessive NSD (Thangavel et al., 2015). Therefore, metabolic stress could lead to dissociation of Timeless and inhibition of fork restart thereby leading to aberrant NSD. The system that we have developed to study site-specific uncoupling in *Xenopus* egg extracts could be easily adapted to include other genotoxins and analyze whether rampant NSD and fork reversal also occur in response to other insults and whether this is linked to defective fork restart. Although Xenopus egg extracts are supplemented with

a reducing agent DTT in order to stabilize enzymes and it remains untested whether oxidative stress can occur in a reducing environment.

The role of the retention of CMG helicase during NSD and Fork Reversal

CMG unloading from chromatin is a very tightly regulated process. A critical licensing factor CDT1 is completely proteolytically degraded in order to prevent re-licensing and re-replication of DNA during S phase of the cell cycle (Zhong et al., 2003). If CMG is unloaded from chromatin prematurely, this could lead to stretches of unreplicated DNA and possible mis segregation of chromosomes during mitosis. This could have catastrophic implications for mitosis, chromatin establishment and genome stability. In order to avoid premature CMG disassembly, nascent strands at the replication fork suppresses CMG unloading before DNA replication termination (Deegan et al., 2020; Low et al., 2020). Uncoupling however dissociates CMG from the nascent strands, as helicase continues unwinding but the nascent strands are not being elongated (Byun et al., 2005). Prior work has shown that even under prolonged genotoxic stress, components of the replisome can be detected by nascent chromatin capture followed by mass spectrometry and additionally synthesis can be readily resumed once the genotoxin is washed out, suggesting that forks can restart and CMG is present (Dungrawala et al., 2015). My work has shown that CMG components remain bound to DNA during fork reversal and NSD. So an important question is how does CMG stay bound when the canonical fork structure is altered by either NSD or fork reversal? One appealing model is that CMG resides in the ssDNA bubble of parental

DNA ahead of the fork. In principle, CMG could backtrack (Kose et al., 2020) but this would cause reannealing of parental DNA, which was not observed in our NSD assays. Another possibility is that CMG could translocate onto dsDNA. However, translocation of CMG onto dsDNA would trigger its ubiquitylation and removal from chromatin (Dewar et al., 2017). But the possibility that some mechanism counteracts CMG ubiquitylation during fork reversal and NSD cannot be discounted. A recent study has found that eukaryotic CMG helicase has a gate in its ring that allows it to switch from dsDNA to ssDNA and enables the CMG to vacate the replication fork when uncoupled from the polymerase (Wasserman et al., 2019). During the gating process, a replisome factor MCM10 tethers CMG to DNA to ensure it does not get displaced. This study hypothesized that this form of gate switching could take place during fork reversal, recombinative repair and/or translesion synthesis. However, how CMG diffusing on dsDNA in a cellular context would be able to stay on chromatin and escape ubiquitynation is unclear. The biochemical approach I describe in my thesis could be used to test the role of MCM10 during fork reversal and NSD and see whether depletion of MCM10 might lead to premature disassembly of the CMG.

How does uncoupling elicit NSD?

My thesis work shows that uncoupling of the nascent strand synthesis from the CMG helicase activity stimulates both extensive NSD and fork reversal. This finding formally confirms the previously reported finding that wide variety of genotoxins cause both increased levels of uncoupling as well as fork reversal (Zellweger et al., 2015).

However key questions about the precise molecular trigger for NSD still remain and how exactly uncoupling promotes NSD and fork reversal is unclear. It is unlikely that uncoupled replication fork structure itself promotes NSD because a degraded fork could look identical to an uncoupled fork so there must be other mechanisms and molecular triggers that promote fork reversal and NSD. There are several possibilities on how uncoupling promotes NSD and whether or not it is an absolute requirement. I will discuss these possibilities in more detail below.

Does ssDNA promote NSD?

There are several non-mutually exclusive ways in which ssDNA ahead of the replication fork can promote NSD and fork reversal. Firstly, ssDNA ahead of the uncoupled nascent strands could serve as a loading dock for RPA, RAD51 and fork remodeling enzymes such as SMARCAL1. In addition, physical dissociation of CMG from the proximity of the nascent strands could provide space for nuclease and/or fork reversal enzyme entry. Certain length of parental ssDNA could also be necessary in order to reanneal them and promote fork reversal. Interestingly, my thesis work has found that even when uncoupling is severely inhibited by a physical barrier to helicase progression, Y-shaped forks can still undergo degradation but they do not remodel into reversed forks. This is interesting because in theory, degraded Y-shaped forks should resemble an initial uncoupled fork. However, degradation of Y-shaped forks when uncoupling is initially inhibited, does not lead to fork reversal and more excessive degradation. This probably signifies that initial uncoupling serves some sort of a

signaling role in addition to generating a certain substrate that then could be degraded and remodeled. ssDNA can indeed serve as a platform to recruit RPA and activate ATR kinase signaling. One of the key phosphorylation substrates of ATR is SMARCAL1 and phosphorylation of SMARCAL1 by ATR leads to limiting aberrant over-reversal of replication forks to maintain genome stability (Couch et al., 2013).

Is uncoupling an absolute requirement for NSD?

It is clear that uncoupling promotes extensive NSD and fork reversal. However, whether uncoupling is an absolute requirement for NSD remains unclear. Our experiments detected NSD even when uncoupling was severely inhibited, but not fully blocked. A recent study has identified that in addition to HU induced degradation that occurs in BRCA2 deficient cells, ICLs can also experience aberrant hyper resection (Rickman et al., 2020). Interestingly, this mode of NSD is carried out by DNA-WRN nuclease-helicase complex, similarly to the NSD that is triggered in fork protection proficient cells with aphidicolin, as opposed to MRE11. ICLs have been found to stall the CMG complex, with leading strands stalling ~20-40 nucleotides from the ICL due to the CMG footprint (Amunugama et al., 2018).Therefore, fork stalling at an ICL should be incompatible with the type of uncoupling we observe with aphidicolin treatment since CMG should be unable to bypass an ICL. This suggests that NSD can occur in the absence of uncoupling. Although ICLs have been considered an absolute roadblock to DNA replication machinery, recent evidence emerged suggesting that forks might traverse ICLs in human cells. Using single-molecule approaches, a study showed that

that inducing ICL formation leads to ATR kinase mediated global fork slowing and this modulation of fork speed promotes single-fork ICL traverse (Mutreja et al., 2018). Thus, it is possible that uncoupling could occur following an ICL traverse that could trigger NSD. Additionally, ICL repair in *Xenopus* egg extracts has been shown to involve CMG unloading followed by fork reversal. A study found that when two forks converge onto an ICL (Zhang et al., 2015), CMG gets ubiquitylated and unloaded followed by FANCI-FAND2 mediated incisions and ICL unhooking and repair. Importantly, fork reversal here is inhibited when CMG unloading by p97i is inhibited, suggesting that fork reversal occurs following CMG unloading. My thesis findings showed that fork reversal can occur when CMG stays bound to the DNA but it did not rule out that fork reversal cannot occur when CMG dissociates from the DNA. It would be very interesting to know whether reversed forks that form in the presence of absence of the CMG complex are subject to different types of processing or are reversed by a different set of enzymes.

Are post-replicative gaps uncoupled forks or degraded forks?

Recently, evidence has emerged showing that the primary toxic lesion that leads to genomic instability might be ssDNA gaps as opposed to DSBs. Replication fork protection factors such as BRCA1, BRCA2 and Rad51 have critical roles on ssDNA gap suppression (Cong et al., 2021; Vaitsiankova et al., 2022; Wong et al., 2020). However, it is unclear how these gaps are generated and whether they are a function of NSD. Several lines of evidence suggest that these ssDNA gaps in the wake of the replication fork could arise independently from fork degradation. First is that gaps arise even under

low doses of HU treatment, while treatment with the same dose does not lead to NSD (Panzarino et al., 2021). Also, gaps are still detectable after MRE11 nuclease is inhibited (Panzarino et al., 2021). However, in contrast to prior models, my thesis work has found that NSD is an initial and primary response to fork stalling by aphidicolin in wild type *Xenopus* egg extracts and human cells. In addition, my work clearly shows that Y-shaped forks can be subject to degradation, in addition to reversed forks. Thus it is conceivable that initially gaps arise because NSD is deployed under genotoxic stress and then those gaps are subject to processing by BRCA1/2, RAD51 and other fork protection factors. In the absence of fork protection, NSD might generate initial gaps which are then improperly processed and extensively reversed, leading to excessive NSD and chromosomal abnormalities. In fact, inactivation of DNA2, which carries out the NSD that my thesis has described, also inhibits fork degradation in all other genetic backgrounds – such as BRCA2, FANCD2, ABRO1, FANCA VHL, 53BP1 and BOD1L knockdown (Liu et al., 2020). This could point to the possibility that NSD functions upstream of fork protection and generates a substrate that is then processed by fork protection factors. These are all possibilities that require further testing.

How does NSD lead to fork restart?

My work has showed that NSD is an initial and immediate response to aphidicolin mediated fork stalling. If a biochemical mechanism is deployed immediately after genotoxic stress, this might be an indication that this mechanism important for properly dealing with that type of stress. Based on previous work, my inclination is that NSD is

important for proper fork restart after the genotoxic stress is cleared, however, demonstrating this will require further experimentation. Below I will discuss our current understanding of fork restart following HU mediated genotoxic stress and how the system I developed could be adapted to study fork restart.

DNA2/WRN mediated fork processing for fork restart

A study that first showed importance of NSD in fork restart demonstrated that after very prolonged HU mediated genotoxic stress (~8 hours), DNA2 nuclease and WRN helicase cooperate to degrade reversed forks to promote RECQ1 helicase mediated fork restart (Thangavel et al., 2015). First, they subjected wild type cells to 8 hours of HU treatment and measured length of nascent DNA fibers. They found that DNA2 degrades nascent DNA after prolonged genotoxic stress. Subsequently, they measured fork restart after prolonged genotoxic stress and found that ~2 fold less forks are able to restart when DNA2 is knocked down. This study also excluded the role of other nucleases that have previously been implicated in NSD such as EXO1, MRE11, CTIP and MUS81. Similarly to my findings, this study found that inhibiting DNA2 led to an accumulation of reversed forks measured by EM. Two key differences between my thesis study and this study is the amount of time genotoxic stress was applied to cells and the type of genotoxin used (HU versus aphidicolin). I found that NSD occurs rapidly after aphidicolin treatment and not just after 8 hours of prolonged stress. Importantly, my assays measuring radioactive signal as a proxy for amount of nascent strands remaining, are more sensitive than DNA fiber labeling analysis. We are able to detect

small changes in nascent DNA signal, whereas, a single pixel of a DNA fiber could represent anywhere from 300 bp to ~ 1kb of DNA (Bianco et al., 2012; Moore et al., 2022), thereby masking some earlier NSD events. In addition, we compared aphidicolin versus HU induced NSD in human cells and found that HU does not induce rapid NSD like aphidicolin. Therefore it will be important to test how NSD that we are observing contributes to fork restart. We can do this in the *in vitro* biochemical system that my thesis work developed and test it in human cells. In extracts, we can perform an NSD assay and 'wash out' aphidicolin and monitor conversion of Double-Ys to fully replicated linear molecules in the presence of absence of DNA2-i. In cells, we could label with the first nucleotide analog, then treat cells with aphidicolin, wash out the genotoxic and subsequently pulse in the second nucleotide analog and measure the amount of restarted forks. While the cellular approach allows for studying restarted forks, our *in vitro* approach would allow us to monitor both restarted and stalled forks that might fail to restart. This way we can analyze the structure and characteristics of a replication fork that might fail to resume synthesis. Additionally, fork restart after reversal and degradation might not initially include DNA synthesis and instead lead to the restoration of a canonical fork structure. Cellular approaches only measure incorporation of nucleotides and thus, resumption of synthesis. But our *in vitro* approach could help us visualize forks that have been reverted.

Reversed fork conversion to Y-Shaped Forks

Replication fork restart after reversal and degradation should in theory involve conversion of reversed forks back to Y-shaped forks. This is thought to be carried out by RECQ1 helicase (Thangavel et al., 2015). Interestingly, when we induced NSD by aphidicolin, we saw that all replication forks were progressively converted to reversed forks, and at later timepoints majority of the signal was present as reversed forks. We were surprised by this observation because if degraded reversed forks are readily interconverted between Y-shaped forks and reversed forks, we should have expected a different distribution of these structures. However, in our experiments aphidicolin fully blocked DNA synthesis. Therefore, it is possible that conversion of reversed forks to Y-shaped forks requires DNA synthesis or even a small amount of DNA synthesis. It will be important to test whether DNA synthesis is required for converting RFs to Y-shaped forks. We could test this using our *in vitro* system in extracts. First, we could wash out high dose of aphidicolin and replace it with a very low dose of aphidicolin that by itself does not induce NSD but will not allow to forks to elongate at a fast rate and terminate. Then we can assess structures formed before and after aphidicolin washout and measure the percentage of RFs and Y-shaped molecules.

What determines the choice between fork protection and NSD?

A key question that arises given that degradation can occur initially at uncoupled forks, and then following the loss of fork protection factors is – how are these two pathways connected and does fork protection function during initial NSD? Although, there is currently no formal evidence that Y-shaped forks can undergo degradation in

the absence of fork protection factors. Thus, it is possible that deprotected forks only undergo fork reversal mediated degradation. Literature has broadly defined that DNA2 mediated NSD occurs in wild-type cells after prolonged genotoxic stress or both MRE11 and DNA2 mediated NSD occurs in fork protection deficient cells after shorter genotoxic insults. An easy explanation could be that DNA2 carries out NSD at uncoupled Y-shaped forks which then remodel into reversed forks that undergo fork protection. However, my thesis work has shown that DNA2 can degrade both Y-shaped forks and reversed forks. Recent literature showed that inactivation of DNA2 inhibits NSD in at least two distinct fork reversal pathways (Liu et al., 2020), consistent with its role upstream of fork reversal. Collectively, these observations suggest that DNA2 activity at uncoupled forks might somehow promote degradation of reversed forks that are subsequently formed. How this then promotes or counteracts fork protection is unclear. It is also conceivable that fork protection is a completely separate mechanism that only occurs in response to metabolic insults from HU but this is unlikely because excessive NSD in BRCA2 deficient extracts has been documented after treatment with aphidicolin (Kolinjivadi et al., 2017), which does not induce the accumulation of ROS. It will be important to test the relationship between the NSD as a primary response to uncoupling and fork protection proteins that function under genotoxic stress. For instance, does NSD at uncoupled forks negatively regulate fork protection proteins? Or could it be possible that NSD is in fact promoting fork protection which occurs downstream and allows for fork restart after the genotoxic stress is washed out? NSD could in fact be either positively or negatively regulating fork protection. It could promote protection by creating a substrate for fork protection proteins to bind and stabilize stalled replication

forks. Conversely, it could be inhibiting fork protection factors to bind and stabilize reversed forks. These are all testable hypotheses using the systems I have described in my thesis.

APPENDIX A

This appendix contains some unpublished data of the NSD project as well as some supplemental data showing how some factors are not involved in NSD

SAMHD1 and FAN1 nucleases do not aid DNA2 in NSD

My thesis work focused on NSD that is carried out by DNA2 nuclease. DNA2 has a 5' → 3' exonuclease activity and therefore would be expected to be degrading the nascent lagging strands during NSD. To identify a 3' → 5' nuclease that is functioning during NSD, we tested two candidate nucleases. SAMHD1 nuclease has previously been implicated in degrading nascent DNA at stalled forks and restarting DNA synthesis (Coquel et al., 2018). A second candidate, FAN1, is a part of the Fanconi Anemia complex and its nuclease activity helps recover stalled forks (Chaudhury et al., 2014). To test their roles in NSD, we immunodepleted them from extracts (Figure AA.1(A)) and performed an NSD assay (Figure AA.1(B)). In mock depleted extracts, we observed NSD, as expected (Figure AA.1(C, lanes 1-5)). In SAMHD1 and FAN1 depleted extracts, we observed no inhibition of NSD (Figure AA.1(C, lanes 6-15)). These results are quantified in Figure AA.1 D-E. We also repeated these experiments in cells, using siRNAs against SAMHD1 and FAN1 and observed no inhibition of aphidicolin mediated NSD upon nuclease knockdown, confirming what we saw in extracts (Figure AA.1 (F)).

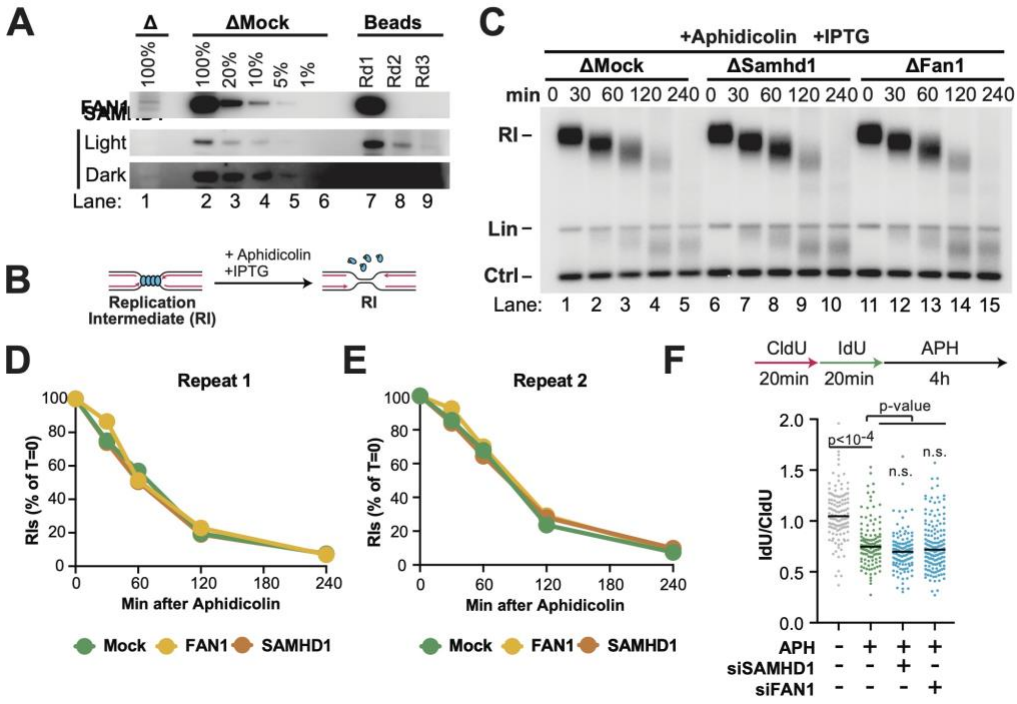

Figure AA.1. SAMHD1 and FAN1 are not involved in NSD
(A) Immunodepleted extracts and the corresponding immunoprecipitates were analyzed by Western blotting to determine the extent of SAMHD1 and FAN1 depletions. (B) Forks were localized to a LacR barrier and NSD was induced by addition of IPTG and aphidicolin in SAMHD1- and FAN1-immunodepleted Xenopus egg extracts. Purified DNA was subjected to restriction digest so that replication fork structures could be visualized (RIs). (C) Samples from (C) were separated on an agarose gel and visualized by autoradiography. (D) Quantification of RI signal from (C). (E) Quantification of RI signal from an experimental replicate of (C). (F) U2OS cells were transfected with the indicated siRNA, pulse labeled with CldU and IdU, then treated with aphidicolin. DNA fiber analysis was performed to determine the lengths of CldU and IdU labeled DNA tracks in each condition.

These data collectively suggest that SAMHD1 and FAN1 nucleases are not involved in NSD that is deployed as a first response to fork uncoupling by aphidicolin.

NSD involves WRN helicase/nuclease

WRN helicase/nuclease cooperates with DNA2 to mediate long-range DNA end resection (Sturzenegger et al., 2014) and has also been implicated in NSD that DNA2 carries out in response to prolonged HU mediated genotoxic stress (Thangavel et al., 2015). Therefore we decided to test its role in the NSD that we were observing. To this end, we induced uncoupling as previously described and treated extracts with DNA2-I, WRN-I or both and purified and digested DNA to monitor NSD (Figure AA.2 (A)). We observed NSD in vehicle treated extracts, as expected (Figure AA.2 (B, lanes 1-5)). We observed that DNA2-I treatment reduced NSD, as previously (Figure AA.2 (B, lanes 5-8)). To our surprise, WRN-I treatment also reduced NSD to the same extent as DNA2-I treatment alone (Figure AA.2 (B, lanes 9-12)). Combination of both inhibitors fully blocked NSD (Figure AA.2 (B, lanes 13-16)). These observations are quantified on a graph in Figure AA.2 (C). Importantly, our results demonstrate that DNA2 and WRN cooperate to carry out NSD and their mutual inhibition has additive effect. This is in contrast to what has been reported in the literature, where DNA2 and WRN are thought to be epistatic in NSD (Thangavel et al., 2015). It is important to point out that our way of measuring NSD, can detect when one strand is degraded but the other one is not, whereas DNA fiber labeling analysis can detect an intact fiber even if either leading or

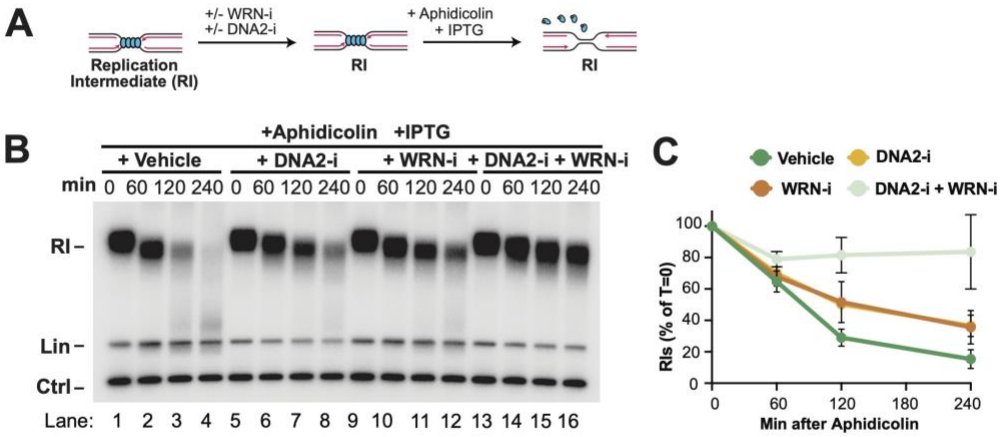

Figure AA.2. WRN and DNA2 function during NSD
(A) Forks were localized to a LacR barrier and NSD was induced by addition of IPTG and aphidicolin in DNA2-I, WRN-I or DNA2-I + WRN-I treated extracts. Purified DNA was subjected to restriction digest so that replication fork structures could be visualized (RIs). (B) Samples from (A) were separated on an agarose gel and analyzed by autoradiography. (C) Quantification of RIs from (B). Mean ± S.D., n=3 independent experiments. v

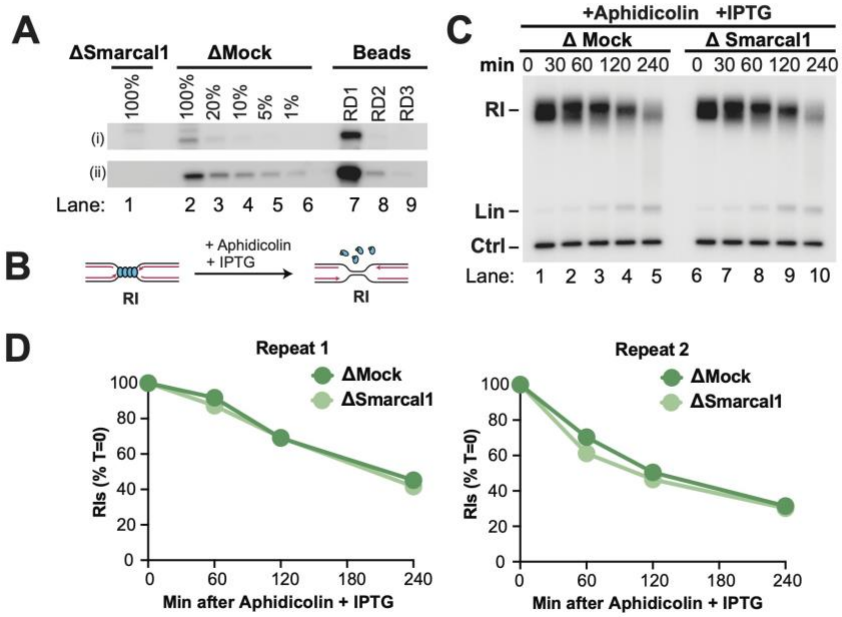

Figure AA.3. NSD in extracts does not involve SMARCAL1
(A) Immunodepleted extracts and the corresponding immunoprecipitates were analyzed by Western blotting to determine the extent of SMARCAL1 immunodepletion. (B) Forks were localized to a LacR barrier and NSD was induced by addition of IPTG and aphidicolin in SMARCAL1-immunodepleted Xenopus egg extracts. Purified DNA was subjected to restriction digest so that replication fork structures could be visualized (RIs). (C) Samples from (B) were separated on an agarose gel and visualized by autoradiography. (D) Quantification of RI signal from (C).

lagging strands are fully degraded. Therefore, additive effects might be masked by cellular assays that we can detect in extracts.

NSD in extracts does not involve Smarcal1

When we previously assessed the requirement of fork reversal enzymes in NSD in cells, we found that SMARCAL1, FBH1 and PICH knockdowns all partially reduced NSD. We decided to test whether these enzymes that we have antibodies for in extracts also have roles in NSD we observe in extracts. To this end, we immunodepleted SMARCAL1 from extracts (Figure AA.3 (A)) and performed an NSD assay (Figure AA.3 (B)). We validated the immunodepletion by probing the Western Blot with a previously published antibody (Kolinjivadi et al., 2017). We surprisingly found no difference in NSD between mock and SMARCAl1 depleted extracts (Figure AA.3 (C-E)). This result suggests that NSD we observe in extracts likely reflects only a subset of pathways observed in cells.

Proximity of the converging forks has no effect on NSD

Our assays that measure NSD all use a plasmid with an approximately 1 kb LacR Array. We wanted to test whether increasing the size of the LacR Array and therefore increasing the distance between converging forks had an effect on NSD (Figure AA.4 (A)). To this end, we induced NSD on two separate plasmids with 1 and 1.5 kb LacR arrays, respectively and monitored the abundance of Double-Ys over time (Figure AA.4 (B)). We found that there is no significant difference in the kinetics of NSD when signal

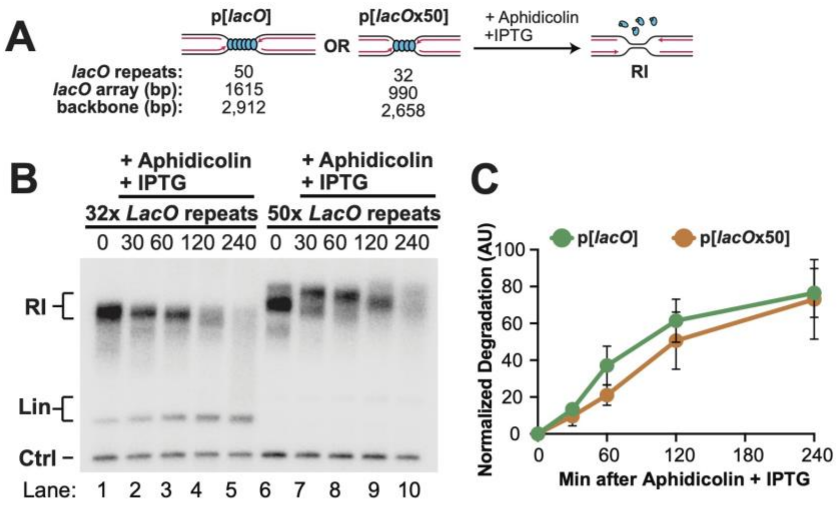

Figure AA.4. Proximity of converging forks has no effect on NSD
(A) Plasmid DNA harboring a 32xlacO array (p[lacO]) or a 50xlacO array (p[lacOx50]) was incubated with LacR then replicated in Xenopus egg extracts. Once forks were localized to the LacR barrier, NSD was induced by addition of IPTG and aphidicolin. Purified DNA was subjected to restriction digest so that replication fork structures (RIs) could be visualized. (B) Samples from (A) were separated on an agarose gel and visualized by autoradiography. (C) Quantification of the amount of DNA degraded in (B). Normalized degradation accounts for the different backbone sizes of the 50x and 32x lacO plasmids. Mean ± S.D., n=3 independent experiments.

was normalized to total degradation (Figure AA.4 (C)). Therefore, these data show that the proximity of the converging forks does not affect NSD.

REFERENCES

1. Achar, Y. J., Balogh, D., & Haracska, L. (2011). Coordinated protein and DNA remodeling by human HLTF on stalled replication fork. *Proc Natl Acad Sci U S A*, *108*(34), 14073-14078. https://doi.org/10.1073/pnas.1101951108

2. Amunugama, R., Willcox, S., Wu, R. A., Abdullah, U. B., El-Sagheer, A. H., Brown, T., McHugh, P. J., Griffith, J. D., & Walter, J. C. (2018). Replication Fork Reversal during DNA Interstrand Crosslink Repair Requires CMG Unloading. *Cell Rep*, *23*(12), 3419-3428. https://doi.org/10.1016/j.celrep.2018.05.061

3. Arias, E. E., & Walter, J. C. (2005). Replication-dependent destruction of Cdt1 limits DNA replication to a single round per cell cycle in Xenopus egg extracts. *Genes Dev*, *19*(1), 114-126. https://doi.org/10.1101/gad.1255805

4. Bai, G., Kermi, C., Stoy, H., Schiltz, C. J., Bacal, J., Zaino, A. M., Hadden, M. K., Eichman, B. F., Lopes, M., & Cimprich, K. A. (2020). HLTF Promotes Fork Reversal, Limiting Replication Stress Resistance and Preventing Multiple Mechanisms of Unrestrained DNA Synthesis. *Mol Cell*, *78*(6), 1237-1251 e1237. https://doi.org/10.1016/j.molcel.2020.04.031

5. Bansbach, C. E., Betous, R., Lovejoy, C. A., Glick, G. G., & Cortez, D. (2009). The annealing helicase SMARCAL1 maintains genome integrity at stalled replication forks. *Genes Dev*, *23*(20), 2405-2414. https://doi.org/10.1101/gad.1839909

6. Berti, M., Cortez, D., & Lopes, M. (2020). The plasticity of DNA replication forks in response to clinically relevant genotoxic stress. *Nat Rev Mol Cell Biol*, *21*(10), 633-651. https://doi.org/10.1038/s41580-020-0257-5

7. Berti, M., Teloni, F., Mijic, S., Ursich, S., Fuchs, J., Palumbieri, M. D., Krietsch, J., Schmid, J. A., Garcin, E. B., Gon, S., Modesti, M., Altmeyer, M., & Lopes, M. (2020). Sequential role of RAD51 paralog complexes in replication fork remodeling and restart. *Nat Commun*, *11*(1), 3531. https://doi.org/10.1038/s41467-020-17324-z

8. Betous, R., Mason, A. C., Rambo, R. P., Bansbach, C. E., Badu-Nkansah, A., Sirbu, B. M., Eichman, B. F., & Cortez, D. (2012). SMARCAL1 catalyzes fork regression and Holliday junction migration to maintain genome stability during DNA replication. *Genes Dev*, *26*(2), 151-162. https://doi.org/10.1101/gad.178459.111

9. Bhat, K. P., & Cortez, D. (2018). RPA and RAD51: fork reversal, fork protection, and genome stability. *Nat Struct Mol Biol*, *25*(6), 446-453. https://doi.org/10.1038/s41594-018-0075-z

10. Bhat, K. P., Krishnamoorthy, A., Dungrawala, H., Garcin, E. B., Modesti, M., & Cortez, D. (2018). RADX Modulates RAD51 Activity to Control Replication Fork Protection. *Cell Rep*, *24*(3), 538-545. https://doi.org/10.1016/j.celrep.2018.06.061

11. Bianchi, V., Pontis, E., & Reichard, P. (1986). Changes of deoxyribonucleoside triphosphate pools induced by hydroxyurea and their relation to DNA synthesis. *J Biol Chem*, *261*(34), 16037-16042. https://www.ncbi.nlm.nih.gov/pubmed/3536919

12. Bianco, J. N., Poli, J., Saksouk, J., Bacal, J., Silva, M. J., Yoshida, K., Lin, Y. L., Tourriere, H., Lengronne, A., & Pasero, P. (2012). Analysis of DNA replication profiles in budding yeast and mammalian cells using DNA combing. *Methods*, *57*(2), 149-157. https://doi.org/10.1016/j.ymeth.2012.04.007

13. Bochman, M. L., & Schwacha, A. (2015). DNA replication: Strand separation unravelled. *Nature*, *524*(7564), 166-167. https://doi.org/10.1038/nature14643

14. Branzei, D., & Foiani, M. (2010). Maintaining genome stability at the replication fork. *Nat Rev Mol Cell Biol*, *11*(3), 208-219. https://doi.org/10.1038/nrm2852

15. Byun, T. S., Pacek, M., Yee, M. C., Walter, J. C., & Cimprich, K. A. (2005). Functional uncoupling of MCM helicase and DNA polymerase activities activates the ATR-dependent checkpoint. *Genes Dev*, *19*(9), 1040-1052. https://doi.org/10.1101/gad.1301205

16. Chaudhury, I., Stroik, D. R., & Sobeck, A. (2014). FANCD2-controlled chromatin access of the Fanconi-associated nuclease FAN1 is crucial for the recovery of stalled replication forks. *Mol Cell Biol*, *34*(21), 3939-3954. https://doi.org/10.1128/MCB.00457-14

17. Chiolo, I., Saponaro, M., Baryshnikova, A., Kim, J. H., Seo, Y. S., & Liberi, G. (2007). The human F-Box DNA helicase FBH1 faces Saccharomyces cerevisiae Srs2 and postreplication repair pathway roles. *Mol Cell Biol*, *27*(21), 7439-7450. https://doi.org/10.1128/MCB.00963-07

18. Cho, W. H., Kang, Y. H., An, Y. Y., Tappin, I., Hurwitz, J., & Lee, J. K. (2013). Human Tim-Tipin complex affects the biochemical properties of the replicative DNA helicase and DNA polymerases. *Proc Natl Acad Sci U S A*, *110*(7), 2523-2527. https://doi.org/10.1073/pnas.1222494110

19. Chou, D. M., & Elledge, S. J. (2006). Tipin and Timeless form a mutually protective complex required for genotoxic stress resistance and checkpoint

function. *Proc Natl Acad Sci U S A*, *103*(48), 18143-18147. https://doi.org/10.1073/pnas.0609251103

20. Chu, W. K., Payne, M. J., Beli, P., Hanada, K., Choudhary, C., & Hickson, I. D. (2015). FBH1 influences DNA replication fork stability and homologous recombination through ubiquitylation of RAD51. *Nat Commun*, *6*, 5931. https://doi.org/10.1038/ncomms6931

21. Ciccia, A., Bredemeyer, A. L., Sowa, M. E., Terret, M. E., Jallepalli, P. V., Harper, J. W., & Elledge, S. J. (2009). The SIOD disorder protein SMARCAL1 is an RPA-interacting protein involved in replication fork restart. *Genes Dev*, *23*(20), 2415-2425. https://doi.org/10.1101/gad.1832309

22. Ciccia, A., Nimonkar, A. V., Hu, Y., Hajdu, I., Achar, Y. J., Izhar, L., Petit, S. A., Adamson, B., Yoon, J. C., Kowalczykowski, S. C., Livingston, D. M., Haracska, L., & Elledge, S. J. (2012). Polyubiquitinated PCNA recruits the ZRANB3 translocase to maintain genomic integrity after replication stress. *Mol Cell*, *47*(3), 396-409. https://doi.org/10.1016/j.molcel.2012.05.024

23. Cong, K., Peng, M., Kousholt, A. N., Lee, W. T. C., Lee, S., Nayak, S., Krais, J., VanderVere-Carozza, P. S., Pawelczak, K. S., Calvo, J., Panzarino, N. J., Turchi, J. J., Johnson, N., Jonkers, J., Rothenberg, E., & Cantor, S. B. (2021). Replication gaps are a key determinant of PARP inhibitor synthetic lethality with BRCA deficiency. *Mol Cell*, *81*(15), 3227. https://doi.org/10.1016/j.molcel.2021.07.015

24. Coquel, F., Silva, M. J., Techer, H., Zadorozhny, K., Sharma, S., Nieminuszczy, J., Mettling, C., Dardillac, E., Barthe, A., Schmitz, A. L., Promonet, A., Cribier, A., Sarrazin, A., Niedzwiedz, W., Lopez, B., Costanzo, V., Krejci, L., Chabes, A., Benkirane, M., . . . Pasero, P. (2018). SAMHD1 acts at stalled replication forks to prevent interferon induction. *Nature*, *557*(7703), 57-61. https://doi.org/10.1038/s41586-018-0050-1

25. Cortez, D. (2019). Replication-Coupled DNA Repair. *Mol Cell*, *74*(5), 866-876. https://doi.org/10.1016/j.molcel.2019.04.027

26. Costanzo, V. (2011). Brca2, Rad51 and Mre11: performing balancing acts on replication forks. *DNA Repair (Amst)*, *10*(10), 1060-1065. https://doi.org/10.1016/j.dnarep.2011.07.009

27. Couch, F. B., Bansbach, C. E., Driscoll, R., Luzwick, J. W., Glick, G. G., Betous, R., Carroll, C. M., Jung, S. Y., Qin, J., Cimprich, K. A., & Cortez, D. (2013). ATR phosphorylates SMARCAL1 to prevent replication fork collapse. *Genes Dev*, *27*(14), 1610-1623. https://doi.org/10.1101/gad.214080.113

28. Deegan, T. D., Mukherjee, P. P., Fujisawa, R., Polo Rivera, C., & Labib, K. (2020). CMG helicase disassembly is controlled by replication fork DNA, replisome components and a ubiquitin threshold. *Elife*, *9*. https://doi.org/10.7554/eLife.60371

29. Deng, L., Wu, R. A., Sonneville, R., Kochenova, O. V., Labib, K., Pellman, D., & Walter, J. C. (2019). Mitotic CDK Promotes Replisome Disassembly, Fork Breakage, and Complex DNA Rearrangements. *Mol Cell*, *73*(5), 915-929 e916. https://doi.org/10.1016/j.molcel.2018.12.021

30. Dewar, J. M., Budzowska, M., & Walter, J. C. (2015). The mechanism of DNA replication termination in vertebrates. *Nature*, *525*(7569), 345-350. https://doi.org/10.1038/nature14887

31. Dewar, J. M., Low, E., Mann, M., Raschle, M., & Walter, J. C. (2017). CRL2(Lrr1) promotes unloading of the vertebrate replisome from chromatin during replication termination. *Genes Dev*, *31*(3), 275-290. https://doi.org/10.1101/gad.291799.116

32. Dewar, J. M., & Walter, J. C. (2017). Mechanisms of DNA replication termination. *Nat Rev Mol Cell Biol*, *18*(8), 507-516. https://doi.org/10.1038/nrm.2017.42

33. Dias, M. P., Moser, S. C., Ganesan, S., & Jonkers, J. (2021). Understanding and overcoming resistance to PARP inhibitors in cancer therapy. *Nat Rev Clin Oncol*, *18*(12), 773-791. https://doi.org/10.1038/s41571-021-00532-x

34. Ding, X., Ray Chaudhuri, A., Callen, E., Pang, Y., Biswas, K., Klarmann, K. D., Martin, B. K., Burkett, S., Cleveland, L., Stauffer, S., Sullivan, T., Dewan, A., Marks, H., Tubbs, A. T., Wong, N., Buehler, E., Akagi, K., Martin, S. E., Keller, J. R., . . . Sharan, S. K. (2016). Synthetic viability by BRCA2 and PARP1/ARTD1 deficiencies. *Nat Commun*, *7*, 12425. https://doi.org/10.1038/ncomms12425

35. Dungrawala, H., Bhat, K. P., Le Meur, R., Chazin, W. J., Ding, X., Sharan, S. K., Wessel, S. R., Sathe, A. A., Zhao, R., & Cortez, D. (2017). RADX Promotes Genome Stability and Modulates Chemosensitivity by Regulating RAD51 at Replication Forks. *Mol Cell*, *67*(3), 374-386.e375. https://doi.org/10.1016/j.molcel.2017.06.023

36. Dungrawala, H., Rose, K. L., Bhat, K. P., Mohni, K. N., Glick, G. G., Couch, F. B., & Cortez, D. (2015). The Replication Checkpoint Prevents Two Types of Fork Collapse without Regulating Replisome Stability. *Mol Cell*, *59*(6), 998-1010. https://doi.org/10.1016/j.molcel.2015.07.030

37. Errico, A., Aze, A., & Costanzo, V. (2014). Mta2 promotes Tipin-dependent maintenance of replication fork integrity. *Cell Cycle*, *13*(13), 2120-2128. https://doi.org/10.4161/cc.29157

38. Errico, A., Costanzo, V., & Hunt, T. (2007). Tipin is required for stalled replication forks to resume DNA replication after removal of aphidicolin in Xenopus egg extracts. *Proc Natl Acad Sci U S A*, *104*(38), 14929-14934. https://doi.org/10.1073/pnas.0706347104

39. Espana-Agusti, J., Warren, A., Chew, S. K., Adams, D. J., & Matakidou, A. (2017). Loss of PBRM1 rescues VHL dependent replication stress to promote renal carcinogenesis. *Nat Commun*, *8*(1), 2026. https://doi.org/10.1038/s41467-017-02245-1

40. Evrin, C., Clarke, P., Zech, J., Lurz, R., Sun, J., Uhle, S., Li, H., Stillman, B., & Speck, C. (2009). A double-hexameric MCM2-7 complex is loaded onto origin DNA during licensing of eukaryotic DNA replication. *Proc Natl Acad Sci U S A*, *106*(48), 20240-20245. https://doi.org/10.1073/pnas.0911500106

41. Feng, W., & Jasin, M. (2017). BRCA2 suppresses replication stress-induced mitotic and G1 abnormalities through homologous recombination. *Nat Commun*, *8*(1), 525. https://doi.org/10.1038/s41467-017-00634-0

42. Fugger, K., Mistrik, M., Neelsen, K. J., Yao, Q., Zellweger, R., Kousholt, A. N., Haahr, P., Chu, W. K., Bartek, J., Lopes, M., Hickson, I. D., & Sorensen, C. S. (2015). FBH1 Catalyzes Regression of Stalled Replication Forks. *Cell Rep*, *10*(10), 1749-1757. https://doi.org/10.1016/j.celrep.2015.02.028

43. Gambus, A., van Deursen, F., Polychronopoulos, D., Foltman, M., Jones, R. C., Edmondson, R. D., Calzada, A., & Labib, K. (2009). A key role for Ctf4 in coupling the MCM2-7 helicase to DNA polymerase alpha within the eukaryotic replisome. *EMBO J*, *28*(19), 2992-3004. https://doi.org/10.1038/emboj.2009.226

44. Georgescu, R., Yuan, Z., Bai, L., de Luna Almeida Santos, R., Sun, J., Zhang, D., Yurieva, O., Li, H., & O'Donnell, M. E. (2017). Structure of eukaryotic CMG helicase at a replication fork and implications to replisome architecture and origin initiation. *Proc Natl Acad Sci U S A*, *114*(5), E697-E706. https://doi.org/10.1073/pnas.1620500114

45. Graham, J. E., Marians, K. J., & Kowalczykowski, S. C. (2017). Independent and Stochastic Action of DNA Polymerases in the Replisome. *Cell*, *169*(7), 1201-1213 e1217. https://doi.org/10.1016/j.cell.2017.05.041

46. Halder, S., Sanchez, A., Ranjha, L., Reginato, G., Ceppi, I., Acharya, A., Anand, R., & Cejka, P. (2022). Double-stranded DNA binding function of RAD51 in DNA protection and its regulation by BRCA2. *Mol Cell*. https://doi.org/10.1016/j.molcel.2022.08.014

47. Han, T., Goralski, M., Capota, E., Padrick, S. B., Kim, J., Xie, Y., & Nijhawan, D. (2016). The antitumor toxin CD437 is a direct inhibitor of DNA polymerase alpha. *Nat Chem Biol*, *12*(7), 511-515. https://doi.org/10.1038/nchembio.2082

48. Hashimoto, Y., Ray Chaudhuri, A., Lopes, M., & Costanzo, V. (2010). Rad51 protects nascent DNA from Mre11-dependent degradation and promotes continuous DNA synthesis. *Nat Struct Mol Biol*, *17*(11), 1305-1311. https://doi.org/10.1038/nsmb.1927

49. He, Y. J., Meghani, K., Caron, M. C., Yang, C., Ronato, D. A., Bian, J., Sharma, A., Moore, J., Niraj, J., Detappe, A., Doench, J. G., Legube, G., Root, D. E., D'Andrea, A. D., Drané, P., De, S., Konstantinopoulos, P. A., Masson, J. Y., & Chowdhury, D. (2018). DYNLL1 binds to MRE11 to limit DNA end resection in BRCA1-deficient cells. *Nature*, *563*(7732), 522-526. https://doi.org/10.1038/s41586-018-0670-5

50. Heintzman, D. R., Campos, L. V., Byl, J. A. W., Osheroff, N., & Dewar, J. M. (2019). Topoisomerase II Is Crucial for Fork Convergence during Vertebrate Replication Termination. *Cell Rep*, *29*(2), 422-436 e425. https://doi.org/10.1016/j.celrep.2019.08.097

51. Higgins, N. P., Kato, K., & Strauss, B. (1976). A model for replication repair in mammalian cells. *Journal of Molecular Biology*, *101*(3), 417-425. https://doi.org/https://doi.org/10.1016/0022-2836(76)90156-X

52. Higgs, M. R., Reynolds, J. J., Winczura, A., Blackford, A. N., Borel, V., Miller, E. S., Zlatanou, A., Nieminuszczy, J., Ryan, E. L., Davies, N. J., Stankovic, T., Boulton, S. J., Niedzwiedz, W., & Stewart, G. S. (2015). BOD1L Is Required to Suppress Deleterious Resection of Stressed Replication Forks. *Mol Cell*, *59*(3), 462-477. https://doi.org/10.1016/j.molcel.2015.06.007

53. Higgs, M. R., & Stewart, G. S. (2016). Protection or resection: BOD1L as a novel replication fork protection factor. *Nucleus*, *7*(1), 34-40. https://doi.org/10.1080/19491034.2016.1143183

54. Hishiki, A., Hara, K., Ikegaya, Y., Yokoyama, H., Shimizu, T., Sato, M., & Hashimoto, H. (2015). Structure of a Novel DNA-binding Domain of Helicase-like Transcription Factor (HLTF) and Its Functional Implication in DNA Damage Tolerance. *J Biol Chem*, *290*(21), 13215-13223. https://doi.org/10.1074/jbc.M115.643643

55. Holloman, W. K. (2011). Unraveling the mechanism of BRCA2 in homologous recombination. *Nat Struct Mol Biol*, *18*(7), 748-754. https://doi.org/10.1038/nsmb.2096

56. Ikegami, S., Taguchi, T., Ohashi, M., Oguro, M., Nagano, H., & Mano, Y. (1978). Aphidicolin prevents mitotic cell division by interfering with the activity of DNA polymerase-alpha. *Nature*, *275*(5679), 458-460. https://doi.org/10.1038/275458a0

57. Ilves, I., Petojevic, T., Pesavento, J. J., & Botchan, M. R. (2010). Activation of the MCM2-7 helicase by association with Cdc45 and GINS proteins. *Mol Cell*, *37*(2), 247-258. https://doi.org/10.1016/j.molcel.2009.12.030

58. Kavlashvili, T., & Dewar, J. M. (2022). Approaches to Monitor Termination of DNA Replication Using Xenopus Egg Extracts. *Methods Mol Biol*, *2444*, 105-123. https://doi.org/10.1007/978-1-0716-2063-2_7

59. Kile, A. C., Chavez, D. A., Bacal, J., Eldirany, S., Korzhnev, D. M., Bezsonova, I., Eichman, B. F., & Cimprich, K. A. (2015). HLTF's Ancient HIRAN Domain Binds 3' DNA Ends to Drive Replication Fork Reversal. *Mol Cell*, *58*(6), 1090-1100. https://doi.org/10.1016/j.molcel.2015.05.013

60. Klein Douwel, D., Boonen, R. A., Long, D. T., Szypowska, A. A., Raschle, M., Walter, J. C., & Knipscheer, P. (2014). XPF-ERCC1 acts in Unhooking DNA interstrand crosslinks in cooperation with FANCD2 and FANCP/SLX4. *Mol Cell*, *54*(3), 460-471. https://doi.org/10.1016/j.molcel.2014.03.015

61. Kolinjivadi, A. M., Sannino, V., De Antoni, A., Zadorozhny, K., Kilkenny, M., Técher, H., Baldi, G., Shen, R., Ciccia, A., Pellegrini, L., Krejci, L., & Costanzo, V. (2017). Smarcal1-Mediated Fork Reversal Triggers Mre11-Dependent Degradation of Nascent DNA in the Absence of Brca2 and Stable Rad51 Nucleofilaments. *Mol Cell*, *67*(5), 867-881.e867. https://doi.org/10.1016/j.molcel.2017.07.001

62. Kose, H. B., Xie, S., Cameron, G., Strycharska, M. S., & Yardimci, H. (2020). Duplex DNA engagement and RPA oppositely regulate the DNA-unwinding rate of CMG helicase. *Nat Commun*, *11*(1), 3713. https://doi.org/10.1038/s41467-020-17443-7

63. Kunkel, T. A., & Bebenek, K. (2000). DNA replication fidelity. *Annu Rev Biochem*, *69*, 497-529. https://doi.org/10.1146/annurev.biochem.69.1.497

64. Langston, L., & O'Donnell, M. (2017). Action of CMG with strand-specific DNA blocks supports an internal unwinding mode for the eukaryotic replicative helicase. *Elife*, *6*. https://doi.org/10.7554/eLife.23449

65. Lebofsky, R., Takahashi, T., & Walter, J. C. (2009). DNA replication in nucleus-free Xenopus egg extracts. *Methods Mol Biol*, *521*, 229-252. https://doi.org/10.1007/978-1-60327-815-7_13

66. Lemacon, D., Jackson, J., Quinet, A., Brickner, J. R., Li, S., Yazinski, S., You, Z., Ira, G., Zou, L., Mosammaparast, N., & Vindigni, A. (2017). MRE11 and EXO1 nucleases degrade reversed forks and elicit MUS81-dependent fork rescue in BRCA2-deficient cells. *Nat Commun*, *8*(1), 860. https://doi.org/10.1038/s41467-017-01180-5

67. Li, N., Zhai, Y., Zhang, Y., Li, W., Yang, M., Lei, J., Tye, B. K., & Gao, N. (2015). Structure of the eukaryotic MCM complex at 3.8 A. *Nature*, *524*(7564), 186-191. https://doi.org/10.1038/nature14685

68. Liao, H., Ji, F., Helleday, T., & Ying, S. (2018). Mechanisms for stalled replication fork stabilization: new targets for synthetic lethality strategies in cancer treatments. *EMBO Rep*, *19*(9). https://doi.org/10.15252/embr.201846263

69. Liu, W., Krishnamoorthy, A., Zhao, R., & Cortez, D. (2020). Two replication fork remodeling pathways generate nuclease substrates for distinct fork protection factors. *Sci Adv*, *6*(46). https://doi.org/10.1126/sciadv.abc3598

70. Liu, W., Zhou, M., Li, Z., Li, H., Polaczek, P., Dai, H., Wu, Q., Liu, C., Karanja, K. K., Popuri, V., Shan, S. O., Schlacher, K., Zheng, L., Campbell, J. L., & Shen, B. (2016). A Selective Small Molecule DNA2 Inhibitor for Sensitization of Human Cancer Cells to Chemotherapy. *EBioMedicine*, *6*, 73-86. https://doi.org/10.1016/j.ebiom.2016.02.043

71. Low, E., Chistol, G., Zaher, M. S., Kochenova, O. V., & Walter, J. C. (2020). The DNA replication fork suppresses CMG unloading from chromatin before termination. *Genes Dev*, *34*(21-22), 1534-1545. https://doi.org/10.1101/gad.339739.120

72. Michael, W. M., Ott, R., Fanning, E., & Newport, J. (2000). Activation of the DNA replication checkpoint through RNA synthesis by primase. *Science*, *289*(5487), 2133-2137. https://doi.org/10.1126/science.289.5487.2133

73. Mijic, S., Zellweger, R., Chappidi, N., Berti, M., Jacobs, K., Mutreja, K., Ursich, S., Ray Chaudhuri, A., Nussenzweig, A., Janscak, P., & Lopes, M. (2017). Replication fork reversal triggers fork degradation in BRCA2-defective cells. *Nat Commun*, *8*(1), 859. https://doi.org/10.1038/s41467-017-01164-5

74. Moore, G., Jimenez Sainz, J., & Jensen, R. B. (2022). DNA fiber combing protocol using in-house reagents and coverslips to analyze replication fork dynamics in mammalian cells. *STAR Protoc*, *3*(2), 101371. https://doi.org/10.1016/j.xpro.2022.101371

75. Moretton, A., & Loizou, J. I. (2020). Interplay between Cellular Metabolism and the DNA Damage Response in Cancer. *Cancers (Basel)*, *12*(8). https://doi.org/10.3390/cancers12082051

76. Mutreja, K., Krietsch, J., Hess, J., Ursich, S., Berti, M., Roessler, F. K., Zellweger, R., Patra, M., Gasser, G., & Lopes, M. (2018). ATR-Mediated Global Fork Slowing and Reversal Assist Fork Traverse and Prevent Chromosomal Breakage at DNA Interstrand Cross-Links. *Cell Rep*, *24*(10), 2629-2642 e2625. https://doi.org/10.1016/j.celrep.2018.08.019

77. Nedelcheva, M. N., Roguev, A., Dolapchiev, L. B., Shevchenko, A., Taskov, H. B., Shevchenko, A., Stewart, A. F., & Stoynov, S. S. (2005). Uncoupling of unwinding from DNA synthesis implies regulation of MCM helicase by Tof1/Mrc1/Csm3 checkpoint complex. *J Mol Biol*, *347*(3), 509-521. https://doi.org/10.1016/j.jmb.2005.01.041

78. Negrini, S., Gorgoulis, V. G., & Halazonetis, T. D. (2010). Genomic instability--an evolving hallmark of cancer. *Nat Rev Mol Cell Biol*, *11*(3), 220-228. https://doi.org/10.1038/nrm2858

79. Nieminuszczy, J., Broderick, R., Bellani, M. A., Smethurst, E., Schwab, R. A., Cherdyntseva, V., Evmorfopoulou, T., Lin, Y. L., Minczuk, M., Pasero, P., Gagos, S., Seidman, M. M., & Niedzwiedz, W. (2019). EXD2 Protects Stressed Replication Forks and Is Required for Cell Viability in the Absence of BRCA1/2. *Mol Cell*, *75*(3), 605-619 e606. https://doi.org/10.1016/j.molcel.2019.05.026

80. O'Donnell, M., Langston, L., & Stillman, B. (2013). Principles and concepts of DNA replication in bacteria, archaea, and eukarya. *Cold Spring Harb Perspect Biol*, *5*(7). https://doi.org/10.1101/cshperspect.a010108

81. Panzarino, N. J., Krais, J. J., Cong, K., Peng, M., Mosqueda, M., Nayak, S. U., Bond, S. M., Calvo, J. A., Doshi, M. B., Bere, M., Ou, J., Deng, B., Zhu, L. J., Johnson, N., & Cantor, S. B. (2021). Replication Gaps Underlie BRCA Deficiency and Therapy Response. *Cancer Res*, *81*(5), 1388-1397. https://doi.org/10.1158/0008-5472.CAN-20-1602

82. Paudyal, S. C., Li, S., Yan, H., Hunter, T., & You, Z. (2017). Dna2 initiates resection at clean DNA double-strand breaks. *Nucleic Acids Res*, *45*(20), 11766-11781. https://doi.org/10.1093/nar/gkx830

83. Pellegrini, L. (2012). The Pol alpha-primase complex. *Subcell Biochem*, *62*, 157-169. https://doi.org/10.1007/978-94-007-4572-8_9

84. Poole, L. A., & Cortez, D. (2017). Functions of SMARCAL1, ZRANB3, and HLTF in maintaining genome stability. *Crit Rev Biochem Mol Biol*, *52*(6), 696-714. https://doi.org/10.1080/10409238.2017.1380597

85. Przetocka, S., Porro, A., Bolck, H. A., Walker, C., Lezaja, A., Trenner, A., von Aesch, C., Himmels, S. F., D'Andrea, A. D., Ceccaldi, R., Altmeyer, M., & Sartori, A. A. (2018a). CtIP-Mediated Fork Protection Synergizes with BRCA1 to Suppress Genomic Instability upon DNA Replication Stress. *Mol Cell*, *72*(3), 568-582 e566. https://doi.org/10.1016/j.molcel.2018.09.014

86. Przetocka, S., Porro, A., Bolck, H. A., Walker, C., Lezaja, A., Trenner, A., von Aesch, C., Himmels, S. F., D'Andrea, A. D., Ceccaldi, R., Altmeyer, M., & Sartori, A. A. (2018b). CtIP-Mediated Fork Protection Synergizes with BRCA1 to Suppress Genomic Instability upon DNA Replication Stress. *Mol Cell*, *72*(3), 568-582.e566. https://doi.org/10.1016/j.molcel.2018.09.014

87. Quinet, A., Lemaçon, D., & Vindigni, A. (2017). Replication Fork Reversal: Players and Guardians. *Mol Cell*, *68*(5), 830-833. https://doi.org/10.1016/j.molcel.2017.11.022

88. Rastogi, R. P., Richa, Kumar, A., Tyagi, M. B., & Sinha, R. P. (2010). Molecular mechanisms of ultraviolet radiation-induced DNA damage and repair. *J Nucleic Acids*, *2010*, 592980. https://doi.org/10.4061/2010/592980

89. Ray Chaudhuri, A., Callen, E., Ding, X., Gogola, E., Duarte, A. A., Lee, J. E., Wong, N., Lafarga, V., Calvo, J. A., Panzarino, N. J., John, S., Day, A., Crespo, A. V., Shen, B., Starnes, L. M., de Ruiter, J. R., Daniel, J. A., Konstantinopoulos, P. A., Cortez, D., . . . Nussenzweig, A. (2016). Replication fork stability confers chemoresistance in BRCA-deficient cells. *Nature*, *535*(7612), 382-387. https://doi.org/10.1038/nature18325

90. Rickman, K. A., Noonan, R. J., Lach, F. P., Sridhar, S., Wang, A. T., Abhyankar, A., Huang, A., Kelly, M., Auerbach, A. D., & Smogorzewska, A. (2020). Distinct roles of BRCA2 in replication fork protection in response to hydroxyurea and DNA interstrand cross-links. *Genes Dev*, *34*(11-12), 832-846. https://doi.org/10.1101/gad.336446.120

91. Santivasi, W. L., & Xia, F. (2014). Ionizing radiation-induced DNA damage, response, and repair. *Antioxid Redox Signal*, *21*(2), 251-259. https://doi.org/10.1089/ars.2013.5668

92. Schlacher, K., Christ, N., Siaud, N., Egashira, A., Wu, H., & Jasin, M. (2011). Double-strand break repair-independent role for BRCA2 in blocking stalled replication fork degradation by MRE11. *Cell*, *145*(4), 529-542. https://doi.org/10.1016/j.cell.2011.03.041

93. Schlacher, K., Wu, H., & Jasin, M. (2012). A distinct replication fork protection pathway connects Fanconi anemia tumor suppressors to RAD51-BRCA1/2. *Cancer Cell*, *22*(1), 106-116. https://doi.org/10.1016/j.ccr.2012.05.015

94. Somyajit, K., Gupta, R., Sedlackova, H., Neelsen, K. J., Ochs, F., Rask, M. B., Choudhary, C., & Lukas, J. (2017). Redox-sensitive alteration of replisome architecture safeguards genome integrity. *Science*, *358*(6364), 797-802. https://doi.org/10.1126/science.aao3172

95. Somyajit, K., Spies, J., Coscia, F., Kirik, U., Rask, M. B., Lee, J. H., Neelsen, K. J., Mund, A., Jensen, L. J., Paull, T. T., Mann, M., & Lukas, J. (2021). Homology-directed repair protects the replicating genome from metabolic assaults. *Dev Cell*, *56*(4), 461-477 e467. https://doi.org/10.1016/j.devcel.2021.01.011

96. Sparks, J. L., Chistol, G., Gao, A. O., Raschle, M., Larsen, N. B., Mann, M., Duxin, J. P., & Walter, J. C. (2019). The CMG Helicase Bypasses DNA-Protein Cross-Links to Facilitate Their Repair. *Cell*, *176*(1-2), 167-181 e121. https://doi.org/10.1016/j.cell.2018.10.053

97. Sturzenegger, A., Burdova, K., Kanagaraj, R., Levikova, M., Pinto, C., Cejka, P., & Janscak, P. (2014). DNA2 cooperates with the WRN and BLM RecQ helicases to mediate long-range DNA end resection in human cells. *J Biol Chem*, *289*(39), 27314-27326. https://doi.org/10.1074/jbc.M114.578823

98. Sun, J., Shi, Y., Georgescu, R. E., Yuan, Z., Chait, B. T., Li, H., & O'Donnell, M. E. (2015). The architecture of a eukaryotic replisome. *Nat Struct Mol Biol*, *22*(12), 976-982. https://doi.org/10.1038/nsmb.3113

99. Taglialatela, A., Alvarez, S., Leuzzi, G., Sannino, V., Ranjha, L., Huang, J. W., Madubata, C., Anand, R., Levy, B., Rabadan, R., Cejka, P., Costanzo, V., & Ciccia, A. (2017). Restoration of Replication Fork Stability in BRCA1- and BRCA2-Deficient Cells by Inactivation of SNF2-Family Fork Remodelers. *Mol Cell*, *68*(2), 414-430.e418. https://doi.org/10.1016/j.molcel.2017.09.036

100. Thangavel, S., Berti, M., Levikova, M., Pinto, C., Gomathinayagam, S., Vujanovic, M., Zellweger, R., Moore, H., Lee, E. H., Hendrickson, E. A., Cejka, P., Stewart, S., Lopes, M., & Vindigni, A. (2015). DNA2 drives processing and restart of reversed replication forks in human cells. *J Cell Biol*, *208*(5), 545-562. https://doi.org/10.1083/jcb.201406100

101. Tian, T., Bu, M., Chen, X., Ding, L., Yang, Y., Han, J., Feng, X. H., Xu, P., Liu, T., Ying, S., Lei, Y., Li, Q., & Huang, J. (2021). The ZATT-TOP2A-PICH Axis Drives Extensive Replication Fork Reversal to Promote Genome Stability. *Mol Cell*, *81*(1), 198-211 e196. https://doi.org/10.1016/j.molcel.2020.11.007

102. Toledo, L. I., Altmeyer, M., Rask, M. B., Lukas, C., Larsen, D. H., Povlsen, L. K., Bekker-Jensen, S., Mailand, N., Bartek, J., & Lukas, J. (2013). ATR

prohibits replication catastrophe by preventing global exhaustion of RPA. *Cell*, *155*(5), 1088-1103. https://doi.org/10.1016/j.cell.2013.10.043

103. Unk, I., Hajdu, I., Fatyol, K., Hurwitz, J., Yoon, J. H., Prakash, L., Prakash, S., & Haracska, L. (2008). Human HLTF functions as a ubiquitin ligase for proliferating cell nuclear antigen polyubiquitination. *Proc Natl Acad Sci U S A*, *105*(10), 3768-3773. https://doi.org/10.1073/pnas.0800563105

104. Vaitsiankova, A., Burdova, K., Sobol, M., Gautam, A., Benada, O., Hanzlikova, H., & Caldecott, K. W. (2022). PARP inhibition impedes the maturation of nascent DNA strands during DNA replication. *Nat Struct Mol Biol*, *29*(4), 329-338. https://doi.org/10.1038/s41594-022-00747-1

105. Vujanovic, M., Krietsch, J., Raso, M. C., Terraneo, N., Zellweger, R., Schmid, J. A., Taglialatela, A., Huang, J. W., Holland, C. L., Zwicky, K., Herrador, R., Jacobs, H., Cortez, D., Ciccia, A., Penengo, L., & Lopes, M. (2017). Replication Fork Slowing and Reversal upon DNA Damage Require PCNA Polyubiquitination and ZRANB3 DNA Translocase Activity. *Mol Cell*, *67*(5), 882-890.e885. https://doi.org/10.1016/j.molcel.2017.08.010

106. Waga, S., Masuda, T., Takisawa, H., & Sugino, A. (2001). DNA polymerase epsilon is required for coordinated and efficient chromosomal DNA replication in Xenopus egg extracts. *Proc Natl Acad Sci U S A*, *98*(9), 4978-4983. https://doi.org/10.1073/pnas.081088798

107. Walter, J., Sun, L., & Newport, J. (1998). Regulated chromosomal DNA replication in the absence of a nucleus. *Mol Cell*, *1*(4), 519-529. https://doi.org/10.1016/s1097-2765(00)80052-0

108. Wasserman, M. R., Schauer, G. D., O'Donnell, M. E., & Liu, S. (2019). Replication Fork Activation Is Enabled by a Single-Stranded DNA Gate in CMG Helicase. *Cell*, *178*(3), 600-611 e616. https://doi.org/10.1016/j.cell.2019.06.032

109. Weston, R., Peeters, H., & Ahel, D. (2012). ZRANB3 is a structure-specific ATP-dependent endonuclease involved in replication stress response. *Genes Dev*, *26*(14), 1558-1572. https://doi.org/10.1101/gad.193516.112

110. Wong, R. P., Garcia-Rodriguez, N., Zilio, N., Hanulova, M., & Ulrich, H. D. (2020). Processing of DNA Polymerase-Blocking Lesions during Genome Replication Is Spatially and Temporally Segregated from Replication Forks. *Mol Cell*, *77*(1), 3-16 e14. https://doi.org/10.1016/j.molcel.2019.09.015

111. Xu, S., Wu, X., Wu, L., Castillo, A., Liu, J., Atkinson, E., Paul, A., Su, D., Schlacher, K., Komatsu, Y., You, M. J., & Wang, B. (2017). Abro1 maintains genome stability and limits replication stress by protecting replication fork stability. *Genes Dev*, *31*(14), 1469-1482. https://doi.org/10.1101/gad.299172.117

112. Yazinski, S. A., Comaills, V., Buisson, R., Genois, M. M., Nguyen, H. D., Ho, C. K., Todorova Kwan, T., Morris, R., Lauffer, S., Nussenzweig, A., Ramaswamy, S., Benes, C. H., Haber, D. A., Maheswaran, S., Birrer, M. J., & Zou, L. (2017). ATR inhibition disrupts rewired homologous recombination and fork protection pathways in PARP inhibitor-resistant BRCA-deficient cancer cells. *Genes Dev*, *31*(3), 318-332. https://doi.org/10.1101/gad.290957.116

113. Yuan, J., Ghosal, G., & Chen, J. (2009). The annealing helicase HARP protects stalled replication forks. *Genes Dev*, *23*(20), 2394-2399. https://doi.org/10.1101/gad.1836409

114. Zellweger, R., Dalcher, D., Mutreja, K., Berti, M., Schmid, J. A., Herrador, R., Vindigni, A., & Lopes, M. (2015). Rad51-mediated replication fork reversal is a global response to genotoxic treatments in human cells. *J Cell Biol*, *208*(5), 563-579. https://doi.org/10.1083/jcb.201406099

115. Zhang, J., Dewar, J. M., Budzowska, M., Motnenko, A., Cohn, M. A., & Walter, J. C. (2015). DNA interstrand cross-link repair requires replication-fork convergence. *Nat Struct Mol Biol*, *22*(3), 242-247. https://doi.org/10.1038/nsmb.2956

116. Zheng, L., Meng, Y., Campbell, J. L., & Shen, B. (2020). Multiple roles of DNA2 nuclease/helicase in DNA metabolism, genome stability and human diseases. *Nucleic Acids Res*, *48*(1), 16-35. https://doi.org/10.1093/nar/gkz1101

117. Zhong, W., Feng, H., Santiago, F. E., & Kipreos, E. T. (2003). CUL-4 ubiquitin ligase maintains genome stability by restraining DNA-replication licensing. *Nature*, *423*(6942), 885-889. https://doi.org/10.1038/nature01747

118. Zhou, B. B., & Elledge, S. J. (2000). The DNA damage response: putting checkpoints in perspective. *Nature*, *408*(6811), 433-439. https://doi.org/10.1038/35044005